การพัฒนาวิธีการเพื่อเพิ่มความเข้มข้น และวิเคราะห์ปริมาณปรอทในน้ำและอากาศ

นายมหิทธิ เพื่อนงาม

วิทยานิพนธ์นี้เป็นส่วนหนึ่งของการศึกษาตามหลักสูตรปริญญาวิทยาศาสตรดุษฎีบัณฑิต
สาขาวิชาเคมี ภาควิชาเคมี
คณะวิทยาศาสตร์ จุฬาลงกรณ์มหาวิทยาลัย
ปีการศึกษา 2553

METHOD DEVELOPMENT FOR PRECONCENTRATION AND DETERMINATION OF MERCURY IN WATER AND AIR

Mr. Mahitti Puanngam

A Dissertation Submitted in Partial Fulfillment of the Requirements
for the Degree of Doctor of Philosophy Program in Chemistry
Department of Chemistry
Faculty of Science
Chulalongkorn University
Academic Year 2010

Thesis Title	METHOD DEVELOPMENT FOR PRECONCENTRATION AND DETERMINATION OF MERCURY IN WATER AND AIR
By	Mr. Mahitti Puanngam
Field of Study	Chemistry
Thesis Advisor	Assistant Professor Fuangfa Unob, Ph.D.

Accepted by the Faculty of Science, Chulalongkorn University in Partial Fulfillment of the Requirements for the Doctoral Degree

…… Dean of the Faculty of Science
(Professor Supot Hannongbua, Dr.rer.nat.)

THESIS COMMITTEE

…… Chairman
(Associate Professor Sirirat Kokpol, Ph.D.)

…… Thesis Advisor
(Assistant Professor Fuangfa Unob, Ph.D.)

…… Examiner
(Associate Professor Orawon Chailapakul, Ph.D.)

…… Examiner
(Assistant Professor Soamwadee Chaianansutcharit, Ph.D.)

…… External Examiner
(Assistant Professor Atitaya Siripinyanond, Ph.D.)

มหิทธิ เพื่อนงาม : การพัฒนาวิธีการเพื่อเพิ่มความเข้มข้น และวิเคราะห์ปริมาณปรอทในน้ำและอากาศ. (METHOD DEVELOPMENT FOR PRECONCENTRATION AND DETERMINATION OF MERCURY IN WATER AND AIR) อ. ที่ปรึกษาวิทยานิพนธ์หลัก : ผศ.ดร.เฟื่องฟ้า อุ่นอบ, 124 หน้า.

พัฒนาวิธีการเพิ่มความเข้มข้นและวิเคราะห์ปริมาณปรอทระดับต่ำในน้ำและอากาศ ทำการสังเคราะห์เอ็มซีเอ็ม-41 และซิลิกาเจลที่ดัดแปรพื้นผิวด้วย 2-(3-(2-อมิโอเอทิลไทโอ)โพรพิลไทโอ)เอทานาไมเพื่อใช้เป็นตัวดูดซับที่มีความจำเพาะเจาะจงกับไอออนปรอท จากนั้นประยุกต์ใช้ตัวดูดซับซิลิกาเจลกับระบบอัตโนมัติสำหรับเพิ่มความเข้มข้นปรอทในน้ำ และนำสารตัวอย่างเข้าสู่เครื่องอะตอมมิกแอบซอบชั่นในสภาวะไอของปรอท โดยทำการวิเคราะห์สารละลายปรอทที่ความเข้มข้น 0.20 และ 4.00 ไมโครกรัมต่อลิตรในการศึกษาประสิทธิภาพในการวิเคราะห์ของระบบที่พัฒนาขึ้น โดยให้ค่าการได้กลับคืนอยู่ในช่วง 85 ถึง 106 เปอร์เซ็นต์ และค่าความแม่นยำในการวิเคราะห์ (%RSD) อยู่ในช่วง 5.5 ถึง 12 เปอร์เซ็นต์ การศึกษาความถูกต้องในการวิเคราะห์ศึกษาโดยใช้ตัวอย่างอ้างอิงมาตรฐาน (HG95-3 และ HG95-10) ซึ่งพบว่าสามารถนำระบบนี้ไปประยุกต์ใช้ในการหาปริมาณของไอออนปรอทที่มีปริมาณน้อยในน้ำตัวอย่างได้ จากนั้นทำการพัฒนาระบบอัตโนมัติสำหรับการวิเคราะห์ปริมาณปรอทในอากาศ บนพื้นฐานของเทคนิคการเปล่งแสงของอะตอมโดยอาศัยการกระตุ้นด้วยกระแสอิเล็คตรอนที่เคลื่อนที่ผ่านตัวกลางที่เป็นฉนวนไฟฟ้า และทำการศึกษาตัวตรวจวัดแสงหลายชนิด ศึกษาประสิทธิภาพของระบบโดยการใช้งานต่อเนื่อง 7 วัน พบว่าค่าความเข้มข้นต่ำสุดของการตรวจวัดปรอทในอากาศคือ 0.12 นาโนกรัมต่อลิตร และมีความสัมพันธ์เชิงเส้นตรงของค่าสัญญาณต่อเนื่องไปถึงความเข้มข้นอย่างต่ำเท่ากับ 6.6 นาโนกรัมต่อลิตร ค่าความแม่นยำในการวิเคราะห์ (%RSD) ปรอทในอากาศในช่วงความเข้มข้นต่ำกว่า 10 นาโนกรัมต่อลิตรอยู่ในช่วง 2.8 ถึง 4.9 เปอร์เซ็นต์ และประสบความสำเร็จในการนำระบบไปใช้วิเคราะห์ปริมาณปรอทในอากาศบริเวณโรงงานแยกและนำกลับมาใช้ใหม่ของหลอดฟลูออเรสเซนต์

ภาควิชา.....เคมี..... ลายมือชื่อนิสิต.....
สาขาวิชา.....เคมี..... ลายมือชื่อ อ.ที่ปรึกษาวิทยานิพนธ์หลัก……..
ปีการศึกษา.....2553.....

4772425723 : MAJOR CHEMISTRY
KEYWORDS : MERCURY / ON-LINE PRECONCENTRATION / PRECONCENTRATION ON GOLD / ATOMMIC EMISSION / DIELECTRIC BARRIER DISCHARGE

MAHITTI PUANNGAM : METHOD DEVELOPMENT FOR PRECONCENTRATION AND DETERMINATION OF MERCURY IN WATER AND AIR. ADVISOR: ASST. PROF. FUANGFA UNOB, Ph.D., 124 pp.

The method for preconcentration and determination of trace mercury in water and air were developed. MCM-41 and silica gel chemically functionalized with 2-(3-(2-aminoethylthio)propylthio)ethanamine were synthesized and used as selective adsorbents for mercury. The functionalized silica gel was further applied to a fully automated sample preconcentration and cold vapor introduction, which was coupled to an atomic absorption spectrometer. The performance of the system was investigated under optimum conditions using the spiked sample containing 0.20 and 4.00 μg L^{-1}. The percentage recovery and the precision (%RSD) of the method were in the range of 85 – 106 % and 5.5 - 12 %, respectively. The accuracy of the proposed method was tested by using certified reference materials (HG95-3 and HG 95-10) and the method gave the analytical results with acceptable accuracy. An automated atmospheric mercury analyzer based on the dielectric barrier discharge (DBD) atomic emission technique was developed. Several types of radiation detector were investigated. The system was operated continuously over 7 days to test the system performance. The limit of detection was 0.12 ng L^{-1} and the linear range extended at least to 6.6 ng L^{-1}, typical RSD values for determination at the single digit ng L^{-1} level ranged from 2.8 to 4.9 %. The system was successfully applied to determine the atmospheric mercury at fluorescence lamp recycling plant area.

Department : Chemistry Student's Signature .....
Field of Study : Chemistry Advisor's Signature .....
Academic Year : 2010

ACKNOWLEDGEMENTS

I would like to thank my kindness advisor, Assistant Professor Dr. Fuangfa Unob for all suggestions, assistance and encouragement. I would like to present my appreciation to Associate Professor Dr. Sirirat Kokpol; Associate Professor Dr. Orawon Chilapakul; Assistant Professor Dr. Soamwadee Chaianansutcharit; Professor Juwadee Shiowatana; and Assistant Professor Dr. Atitaya Siripinyanond for their valuable suggestions as my proposal and/or my thesis committees.

There are some people that I wish to thank. First, I would like to thank Professor Dr. Purnendu K. Dasgupta, Associate Professor Dr. Shin-Ichi Ohira, Lecturer Ponwason Eamchan, Assistant Professor Dr. Wanlapa Aeungmaitripirom, Assistant Professor Dr. Apichat Imyim, and Mr. Sira Nitiyanontakit for their suggestions, teaching and helps. Next, I would like to thank all people in the Environmental Analysis Research Unit for their friendship and good supports. The project is financially supported by a grant for graduate students from Department of Chemistry, Faculty of Science, Chulalongkorn University and the Thailand Research Fund and Chulalongkorn University through the Royal Golden Jubilee Ph.D. program (Grant PHD/37/2550). And I would like to thank Department of Geology, Faculty of Science, Chulalongkorn University for the analytical instruments.

Finally, I am grateful to my beloved family for their support and love. The usefulness of this work, I dedicate to my parents and all the teachers who have taught me since I was a child.

CONTENTS

PAGE

PAGE

PAGE

PAGE

LIST OF TABLES

PAGE

LIST OF FIGURES

FIGURE **PAGE**

LIST OF SCHEME

LIST OF ABBREVIATIONS

SBA	=	Santa Barbara Amorphous
MCM	=	Mobil Crystalline Materials
AAS	=	Atomic absorption spectrometry
ICP	=	Inductively coupled plasma spectrometry
FIA	=	Flow injection analysis
SIA	=	Sequential injection analysis
SPE	=	solid phase extraction
CRM	=	certified reference materials
^{o}C	=	degree Celsius
g	=	gram
mg	=	milligram
μg	=	microgram
ng	=	nanogram
HSAB	=	hard-soft-acid-base principle
L	=	liter
mL	=	milliliter
mol	=	mole
RSD	=	relative standard deviation
SD	=	standard deviation
PTFE	=	polytetrafluoroethylene
SG-NH-L	=	2-(3-(2-aminoethylthio)propylthio)ethanamine functionalized silica gel
MCM-41-NH-L	=	2-(3-(2-aminoethylthio)propylthio)ethanamine functionalized MCM-41

CHAPTER I

INTRODUCTION

1.1 State of the problem

The contamination by heavy metal pollutants, especially mercury, in atmosphere and water source is an important environmental concern due to their high toxicity. The major effects of mercury poisoning manifest as neurological and renal disturbances as it can easily pass the blood-brain barrier and affect the front brain. High concentration of mercury causes impairment of pulmonary function and kidney, chest, pain and dyspnousea. Therefore determination of mercury level in the environment is needed. Generally the concentration of mercury in atmosphere and natural water samples are very low. In order to measure the background level of mercury in an environment, the preconcentration is required.

In this thesis, the methods for preconcentration and determination of mercury in atmosphere and in natural water samples were developed and presented in part I and part II, respectively.

Part I Preconcentration and determination of mercury (II) in natural water samples

The solid phase extraction for trace mercury preconcentration and determination has been widely investigated. Various types of adsorbents are available for extraction of mercury (II) ions in contaminated water samples. Several materials such as activated carbon [1, 2], resin [3, 4], clay [5] and silica [6, 7] have been studied for adsorption of mercury (II) ions. Moreover, the modification of adsorbents with organic functional groups improves the selectivity and capability of the adsorbents for binding target metal ions and has recently drawn much attention. The high selectivity of such adsorbents is the main advantage over traditional adsorbents. Regarding mercury ions, the most effective modification is surface functionalization with coordinating ligands containing sulfur atoms [6-12].

Recently, surface functionalization of ordered mesoporous silica has garnered intense interest for the use as solid supports due to its large surface area, fast adsorption kinetics and controllable pore size and pore arrangement in comparison to amorphous silica gel [9, 10]. Several mesoporous silicas have been functionalized with different ligands and used for mercury removal from water. The modifications of SBA-15 and MCM-41 with 2-mercapto thiazoline, 2-mercaptopyridine, or 2-mercapto benzothiazol and MCM-48 with benzoyl thiourea were reported [8, 10-12]. Although mesoporous silica has several advantages over amorphous silica gel, it seems to be less suitable for the column methods, due to smaller particle sizes. However, there are few works that compared the adsorption behavior of the functionalized amorphous silica gel and ordered mesoporous silica. In this work, silica gel and MCM-41 were functionalized with 2-(3-(2-aminoethylthio)propylthio)ethanamine and applied in mercury extraction from water. Their mercury adsorption behavior was then compared in batch method. Furthermore, the application of the materials in determination of mercury in water samples was also studied.

Due to the toxicity of mercury (II) ions, the concentration of mercury (II) ions in natural water should be monitored. Normally the concentration level of mercury (II) ions in contaminated natural water is very low, thus the preconcentration is needed in most cases [13-15]. The sensitive detection techniques are also required. Cold vapor technique is the most useful sample introduction technique for determination of mercury (II) ions in water sample because the mercury is isolated from sample by changing their state from solution to gas phase. Atomic absorption spectrometry (AAS) is one of the most famous techniques for determination of mercury and it offers many advantages, for example, good precision and accuracy and low cost operation. However, the lack of sensitivity is a major concern for the atomic absorption technique, the preconcentration process prior to the determination of mercury (II) ions can be applied in order to improve the sensitivity of the detection. Solid phase extraction (SPE) is the most suitable technique which can be easily coupled with the online sample preconcentration and determination method. On-line methods provide some advantages over the offline column method or the batch method such as automated and rapid analysis with simple apparatus and easy

operation, low reagents and samples consumptions, less contamination, good reproducibility and accuracy [16].

In this research, a fully automated system of sample preconcentration and introduction was coupled to AAS for determination of low level of mercury ions in water samples. Silica gel functionalized with 2-(3-(2-aminoethylthio)propylthio) ethanamine was applied as the solid phase in SPE preconcentration column. The conditions in preconcentration and determination of mercury (II) ions were optimized. The method was validated and applied to determine trace mercury in natural water samples and certified reference materials (CRMs).

Part II Preconcentration and determination of atmospheric mercury

The cycling of mercury through the atmosphere is a major vector for mobilizing mercury in the environment; the atmospheric chemistry of mercury has been concisely reviewed [17]. The majority (95%) of mercury in the atmosphere is in the elemental (Hg^0) form. Although the residence time of mercury is only few months as reported recently [18], it is enough for mercury emitted in any region to be dispersed globally that led to a need in measurements of elemental Hg. Particularly an inexpensive measurement and a portable device able to measure ambient background levels will be highly desirable. A variety of options are available for the measurement of gaseous Hg^0 and in almost all cases some preconcentration is needed to measure background levels. Atomic spectrometry, especially emission spectrometry, is one of the most sensitive techniques for determination of Hg^0. This includes atomic fluorescence [19], inductively coupled plasma [20], microwave induced plasma [21] and glow discharge spectrometry [22], etc. Very recently Yu et al. [23] and Zhu et al. [24] independently introduced dielectric barrier discharge (DBD) plasma spectrometry. The DBD or silent discharge is non-thermal plasma generated between two electrodes in the presence of at least one dielectric barrier in the current flow path [25].

In this work, a fully automated system for the preconcentration and atmospheric pressure DBD-atomic emission based determination of atmospheric Hg^0 were described. This research focused on a portable and inexpensive instrument. The performance of several inexpensive to moderately priced detectors for their

relative sensitivities in measuring the mercury emission was studied. Mercury preconcentration was carried out on gold-plated tungsten filaments from a pair of quartz-halogen lamps. This has the advantage of a "built-in" heater and rapid desorption due to a low thermal mass. System operation was controlled by an in-house program written in Labview software (http://www.ni.com).

1.2 Objectives of the thesis

The objectives of this work were (i) to prepare selective adsorbents for mercury (II) ions adsorption which provides an alternative in preconcentration of mercury (II) ions in water sample, (ii) to develop a fully automated sample preconcentration and sample introduction system coupled to AAS for determination of mercury (II) ions in water sample and (iii) to develop a fully automated system for atmospheric mercury measurement.

1.3 Scope of the thesis

Part I;

The scope of this part includes the preparation and characterization of the MCM-41, 2-(3-(2-aminoethylthio)propylthio)ethanamine chelating ligand, MCM-41 and silica gel functionalized with 2-(3-(2-aminoethylthio)propylthio)ethanamine. The adsorbents extraction properties under various conditions such as solution pH, extraction time, ionic strength, interfering ions were investigated by batch method. The automated sample preconcentration and introduction system was built and coupled to the atomic absorption spectrometer. The modified silica gel was further used as the adsorbent for the mercury (II) ions preconcentration. The effect of parameters affecting the determination of mercury including argon flow rate, the presence of chloride ions, sample loading flow rate and interfering ions effect were studied. Then the gold plated Tungsten filament was used as the focusing material for cold vapor mercury (0) before vapor introduction to AAS. The proposed system was validated using standard mercury (II) ions solution, spiked samples and CRMs. Finally, the proposed method was applied in the determination of sub parts-per-billion (ppb) of mercury (II) ions in water samples.

Part II;

The scope of this part includes the preparation of DBD emission cell, gold-plated Tungsten filament preconcentration chamber and standard elemental mercury source. Two types of emission detector such as band pass filter + phototube (PT) or photomultiplier tubes (PMTs) and charge couple devices (CCD) spectrometer were investigated. The automated atmospheric mercury preconcentration and detection system was built and controlled by in-house program written in Labview software. The effect of parameters affecting the signal response and sensitivity of elemental mercury determination including plasma potential and plasma gas flow rate, detectors type, electrode area and placement, desorption voltage and time were studied. The major parameters in atmospheric mercury determination such as argon flush flow rate during desorption step, sampling rate during preconcentration, repeatability and limit of detection were also examined. The developed instrument was applied to monitor the level of atmospheric mercury in field.

CHAPTER II

THEORY AND LITERATURE REVIEW

2.1 Chemistry of silica materials

2.1.1 What is a silica material?

Silica is a solid and hard material which is an oxide of silicon. The ratio of Si:O is 1:2 as known as silicon dioxide (SiO_2). Silica is naturally found as sand or quartz, and it provides many advantages such as high mechanical strength, good thermal and chemical stability under various conditions.

2.1.2 Type and properties of silica material

Silica materials can be classified in 2 categories as the silica with crystalline forms (polymorphs) and amorphous forms. Crystalline silica material is the silicon dioxide compound that has a regular repeating pattern in the structure such as MCM-41, MCM-48 and SBA-15, while an amorphous silica material does not have the repeating pattern or no repeat unit such as silica gel. In this research, two types of silica material are employed i.e. MCM-41 and silica gel.

MCM-41 is an ordered structure mesoporous silica material containing the hexagonal arrays with a pore size range of 1.5 to 20 nm, which is controlled by varying the surfactant molecules used as template during preparation step.

Silica gel is an amorphous highly porous granular solid which is prepared from sodium silicate.

2.1.3 Modification of silica surface

The surface of silica materials consists of the hydroxyl groups (-OH) which are capable of reacting with silane reagents to form Si-O-Si bond. This method produces a strong covalent bond between silica surface and modified molecules, which has the advantage of reusing the material because there is no leaching out of modified molecule when contacts with solvent.

2.2 Mercury in environment

Mercury is a toxic element naturally found in several forms, such as elemental mercury, inorganic mercury compounds and organic mercury compounds. The primary source of mercury is the earth's crust and it is also found in many types of rock. Human activities (such as industrial combustion and mining) also release the mercury to the environment.

2.2.1 Species and toxicology

Elemental mercury and most of its compounds are toxic, however the level of toxicity are different for the different species. Elemental mercury (Hg^0) is a silvery-white liquid at room temperature; it has low boiling point and high vapor pressure. It is the major species of mercury in atmosphere. Also the elemental mercury can be oxidized or react to form compounds in either the Hg^+ or Hg^{2+} oxidation state. The most toxic species is organic-mercury compounds such as methyl and dimethyl mercury, which can bioaccumulate and cause neurological impairment especially for very young children.

2.2.2 Mercury measurement

According to the high toxicity of mercury, the monitoring and measurement of mercury in environment is important. There are several sensitive and robust methods for mercury measurement [26]. Most of detection techniques response to the elemental mercury, therefore the mercury compounds have to be converted into the elemental form before detection. In the measurement of mercury compounds in aqueous sample, cold vapor generation is a famous method that converts the mercury compounds in sample into the elemental from. Moreover the cold vapor generation also cuts off the matrix interfering effect due to the phase separation between analyte and sample before detection. The recent cold vapor generation has succeeded in reducing a risk of contamination from reagents by using electrochemical method [27, 28] instead of the chemical reduction method.

Atomic fluorescence technique is often used to determine mercury in the low level concentration due to its relatively high sensitivity compared to other techniques. In trace mercury analysis, the commonly used detection techniques are not sensitive enough to determine the concentration of mercury directly, therefore the mercury preconcentration is needed prior to the detection. Many types of adsorbents are used to preconcentrate the mercury compounds in aqueous sample before conversion to elemental mercury by cold vapor generation method [29]. Furthermore, gold surface is a famous material to be used as elemental mercury preconcentrator, because it takes up the mercury efficiently and simply releases the trapped mercury by heating.

2.3 Extraction of mercury in water

2.3.1 Sorption isotherms

The adsorption isotherms are the models describing the adsorption behavior of the analytes onto sorbent surface under thermodynamic equilibrium and constant temperature. Many types of isotherm have been proposed base on different assumptions. The Langmuir and Freundlich isotherm are wildly used to describe the adsorption phenomena at solid-liquid interface.

2.3.1.1 Langmuir isotherm

The Langmuir relation assumes that the analytes accumulate onto the homogeneous sorbent surface in a monolayer adsorption at a constant temperature. The Langmiur equation [30] and the linearized expression are presented in equation (2.1) and (2.2), respectively,

$$N_f = \frac{bN_f^S C}{1+bC} \tag{2.1}$$

$$\frac{C}{N_f} = \frac{C}{N_f^S} + \frac{1}{bN_f^S} \tag{2.2}$$

where N_f is the amount of analyte adsorbed per gram of adsorbent (mg g^{-1}), C is the equilibrium concentration of the analyte (mg L^{-1}), $b = K_{eq}/a$ (where a represents the activity of the analyte in solution, K_{eq} is the equilibrium constant) and N_f^S is the maximum sorption capacity of the sorbent (mg g^{-1}). The Langmuir constant (b) is related to the bonding energy between the analyte and the adsorbent. The plot of $\frac{C}{N_f}$ against C yields a straight line with a slope of $\frac{1}{N_f^S}$ and intercept of $\frac{1}{bN_f^S}$ (Figure 2.1).

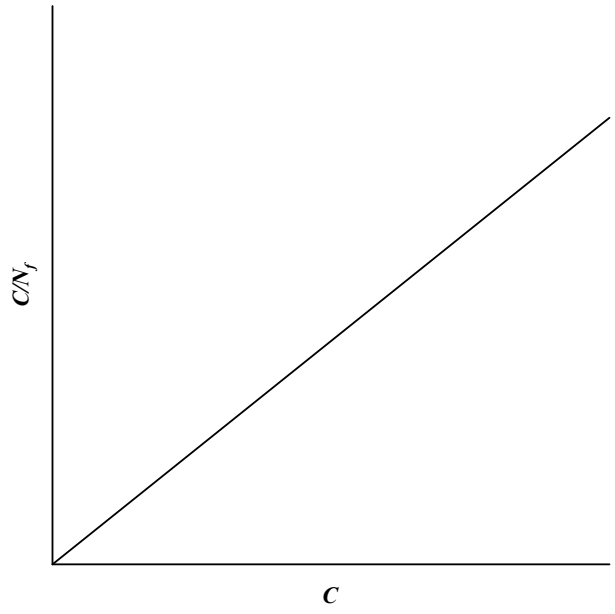

Figure 2.1 The linear plot of Langmuir isotherm.

2.3.1.2 Freundlich isotherm

The Freundlich isotherm assumes that the multilayer adsorption of analyte occurs on adsorbent surface. The Freundlich relation [31] can be expressed in equation (2.3),

$$N_f = K_f C^{\frac{1}{n}} \tag{2.3}$$

where N_f is the amount of analytes adsorbed per gram of sorbent (mg g^{-1}), C is the equilibrium concentration of the analytes (mg L^{-1}), K_f is Freundlich constants and *n* is the numerical value of Freundlich constant. The linear relation can be plotted using the following equation.

$$\log N_f = \log K_f + \frac{1}{n} \log C \tag{2.4}$$

The value of 1/*n* and K_f can be obtained from the slope and the intercept, respectively.

2.4 Determination of mercury

2.4.1 Flow injection analysis (FIA)

Flow injection analysis (FI, Scheme 2.1) was first described by Ruzicka and Hansen in 1975 [32], where a plug of sample is injected into a flowing carrier stream of reagent, then the sample solution disperses and reacts with reagent to form the detectable product. The signal response of product is recorded by a flow through detector placed downstream. Nowadays the modern technology is applied to flow injection analysis system providing ability to deal with complicated reaction, combining the sample preparation or preconcentration step to the detection [33]. The FIA instrument usually consists of peristaltic pump, injection valve, coiled reactor and detector. Some components such as a flow through heater, preconcentration column, membranes, filters and debubblers can also be added into the system.

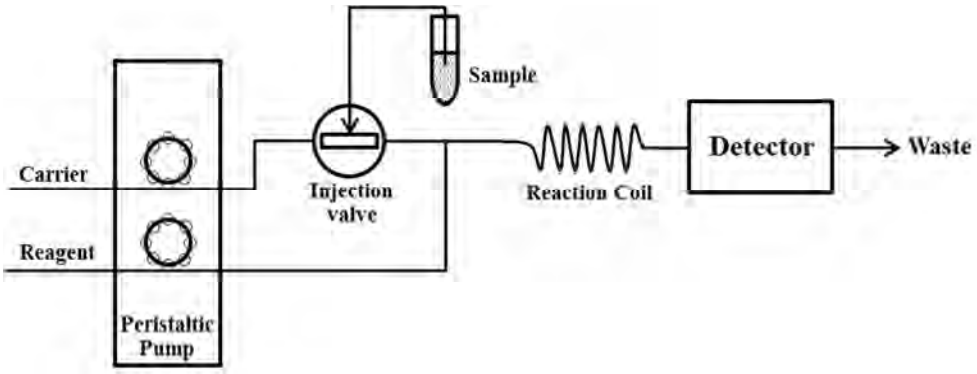

Scheme 2.1 Example of a flow injection system.

The second generation of FIA (Scheme 2.2) is sequential injection analysis (SIA) which uses a high precision bi-directional pump to move the solution through multiposition valve which chooses the proper position. In the common operation of SIA, firstly the system is filled with a carrier stream, then sample and reagent(s) are sequentially aspirated into holding coil, the detectable product is formed due to dispersion of sample and reagent(s) with parabolic profiles. Moreover the reversals of accelerated flow stream promote mixing, while the multiposition valve is switched to the detector position and the flow direction is reversed, finally the detectable product is detected at the flowcell.

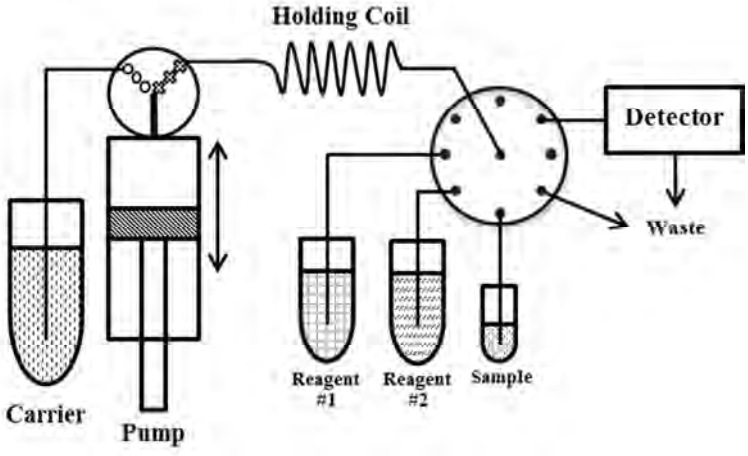

Scheme 2.2 Example of a sequential injection system.

The SIA has more advantage than the first generation FIA in less chemical consumption, less waste generation, however the disadvantage of SIA compared to the first generation FIA is lower analysis frequency due to slower operation.

2.5 Literature review

2.5.1. Preconcentration and determination of mercury (II) in natural water samples

2.5.1.1 Extraction of mercury

Many works have been published on mercury in water extraction. The adsorption process is one of the famous methods for this proposes. Several types of adsorbent were used such as ion-exchange resin, activated carbon and silica materials. Moreover, the surface modification of the adsorbent was performed to improve the selectivity and capacity of the adsorbent in mercury extraction. The chemically modification is one of the effective method which provides a good stability of the modified surface and high possibility to reuse the adsorbent. In order to improve the selectivity of the adsorbent toward mercury ions, the functional groups containing sulfur atom are modified onto the adsorbents surface. Some of literatures that mentioned about extraction of mercury in water, surface modification, chemical modification especially for the silica materials are listed below.

Chiarle *et al.* [34] used the Duolite GT-73 ion-exchange resin for mercury (II) ion removal. The effect of pH on adsorption kinetics in batch method was studied. It was found that the extraction efficiency decreased by decreasing the solution pH due to the competitive adsorption of proton in solution.

Dujardin *et al.* [35] synthesized the ion-exchange resin containing thiol groups. The resin could remove mercury from industrial wastewater (10 mg L^{-1} Hg) and the final concentration about 1 μg L^{-1} was achieved after treatment.

Starvin and Rao [36] used the 1-(2-thiazolylazo)-2-napthol modified activated carbon as the adsorbent for mercury. It was found that the modified activated carbon provided higher extraction efficiency over the unmodified activated carbon.

Olkhovyk *et al*. [37] modified the MCM-48 surface with benzoylthiourea, and applied to extract the mercury (II) ions in water. The modified adsorbent has a surface area of 505 m^2 g^{-1} and the approximate pore size of 2.8 nm. While the ligand loading on the adsorbent surface was 1.55 mmol g^{-1} which provided the maximum adsorption capacity in the mercury (II) ions extraction of 6.7 mmol of mercury (II) ions per gram of adsorbent. The 10 % decreasing of the maximum adsorption capacity was observed after regenerated with 10 % Thiourea in 0.05 M HCl.

Walcarius and Delacôte [38] evaluated the adsorption properties of several types of mesoporous silica material in mercury (II) ions extraction. The mesoporous silicas were modified to have thiol groups (–SH) on their surfaces. The extraction was performed in solution at pH range of 0 – 8 and in the presence of other metals ion. It was found that the mercury (II) ions could not be hydrolyzed in the solution pH less than 4, and the efficiency in mercury extraction from solution was higher when mercury was in their hydrolyzed form, compared to non-hydrolyzed form.

Aguado *et al*. [39] synthesized the mesoporous silica SBA-15 for mercury (II) removal by co-condensation method between tetraethoxysilane and mercaptopropyl trimethyloxysilane in the different ratio. It was found that the SBA-15 structure was distorted when the amount of mercaptopropyl trimethyloxysilane more than 15 % in the preparation step. The maximum adsorption capacity of the adsorbent was about 2.9 mmol of mercury (II) ions per gram of the adsorbent.

Pérez-Quintanilla *et al*. [11] synthesized the modified MCM-41 and SBA-15 adsorbents for mercury (II) removal. The MCM-41 and SBA-15 were chemically modified by 2-mercaptothiazoline. Two different surface modification pathways were studied; (i) the homogeneous reaction between 3-chloropropyltriethoxysilane and 2-mercaptothiazoline was performed before the functionalization of the obtained product on the adsorbents surface, (ii) the heterogeneous reaction between 3-chloropropylteiethoxysilane and adsorbents surface was carried out before further

modification with 2-mercaptothiazoline. It was found that the adsorbents prepared by homogeneous pathway provided higher adsorption capacity and the maximum adsorption capacity of the MCM-41 and SBA-15 were 1.10 and 0.7 mmol of mercury (II) per gram of the adsorbents, respectively.

2.5.1.2 Determination of mercury in water by solid phase preconcentration methods

The most commonly used techniques for mercury (II) determination are atomic spectrometric techniques, in many cases the preconcentration is needed to achieve the low level measurement. Solid phase extraction shows a good potential for mercury (II) preconcentration and the example works are listed in the Table 2.1. Moreover the on-line system provides higher precision, less time consumption and reduces the risk of contamination in sample preparation steps, resulting in higher sample throughput and more reliable results. The example of on-line preconcentration and determination of mercury (II) in water are shown in Table 2.2

Table 2.1 Solid phase preconcentration methods for determination of mercury (II) in waters by cold vapor atomic absorption spectrometry (off-line)

Support material	**Ligand**	**Eluent**	**[a] Working range or [b] LOD**	**Samples investigated / sample volume (enrichment factor)**	**Reference**
Dowex 50Wx4 cation-exchange resin microcloumn (500 mg)	-	0.1 % thiourea in 8 % HCl	[b] 27 ng L^{-1}	spiked mineral water, spring water, tap water / 100 mL (6.67)	[40]
Agar minicolumn (200 mg)	2-mercapto-benzimidazole	3 M HCl	[a] 40 – 2400 μg L^{-1} [b] 20 ng L^{-1}	drinking water, waste water / 250 mL (100)	[41]
Neutral alumina microcolumn (100 mg)	Dimethylsulfoxide	concentrated HNO_3	[a] ≥ 10 ng L^{-1}	spiked river water, tap water / 2000 mL (1000)	[42]
Neutral alumina microcolumn (100 mg)	Thiosemicarbazide	concentrated HNO_3	[a] 10 – 25 ng L^{-1}	spiked tap water, river water / 2000 mL (1000)	[43]
Silica gel (1000 mg)	Dithizone	10.0 M HCl	[b] 20 ng L^{-1}	tap water / 1000 mL (200)	[44]
Silica gel microcolumn (500 – 1000 mg)	(*E*)-*N*-(1-thien-2'-ylethylidene)-1,2-phenylenediamine	10.0 M HCl	[a] ≥ 30 ng L^{-1}	spiked tap water / 2000 mL (200)	[45]

Table 2.2 On-line preconcentration and determination of mercury (II) in water

Support material	**Ligand**	**Eluent**	**Detection method / [a] Working range or [b] LOD**	**Samples investigated / sample volume**	**Reference**
Vinyl co-polymer Toyopearl gel minicolumn (5.5 cm length and 5.0 mm i.d.)	8-hydroxiquinoline	2 M HCl + 1 M HNO_3	CV-AAS [a] 5.0 – 25 μg L^{-1} [b] 0.23 μg L^{-1}	sea water / 1.00 mL	[13]
PTFE powder (packed in 100 μL pipette tip)	Cyanex 923	10 % HNO_3	CV-AAS [a] 20 – 2000 ng L^{-1} [b] 0.2 ng L^{-1}	city lake water, deep well water / 25.0 mL	[14]
C18-silica microcolumn	O,O-diethyl dithiophos-phoric acid	Methanol	CV-ICP-MS [a] 25 – 500 ng L^{-1} [b] 5.0 ng L^{-1}	Sea water / 2.3 mL	[46]

CV-AAS = Cold vapor atomic absorption spectroscopy

CV-ICP-MS = Cold vapor inductively coupled plasma mass spectrometry

2.5.2 Determination of atmospheric mercury

All available detectors for mercury are mostly response to the elemental mercury which is the major species (~ 95%) of mercury in atmosphere, especially, the high sensitive optical emission spectrometry such as atomic fluorescence [19], inductively coupled plasma [20], microwave induced plasma [21] and glow discharge spectrometry [22], dielectric barrier discharge (DBD) plasma spectrometry [23, 24]. Normally the concentration of mercury in atmosphere is very low, therefore the preconcentration is needed in the measurement of the background levels of atmospheric mercury. The most common preconcentration method for Hg^0 is trapping on gold, typically the gold is supported on glass beads [47], silica [48], glass/quartz wool [49], etc. Therefore, a separate heater is needed to thermally desorb the trapped mercury. Gold not only takes up mercury efficiently, the resistivity of gold changes [50] upon mercury uptake enabling thin gold film based resistive sensors for mercury [51].

In this research, the DBD plasma spectrometry was employed in combination with gold trapping preconcentration for atmospheric mercury determination. There are a few works reporting the measurement of mercury ions in solution by DBD plasma spectrometry as described following.

In 2008, the DBD was used for the first time as a radiation source for a miniaturized optical emission spectrometric system by Yu *et al* [23]. The system was used to determine the concentration of mercury (II) ions in water. The DBD emission cell ($50 \times 5 \times 1$ mm^3) was made from two quartz plates and two glass plates. Two pieces of aluminum foil were used as the discharging electrodes; the neon power supply was used as the power source with input voltages of 55 to 75 V at 50 Hz. The emission spectra were recorded by a QE65000 CCD spectrometer (Ocean Optics), equipped with wavelength selector (~8 nm resolution) and the integration time was set at 50 milliseconds (ms). Argon was used as a carrier gas and the plasma source, and no plasma was generated at a discharge voltage less than 1.1 kV. The system provided 0.2 μg L^{-1} limit of detection (LOD) and 2.1 percentages of relative standard deviation for the determination of 10 μg L^{-1} of mercury (II) ions.

The percentage of recovery was found to be over 97 % for the determination of city waste incineration ash (CRM 176), sea water (NASS-5) and riverine water (SLRS-4).

Zhu *et al*. [24] studied two of plasma gas types (argon and helium) on the determination of mercury (II) ions in water. The DBD cell (15 × 0.6 × 1 mm^3) was formed using two glass plates and two glass spacers of 1 mm thickness. The discharging electrode was made from two copper strips and the power supply of commercial ozone generator was used to sustain the plasma. The emission radiation from the DBD cell was imaged by a fused-silica lens (focal length, 75 mm) onto a 0.5-m Czerny-Turner monochromator. A Hamamatsu R928 photomultiplier tube (PMT) biased at −850 V was used as the detector. The obtained detection limit was 14 pg mL^{-1} for He-DBD and 43 pg mL^{-1} for Ar-DBD without removal of the residual moisture. The relative standard deviation was less than 2% for a10 ng mL^{-1} standard mercury (II) ions determination.

The gold-plated Tungsten filament preconcentrator coupled with the DBD emission spectrometry for atmospheric mercury determination was firstly explained in this research.

CHAPTER III

EXPERIMENTAL SECTION

This chapter is divided into two parts: part I preconcentration and determination of mercury (II) in natural water samples and part II preconcentration and determination of atmospheric mercury. The list of instruments and chemicals used in these parts are given below.

3.1 Instruments

The instruments used in this study are listed in Table 3.1

Table 3.1 Instruments list

Instruments	**Model (company)**	**Purpose**
Thermogravimetric analyzer (TGA)	Pyris 1 (Perkin-Elmer)	Measurement of functional group amount on sorbent
Atomic absorption spectrometer (AAS)	AAnalyst 300 (Perkin-Elmer)	Mercury (II) ions determination
Flow Injection Instruments (FIAS)	FIAS-400 (Perkin-Elmer)	Reducing agent delivering and argon flow rate controlling
pH meter	pH 211 (Hanna Instruments)	pH measurement
Syringe Pump	V6 - 55022 (Kloehn)	Controlling the fluid flow in the system
NIST traceable primary flow calibrator	Gilibrator (Gilian)	Flow calibration for mass flow controller devices
Charge coupled device (CCD) spectrometer	C9404CA (Hamamatsu) QE65000 (Ocean Optics) USB2000 (Ocean Optics)	Recording of emission spectrum

3.2 Chemicals

The reagents and solvents in all experiments were of analytical grade and summarized in Table 3.2

Table 3.2 Chemicals and suppliers

Chemicals	**Supplier**
Silica gel, 70-230 mesh, 60	Merck
Tetraethoxysilane (TEOS)	ACROS Organics
Cetyltrimethyl ammoniumbromide (CTAB)	Merck
Cystamine hydrochloride	Merck
1,3-Dibromopropane	Merck
3-Aminopropyltriethoxysilane	Merck
Ethyl-2-bromo propionate	Sigma-Aldrich
Hydrochloric acid (37% w/w)	Merck
Nitric acid (65% w/w)	Merck
Sulfuric acid (95 - 97% w/w)	Merck
Toluene	CARLO ERBA
Ethanol	Merck
Dichloromethane	Fisher Chemicals
Mercury (II) nitrate monohydrate ($Hg(NO_3)_2 \cdot H_2O$)	Merck
Cadmium (II) nitrate tetrahydrate ($Cd(NO_3)_2 \cdot 4H_2O$)	Sigma-Aldrich
Nickel (II) nitrate hexahydrate ($Ni(NO_3)_2 \cdot 6H_2O$)	Merck
Cobalt(II) nitrate hexahydrate ($Co(NO_3)_2 \cdot 6H_2O$)	Merck
Sodium hydroxide (NaOH)	Merck
Potassium bromide (KBr)	Merck
Sodium chloride (NaCl)	Merck
Sodium nitrate ($NaNO_3$)	Merck
Sodium sulfate (Na_2SO_4)	Merck
Potassium nitrate (KNO_3)	Merck
Magnesium nitrate ($Mg(NO_3)_2$)	Merck

Table 3.2 Chemicals and suppliers (cont.)

Chemicals	**Supplier**
Calcium nitrate ($Ca(NO_3)_2$)	Merck
Hg standard solution (1000 mg L^{-1})	BDH SpectrosoL®
Pb standard solution (1000 mg L^{-1})	BDH SpectrosoL®
Ag standard solution (1000 mg L^{-1})	BDH SpectrosoL®
Au standard solution (1000 mg L^{-1})	BDH SpectrosoL®
Sodium borohydride	Merck
Thiourea	BDH SpectrosoL®
Certified reference materials: - HG95-3 - HG95-10	National Water Research Institute, Canada

Part I Preconcentration and determination of mercury (II) in natural water samples

3.3 Preconcentration and determination of mercury (II) in natural water samples

3.3.1 Preparation of chemicals and reagents

All reagents and organic solvents were of analytical grade and used without further purification. All solutions were prepared by using de-ionized (DI) water except the solutions used in the mercury preconcentration and determination experiments that were prepared in ultrapure water (Milli-Q water).

a) Metal ions standard solutions

All metal ions solutions were prepared by dilution of 1000 mg L^{-1} stock standard solution to desired concentrations with DI water or Milli-Q water. The pH value was adjusted using sodium hydroxide and nitric acid solutions.

b) Sodium hydroxide solutions for pH adjustment

Sodium hydroxide solutions (1, 5 and 10 % w/v) were prepared daily by dissolving the appropriate amount of sodium hydroxide in DI water.

c) Nitric acid solutions for pH adjustment

Nitric acid solutions (1, 5 and 10 % v/v) were prepared daily by direct dilution of the concentrated solution (65% w/w).

d) Solution containing different salts

The mercury ions solution containing sodium salt of different anions (NO_3^-, SO_4^{2-} or Cl^-) or nitrate salt of different cations (Na^+, K^+, Mg^{2+} or Ca^{2+}) of 0.1 and 1.0 M, used in the study of coexisting ions effect were prepared by dissolving the appropriate amount of each salt in DI water.

e) Solution containing different metal ions

The mercury ions solution containing nitrate salt of different transition metal ions (Ni^{2+}, Cd^{2+} or Co^{2+}), used in the study of coexisting ions effect were prepared by dissolving the appropriate amount of each salt in DI water. In mercury preconcentration and determination experiment, Pb^{2+}, Au^{3+} or Ag^{+} solutions were prepared by dilution of 1000 mg L^{-1} stock standard solution with Milli-Q water to the desired concentrations.

f) Acid carrier and cleaning solution for mercury preconcentration experiments (1% H_2SO_4)

A sulfuric acid solution (1% w/v) was prepared daily by direct dilution of the concentrated solution (95% w/w) with Milli-Q water.

g) Reducing agent (5% $NaBH_4$ in 0.2 M NaOH)

A reducing agent solution was prepared daily by dissolving the appropriate amount of $NaNH_4$ and NaOH in Milli-Q water.

h) Eluent (1% Thiourea in 1% H_2SO_4)

An eluent solution was prepared daily by dissolving the appropriate amount of thiourea with the acid carrier solution.

3.3.2 Synthesis of MCM-41 mesoporous silica

In the synthesis of MCM-41, the method reported by Chen and Wang was adopted [52]. Source of silicon was TEOS and the structure directing agent was CTAB. MCM-41 was prepared by adding 5.78 g of TEOS (27.7 mmol) into a solution containing 1.01 g of CTAB (2.8 mmol) and 0.34 g of NaOH (8.5 mmol) in 30 mL of DI water in a 125 mL polytetrafluoroethylene (PTFE) bottle. The mixture was stirred for 1 hour at room temperature. Then close tightly the bottle cap before kept in the oven at 110 ^{o}C for 96 hours. The molar composition of the initial gel mixture was 1.0:0.1:0.3:60 TEOS/CTAB/NaOH/H_2O. The solid product was obtained by filtration, washed with DI water, ethanol and dichloromethane, respectively. This MCM-41 was dried in air at room temperature.

3.3.3 Synthesis of chelating ligand

The synthesis of 2-(3-(2-aminoethylthio)propylthio)ethanamine [53] was performed by dissolving the sodium metal (1 g, 42.9 mmol) with 20 mL of ethanol in 150 mL two-necked round bottom flask and the solution was kept at 10 – 20 ^{o}C. Cystamine hydrochloride (2.3 g, 20 mmol) was added to the solution. The mixture was stirred for 15 minute before adding 1,3-dibromopropane (1.0 mL, 9.8 mmol). Then the mixture was stirred for 4 hours at 40^{o}C under nitrogen atmosphere. After 4 hours of stirring, the solvent was subsequently removed by rotary evaporator. Sodium hydroxide solution (30%, w/v, 15 mL) was added to the residue and the resulting mixture was left to stand overnight. The mixture was transferred to a separatory funnel and extracted with dichloromethane (3 × 20 mL). The dichloromethane phase was separated and washed with DI water. A yellow oil product (1.3 g, %68 yield) was obtained after evaporating the dichloromethane.

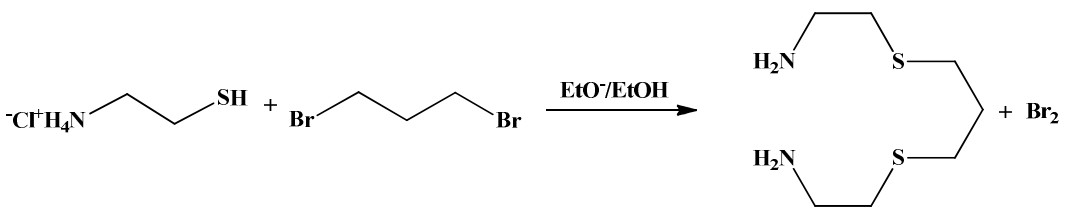

Scheme 3.1 Preparation of 2-(3-(2-aminoethylthio)propylthio)ethanamine.

The obtained product was characterized by ^{1}H-NMR and ^{13}C-NMR: ^{1}H NMR (400 MHz, CDCl3) δ: 1.7 (q, 2H), 2.5 (t, 8H), 2.8 (t, 4H); ^{13}C NMR (400 MHz, CDCl3) δ: 29.5, 30.4, 36.2, 41.2.

3.3.4 Modification of MCM-41 and silica gel

The method for modification of MCM-41 and amorphous silica gel is illustrated in Scheme 3.2. In the first step, MCM-41 or silica gel (25 g) was suspended in 200 mL of dried toluene, refluxed and stirred under nitrogen atmosphere for 2 hours. Ten millilitres of 3-aminopropyltriethoxysilane was added drop wise and the mixture was refluxed for 24 hours. The solid (Scheme 3.2a) was filtrated, washed with toluene (2 × 50 mL), ethanol (2 × 50 mL), dichloromethane (4 × 50 mL) and subsequently dried in vacuum. The modified MCM-41 and silica gel obtained from the first step were named **MCM-41-NH_2** and **SG-NH_2**, respectively. In the second step, MCM-41-NH_2 or SG-NH_2 was immersed in 200 mL of dried toluene, refluxed and stirred for 2 hours under nitrogen atmosphere. Then ethyl-2-bromopropionate (6.25 mL) was added and the mixture was refluxed for 24 hours. The resulting product (Scheme 3.2b) was filtered and washed with toluene (2 × 50 mL), ethanol (4 × 50 mL) and dichloromethane (4 × 50 mL). The product was dried at room temperature under vacuum. The second step modified MCM-41 and silica gel were named **MCM-41-NH-Br** and **SG-NH-Br**, respectively. In the final step, dried acetonitrile was used as solvent. The MCM-41-NH-Br or SG-NH-Br was dispersed in 200 mL dried acetonitrile, refluxed and stirred for 2 hours before adding the ligand 2-(3-(2-aminoethylthio)propylthio)ethanamine (8.3 g). The mixture was stirred and refluxed for 24 hours under nitrogen atmosphere. The final product (Scheme 3.2c) was filtered and washed with acetonitrile (2 × 50 mL), ethanol (6 × 50 mL) and dichloromethane (4 × 50 mL). These products were dried at room temperature under vacuum before further use and named **MCM-41-NH-L** and **SG-NH-L**.

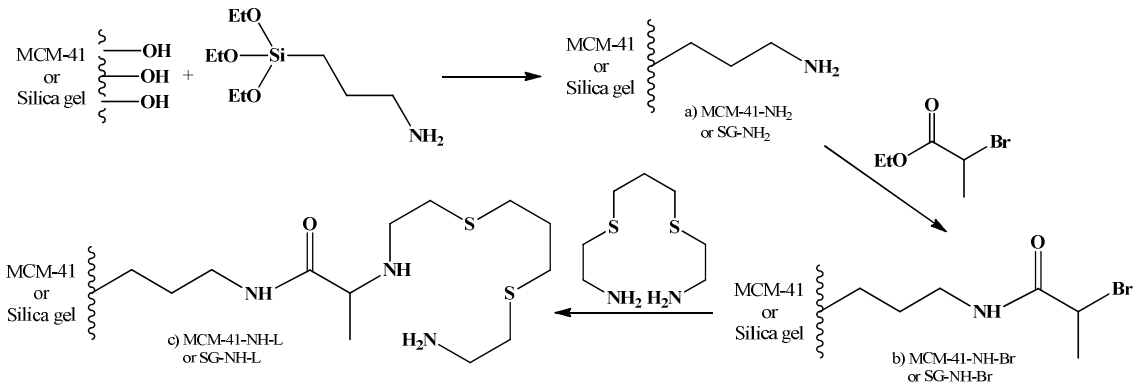

Scheme 3.2 Modification of MCM-41 and silica gel.

3.3.5 Characterization

3.3.5.1 Characterization of chelating ligand

The characterization of the synthesized 2-(3-(2-aminoethylthio)propylthio) ethanamine was performed by using ^{1}H-NMR and ^{13}C-NMR spectroscopy.

3.3.5.2 Characterization of modified MCM-41 and silica gel

The characterization of the modified MCM-41 and silica gel was performed by X-ray diffraction (XRD), surface area and porosity analyzer, thermogravimetric analyzer and solid state ^{13}C-NMR.

The XRD was used to confirm the uniform mesoporous structure of the synthesized MCM-41 and also modified MCM-41. The XRD pattern of MCM-41 and modified MCM-41 were recorded from 1.5 to 8 of 2-Theta (2Θ) values.

The surface area, total pore volume and average pore diameter of unmodified adsorbents and modified adsorbents were measured by the surface area analyzer.

The thermogravimetric measurements were performed using a heating rate of 20 ^{o}C min^{-1} under nitrogen atmosphere. The amount of 2-(3-(2-aminoethylthio) propylthio)ethanamine (mmol) per adsorbent amount (g) were calculated from the thermogram obtained.

The solid state ^{13}C-NMR was used to confirm the presence of functional groups on MCM-41 and silica gel.

3.3.6 Adsorption study with batch method

The effect of various parameters on the extraction efficiency was investigated. The ionic strength of all solutions was controlled using 0.01 M $NaNO_3$. Ten milligrams of adsorbent were used in the extraction of mercury ions in 5 mL solution. All experiments were performed in triplicate.

3.3.6.1 Effect of mercury (II) ions solution pH

The effect of mercury (II) ions solution pH was investigated by monitoring percentages of mercury (II) ions sorption at different initial pH values. Ten milligrams of adsorbent (MCM-41-L or SG-L) was placed in a test tube, then 5.0 mL of pH adjusted mercury (II) solution (20 mg L^{-1} for SG-L, 100 mg L^{-1} for MCM-41-L) was added. The mixture was stirred for 30 minutes at 600 rpm and the solid was separated. The concentration of mercury (II) ions was determined using CVAAS.

3.3.6.2 Effect of extraction time

The influent of the contact time on the adsorption efficiency and adsorption kinetics were evaluated. The mercury (II) ions solutions (20 mg L^{-1} for SG-L, 100 mg L^{-1} for MCM-41-L) were prepared at the optimum pH for adsorption. The stirring time used was 2.5, 5, 10, 20, 30, 40, 50 or 60 minutes for both adsorbents. The concentration of mercury (II) ions was determined using CVAAS.

3.3.6.3 Effect of ionic strength

The various concentration of $NaNO_3$ was used in order to study the effect of ionic strength on the sorption efficiency. Mercury (II) ions solutions containing 0, 0.01, 0.1, 0.5, 1.0 or 1.5 M $NaNO_3$ were prepared at optimum pH. A 10 mg of adsorbent was placed in a test tube, then 5.0 mL of mercury (II) ions solution was added into the test tube. The mixture was stirred for 30 minutes at 600 rpm and the solid was separated. The concentration of mercury (II) ions was determined using CVAAS.

3.3.6.4 Effect of coexisting ions

The effect of coexisting ions was examined by adding the common salt usually found in natural water and some of heavy metals into mercury (II) ions solutions. The selected ions were individually mixed with mercury (II) ions in solution and the mercury (II) extraction efficiency of modified adsorbents was evaluated in the presence of the coexisting ions. The following solutions were prepared and investigated;

- The mercury (II) ions solutions containing nitrate salt of Na^{+}, K^{+}, Mg^{2+} or Ca^{2+} in concentration of 0.1 and 1.0 M

- The mercury (II) ions solutions containing sodium salt of NO_3^{-}, SO_4^{2-} or Cl^{-} in concentration of 0.1 and 1.0 M

- The mercury (II) ions solutions containing nitrate salt of Ni^{2+}, Cd^{2+} or Co^{2+} in concentration of 0.01, 0.05, 0.10 and 0.50 mM

3.3.6.5 Adsorption isotherms

The concentration of mercury (II) ions in solutions (5 mL) was varied when used adsorbent in fixed amount (10 mg). The experiments were carried out at concentration of mercury (II) ions in the range of 100 to 800 mg L^{-1} (pH 3.0). The extraction condition was 30 minutes of stirring time. The supernatant was separated and properly diluted before determination by CVAAS.

3.3.7 Development of an automated system for online preconcentration

An automated sample preconcentration and cold vapor introduction to atomic absorption spectrometer (AAS) was developed. The SG-NH-L was applied for the extraction and preconcentration of the mercury (II) ions in the preconcentration column. Two different systems were setup. The first setup was the simple system which preconcentrated the mercury (II) ions from aqueous sample, then converted the preconcentrated mercury (II) ions to elemental mercury and introduced to AAS (Topic 3.3.7.1). In the second setup (Topic 3.3.7.2), the gold plated filament [54] was added into the setup to improve sensitivity.

3.3.7.1 The SG-NH-L mercury preconcentrator (SG-PT)

The syringe pump equipped with 8-ports (1/4”-28 connector type) selection valve was used for the solution delivery. The syringe pump stored the input command in its own memory and was sequentially operated by the input signal from FIAS-400 (AAS system). The syringe pump was not only operated by the input signal, it also sent the output signal to an in-house made microcontroller and circuits for all four 3-ways solenoid valves operation and powering the gold plated filament in the second setup (Topic 3.3.7.2). The common port of selection valve was connected with syringe allow the syringe connected to any other ports. The port number 1 to number 8 (A to H, Scheme 3.3) of selection valve was connected to waste, Milli-Q water, preconcentration column, cleaning line, air, eluent, sample and acid carrier, respectively. The cold vapor generation chamber was a custom made glass material with syringe-like shape (1.5 cm i.d., 5.0 cm long). The preconcentration column was made by PTFE tube (2.5 cm, 6.4 mm o.d., 4.8 mm i.d.) containing SG-NH-L that were held in place by custom-cut Teflon frits (P/N 57185, Supelco) and two PTFE adapters (6.4 mm and 1/4"-28 screw thread, B0196857; Perkin-Elmer). The silicone bung was drilled to make the airtight holes for the PTFE tubes and seal the chamber. One channel of peristaltic pump from FIAS-400 was used as the reducing agent deliverer. The 3-ways solenoid valves were used to switch the solution or gas from each port of normally open or normally close to the common port by powering and non-powering. The soda lime was used to trap the moisture and acid fumes produced during reducing step [55]. This trapping column was made from a 9 cm PTFE tube (6.4 mm o.d., 4.8 mm i.d.) containing granules of soda lime that were held in place by two PTFE adapters (6.4 mm and 1/4"-28 screw thread, B0196857; Perkin-Elmer). All lines were made of flexible PTFE tubing (1/16” o.d., 0.79 mm i.d. or 1/8” o.d., 1.59 mm i.d.). The system communication and operation is illustrated in scheme 3.4

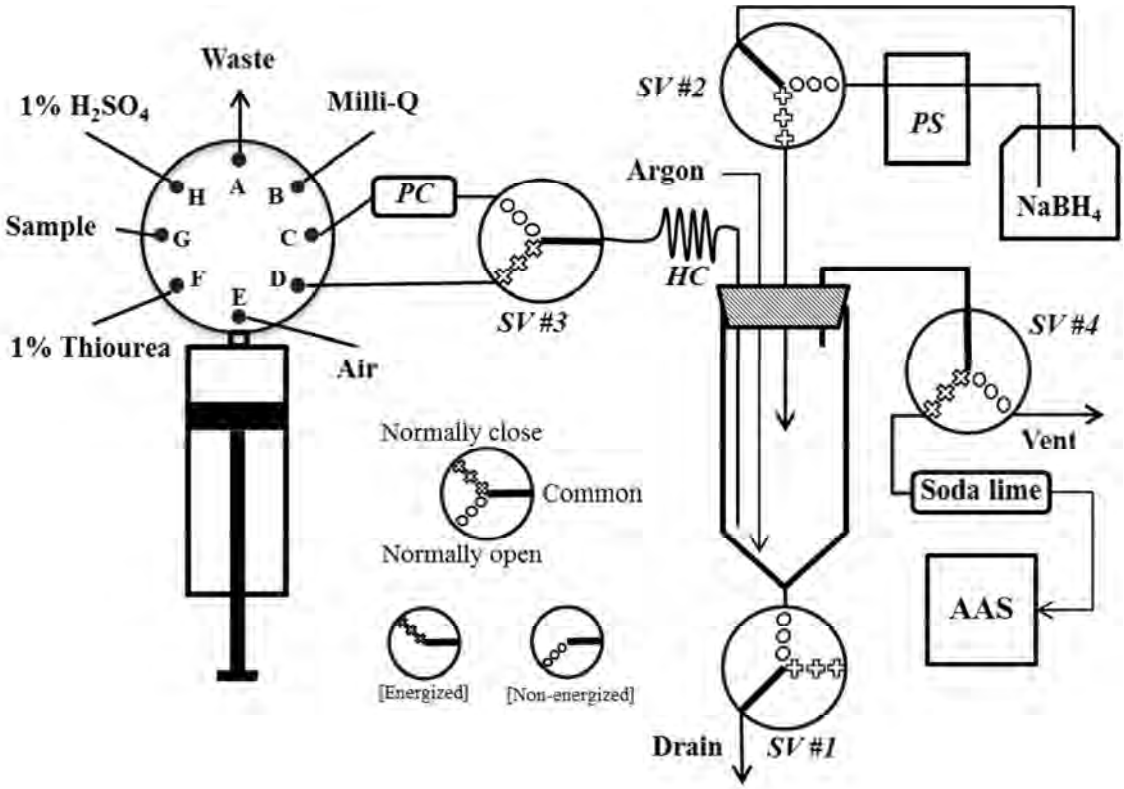

Scheme 3.3 The automated sample preconcentration and cold vapor introduction to atomic absorption spectrometer, SG-PT. (PC = preconcentration column, HC = holding coil, PS = peristaltic pump, SV = solenoid valve)

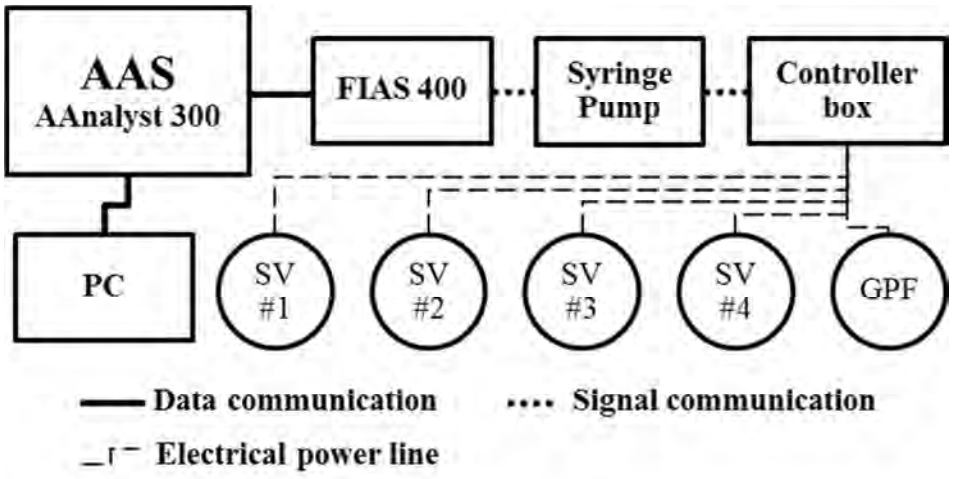

Scheme 3.4 System communication and operation diagram (Controller box contains in-house programmed microcontroller and circuits, PC = personal computer, SV = 3-ways solenoid valve, GPF = gold plated filament).

The in-house made microcontroller and circuits was developed. The 8-bits PIC microcontroller (16F648A, Microchip) was used to control the operation of solenoid valves (SV #1 - #4) and gold-plated filament. The control circuits are presented in scheme 3.5. The microcontroller had two ports (port A and B) with 8 pins each. One pin of port A was used as input pin which picked up the signal from syringe pump. The output of microcontroller was performed by 5 pins of port B. The circuit indicates that pin 0 to 4 of port B sent individually the output signal to each solid state relay (LH1540, Siemens) connected to each solenoid valve (SV) or mechanical relay. The solenoid valve was connected directly to power source (+12 VDC) and solid state relay. In the second setup which was equipped with gold-plated filament, the powering of gold-plated filament was controlled by a mechanical relay to avoid some current leak to the filament. The program for microcontroller was written by C programing language via PIC-C compiler software. And the PIC16F648A was programed by MPLAB IDE software (V8.56, Microchip).

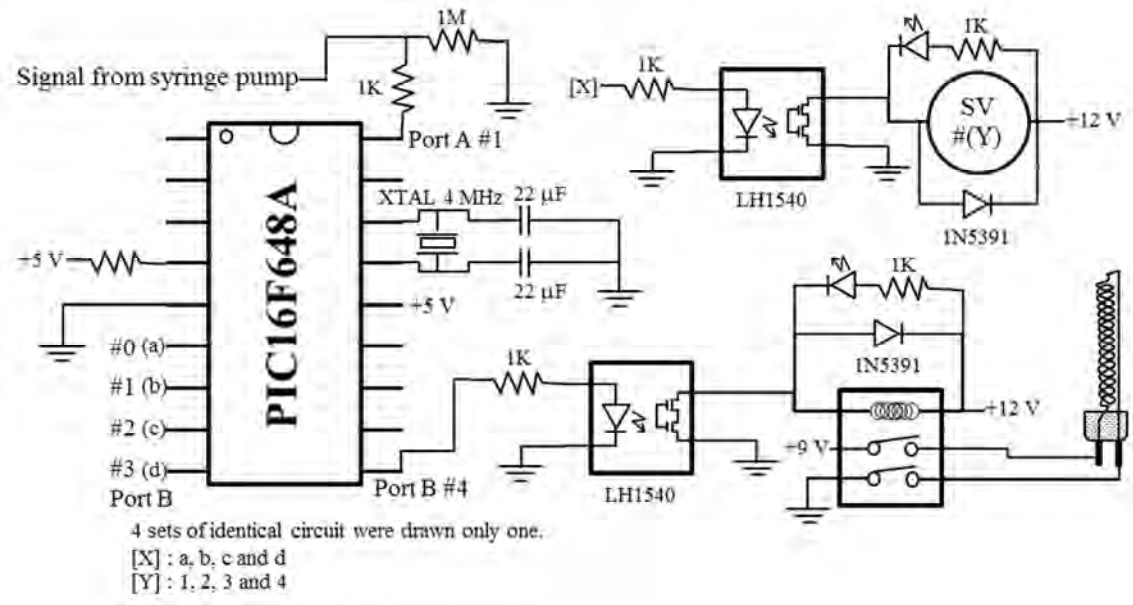

Scheme 3.5 Microcontroller and control circuits.

For the SG-PT (Scheme 3.3), the reducing chamber was connected to 3-ways solenoid valve (SV #1, P/N 003-0636-900, http://www.parker.com) through a normally open port (N.O.) which allowed the solution in chamber to drain through

a common port (COM). The solution could be held in the chamber by applying an electric current to SV #1. The PTFE holding coil (HC), argon gas, reductant and mercury gas lines were put through the drilled silicone bung on top of the chamber for their propose. The filling of reductant was conducted by peristaltic pump and SV #2 (P/N 225T031, http://www.nresearch.com), the peristaltic pump drove the reductant to the chamber via the common port through normally close port of powered SV #2 in the filling step. The SV #3 (P/N 01540-11, http://www.coleparmer.com) was used to switch between preconcentration column and cleaning line connected to the holding coil. The holding coil was made from a 25 cm PTFE tube (1/8" o.d., 1.59 mm i.d.) which sufficiently held the eluted solution inside. The converted mercury gas was transferred to AAS by the argon carrier gas. The argon flow rate was controlled by argon flow controller in FIAS-400. The SV #4 (P/N 225T031, http://www.nresearch.com) was used to vent the gas stream from reducing chamber or let the stream flow through the AAS for detection. A non-powered SV #4 allowed stream to flow from the chamber through a common port and vent via a normally open port, on the other hand, the powered SV #4 allowed the stream to flow through soda lime column and enter to AAS. The operating procedures are described in Table 3.3.

Table 3.3 Operation procedures of the SG-PT system

The operations of solenoid valve (SV) are represented by 0 and 1. The energized and non-energized solenoid valve is indicated by 1 and 0, respectively.

Procedures	**SV #1**	**SV #2**	**SV #3**	**SV #4**
Conditioning of the preconcentration column with Milli-Q water				
- (a) The Milli-Q water (10.00 mL) was aspirated into the syringe through port B at a flow rate of 10.0 mL min^{-1}.	0	0	0	0

- (b) The selection valve was switched to port C then the syringe was emptied at a flow rate of 10.0 mL min^{-1}. The milli-Q water was passed through the column and drained through SV #1.	0	0	0	0
Sample loading step				
Rinse the syringe - (c) The selection valve was rotated to port G then the syringe was filled with the sample. The syringe was emptied to waste via port A at a flow rate of 10.0 mL min^{-1}.	0	0	0	0
Load the sample - (d) The syringe was again filled with sample (10.00 mL) at a flow rate of 10.0 mL min^{-1} - (e) The selection valve was rotated to port C then the sample in the syringe was passed through the preconcentration column **at designed flow rate.**	0	0	0	0
Wash the column - (f) The Milli-Q water (1.00 mL) was aspirated into the syringe then dispensed to the column via port C at same flow rate as sample loading (e) and drained through SV #1.	0	0	0	0
Elution step				
Clean the holding coil and reducing chamber - (g) The syringe was filled with Milli-Q water (5.00 mL) through port B then the syringe was emptied via port D at a flow rate of 10.0 mL min^{-1}.	1	0	1	0
- (h) The air (2.00 mL) was aspirated into the syringe from port E, then flushed the holding coil with air at a flow rate of 10.0 mL min^{-1} and drained through SV #1.	0	0	1	0

- (i) The syringe was rinsed with eluent (1% Thiourea, 0.50 mL) by aspirated the eluent via port F then emptied the syringe to waste (port A) at a flow rate of 5.0 mL min^{-1}.	0	0	0	0
- (j) The eluent (0.50 mL) was again filled into the syringe at a flow rate of 5.0 mL min^{-1}.	0	0	0	0
- (k) The sorbed mercury (II) ions in the preconcentration column were eluted in the holding coil at a flow rate of 1.0 mL min^{-1}.	0	0	0	0
- (l) The acid solution (1% H_2SO_4, 0.25 mL) was aspirated in to the syringe at a flow rate of 5.0 mL min^{-1}. Then the acid solution was passed through the preconcentration column at a flow rate of 1.0 mL min^{-1} and retained in the holding coil along with the eluted mercury.	0	0	0	0
Analyzing step				
Fill the reducing agent in the reducing chamber - (m) The peristaltic pump was operated then the SV #1 and SV #2 were energized to allow reducing agent (5% $NaBH_4$, ~ 0.5 mL) to fill into the chamber.	1	1	0	0
- (n) The SV #4 was powered to allow the flow stream from the reducing chamber through AAS.	1	0	0	1
- (o) The syringe pump was filled with the air (1.50 mL) then the SV #3 was energized. The solution in the holding coil was flushed into the chamber by the air via port D at a flow rate of 15.0 mL min^{-1} **(The mercury signal was acquired here.)**	1	0	1	1
Cleaning step				
- (p) The mixture in reducing chamber was drained by cutting the SV #1 power off.	0	0	0	0

- (q) The syringe was washed with acid solution by aspirated the acid solution (10.00 mL) into the syringe and then emptied through port A at a flow rate of 10.0 mL min^{-1}.	0	0	0	0
- (r) The Milli-Q water (5.00 mL) and acid solution (5.00 mL) were sequentially aspirated into the syringe. Then the mixture (5.00 mL) was transferred into the chamber via port D at a flow rate of 10.0 mL min^{-1}, meanwhile the SV #1 and SV #3 were energized.	1	0	1	0
- (s) The chamber solution was drained.	0	0	1	0
- (t) Wait for 5 seconds, the syringe was emptied through port D at a flow rate of 10.0 mL min^{-1}.	1	0	1	0
- (u) Wait for 5 seconds, the chamber solution was drained.	0	0	0	0

3.3.7.2 The SG-NH-L mercury preconcentrator coupled with gold-plated filament (SG-PT-GF)

This setup consisted of the same devices and elements as the SG-PT system except the addition of gold-plated filament preconcentration chamber. To make gold plating of Tungsten filament, the glass envelopes of high-power halogen light bulbs (Hikari JCD 250 W @ 130 V) were removed at the base by scoring. The metallic supported filament was removed and non-filament metallic portions were coated with silicone (aquarium sealant) to prevent the gold deposition on the non-heated areas. The filament was then coated with gold by, (a) the filament surface was activated by immersing the filament in 20% H_2O_2 in 0.5 M NaOH for 10 min; (b) the filament was washed thoroughly with DI water; (c) the filament was connected as the (−)ve electrode and a stainless steel wire was connected as the (+)ve electrode and these were dipped into 10 mL of a solution containing 5 g L^{-1} of $KAu(CN)_2$ and 50 g L^{-1} of Na_2EDTA and placed 15 mm apart; (d) 1 VDC was applied for 30 minutes; (e) 3 VDC was applied for 2 hours; (f) the filament was rinsed with dichloromethane to remove the silicone, methanol and DI water, respectively; (g) finally the gold

plated filament was dried at 60 °C before further use. The gold plated filament was inserted into one end caps machined from PTFE with a glass tube (4.2 cm long, 5 mm i.d., 7 mm o.d.) providing the flow enclosure. Each end cap was equipped with 1/4-28 threaded apertures for gas in/out connections through the preconcentration chamber (Scheme 3.6). The lamp base was sealed in place by silicone adhesive and the glass tube was sealed into the PTFE holders with PTFE tape. The filament was electrical connected (9 VDC supplied, 15 s) for mercury desorption.

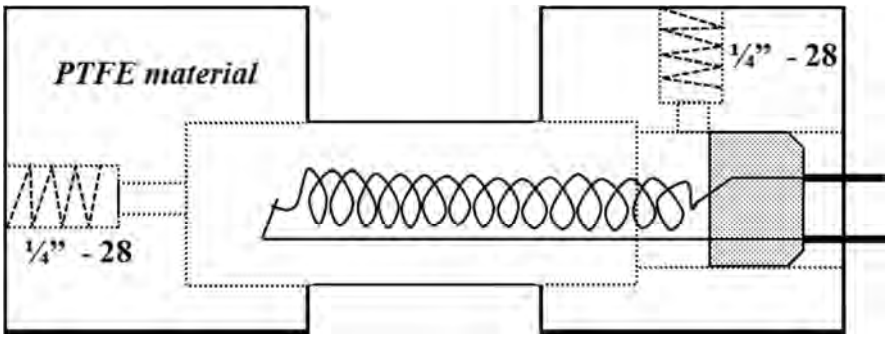

Scheme 3.6 The gold plated filament preconcentration chamber.

The gold plated filament preconcentration chamber was coupled to the setup system (Scheme 3.7). The gold trap chamber (GT) was inserted between reducing chamber and AAS. The mercury re-focusing process was occurred in this part. The mercury vapor from reducing chamber was trapped on the gold surface and then all of trapped mercury was released at almost the same time to reduce the dispersible volume.

In this setup, one more argon source was added. The holding coil was connected directly to the preconcentration column and port D of selection valve was also directly connected to reducing chamber. The SV #1 and SV #2 were operated and functioned in the same way as in the first setup. The soda lime column was connected between SV #3 and SV #4 via normally close port. The common port of SV #3 connected to the reducing chamber allowed the flow from chamber to vent or to enter the SV #4. The flow rate of argon for flushing the gold trap chamber (Argon #2, Scheme 3.7) was controlled by a flow tube meter (FM082-03, AALBORG

instruments). The argon flushing line was connected to SV #4 via a normally open port, which allowed the argon to flow through the gold trap chamber to AAS. The re-focusing step or analyzing step was controlled by SV #4. The heating of gold-plated filament was performed by applying the electric current to the filament via a relay (12 VDC, DS2E-M, Matsushita).

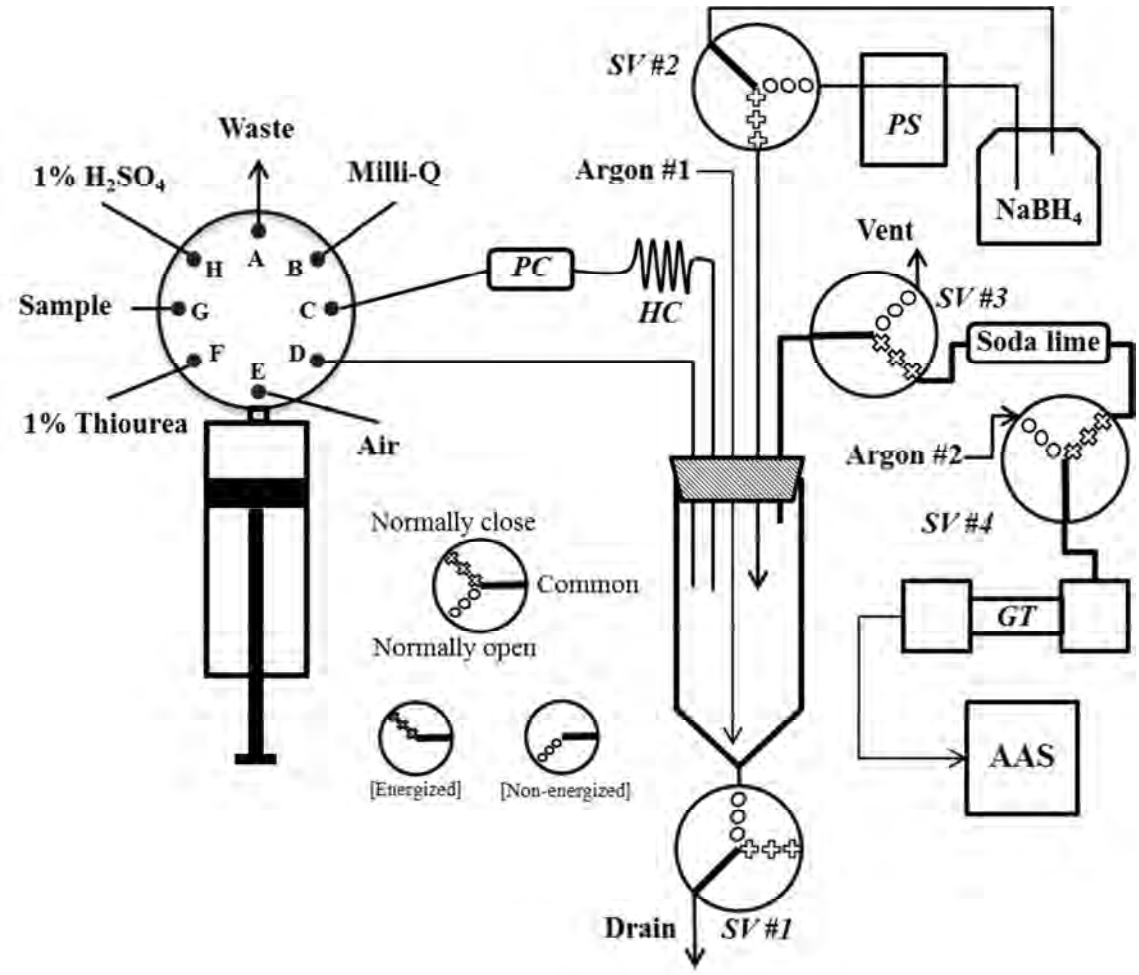

Scheme 3.7 The automated sample preconcentration with gold trap and cold vapor introduction to atomic absorption spectrometer, SG-PT-GF. (PC = preconcentration column, HC = holding coil, PS = peristaltic pump, SV = solenoid valve, GT = gold trap)

The operating procedure of this setup is described in Table 3.4.

Table 3.4 Operation procedures of the SG-PT-GF system

The operations of solenoid valve (SV) are represented by 0 and 1. The energized and non-energized solenoid valve is indicated by 1 and 0, respectively.

Procedures	**SV #1**	**SV #2**	**SV #3**	**SV #4**
Conditioning of the preconcentration column with Milli-Q water				
- (a) The Milli-Q water (10.00 mL) was aspirated into the syringe through port B at a flow rate of 10.0 mL min^{-1}.	0	0	0	0
- (b) The selection valve was switched to port C then the syringe was emptied at a flow rate of 10.0 mL min^{-1}. The milli-Q water was passed through the column and drained through SV #1.	0	0	0	0
Sample loading step				
Rinse the syringe - (c) The selection valve was rotated to port G. Then the syringe was filled with the sample and emptied to waste via port A at a flow rate of 10.0 mL min^{-1}.	0	0	0	0
Load the sample - (d) The syringe was again filled with sample (10.00 mL) at a flow rate of 10.0 mL min^{-1}. - (e) The selection valve was rotated to port C then the sample in the syringe was passed through the preconcentration column **at designed flow rate**.	0	0	0	0
Wash the column - (f) The Milli-Q water (1.00 mL) was aspirated into the syringe, then dispensed to the column via port C at same flow rate as sample loading (e) and drained through SV #1.	0	0	0	0

Elution step				
Empty the holding coil - (g) The air (2.00 mL) was aspirated into the syringe from port E, and then flushed through the holding coil with a flow rate of 10.0 mL min^{-1}.	0	0	0	0
Clean the reducing chamber - (h) The syringe was filled with Milli-Q water (5.00 mL) and then emptied via port A at a flow rate of 10.0 mL min^{-1}.	0	0	0	0
- (i) The syringe was filled with Milli-Q water (5.00 mL) and then emptied via port D at a flow rate of 10.0 mL min^{-1}.	1	0	0	0
- (j) The syringe was rinsed with eluent (1% Thiourea, 0.50 mL) by aspirating the eluent via port F and then emptied to waste (port A) at a flow rate of 5.0 mL min^{-1}.	0	0	0	0
- (k) The eluent (0.50 mL) was again filled into the syringe at a flow rate of 5.0 mL min^{-1}.	0	0	0	0
- (l) The sorbed mercury (II) ions in the preconcentration column were eluted into the holding coil at a flow rate of 1.0 mL min^{-1}.	0	0	0	0
- (m) The acid solution (1% H_2SO_4, 0.25 mL) was aspirated into the syringe at a flow rate of 5.0 mL min^{-1}. And then the acid solution was passed through the preconcentration column at a flow rate of 1.0 mL min^{-1} and retained in the holding coil along with the desorbed mercury ions.	0	0	0	0

Re-focusing step				
Fill the reducing agent in the reducing chamber - (n) The peristaltic pump was operated then the SV #1 and SV #2 were energized to allow reducing agent (5% $NaBH_4$, ~ 0.5 mL) to fill into the chamber.	1	1	0	0
- (o) The SV #3 and SV #4 were powered to allow the flow stream from the reducing chamber to pass through GT. Then the acid solution (2.00 mL) was aspirated into the syringe and then dispensed through the holding coil at a flow rate of 5.0 mL min^{-1}. The desorbed mercury (II) solution in the holding coil was replaced by the acid solution and passed to the reducing chamber. The desorbed mercury (II) was converted to elemental mercury (0) and was transferred to GT by the argon gas (argon #1, 50 mL min^{-1}). Wash the syringe - (p) The syringe was filled with acid solution then emptied via port A at a flow rate of 10.0 mL min^{-1}.	1	0	1	1
Analyzing step				
- (q) The SV #3 and SV #4 were switched off to allow the argon (argon #2) flush the GT to AAS. (**Argon #2 was flow at designed flow rate**.) Meanwhile the mixture was drained through SV #1.	0	0	0	0
- (r) The argon was flushed to AAS for 60 seconds, and then the gold-plated filament was heated by applying the electrical current for 15 seconds. **(The mercury signal was acquired here.)**	0	0	0	0

Cleaning step				
- (s) The Milli-Q water (5.00 mL) and acid solution (5.00 mL) were sequentially aspirated into the syringe. Then the mixture (5.00 mL) was transferred into the chamber at a flow rate of 10.0 mL min^{-1} via port D and retained in the chamber while the SV #1 was energized.	1	0	0	0
- (t) The chamber solution was drained while cut off the power of SV#1.	0	0	0	0
- (u) Wait for 5 seconds, the syringe was emptied through port D at a flow rate of 10.0 mL min^{-1}.	1	0	0	0
- (v) Wait for 5 seconds, the chamber solution was drained.	0	0	0	0

3.3.8 Preconcentration and quantification of mercury (II) ions in sample by SG-PT system

3.3.8.1 Effect of argon flushing flow rate

The effect of argon flushing flow rate was investigated in the flow rate at 50, 100 and 150 mL min^{-1}. The triplicated experiments were conducted by the described procedures with the sample loading flow rate of 7 mL min^{-1}. The mercury solutions (0.50 and 5.00 μg L^{-1}) were selected as the sample for all experiments and the background corrected peak height was recorded.

3.3.8.2 Effect of sample loading flow rate

The sample loading flow rate is an important parameter to be optimized in order to obtain quantitative retention of mercury (II) ions on the adsorbent with a reasonable analysis time. Experiments were performed at the loading flow rate of 3, 5 and 7 mL min^{-1} controlled by the speed of syringe pump. The mercury (II)

solution (0.50 and 5.00 μg L^{-1}) was selected as the sample for all experiments and the background corrected peak height was deliberated.

3.3.8.3 Effect of chloride ions on the extraction efficiency

The effect of chloride ions was examined by adding the chloride ions in the concentration of 10, 100 or 1000 mg L^{-1} to the mercury (II) sample solution. The mercury (II) sample solutions were prepared in the concentration of 1.00 and 4.00 μg L^{-1}. The background corrected peak height was used to study the effect of chloride ions on extraction efficiency.

3.3.8.4 Comparison of the calibration curve obtained from direct determination and preconcentration procedure

The mercury (II) ions calibration solutions were prepared in four sets; 10.00 to 100.00 μg L^{-1} of mercury (II) ions in (a) 1% H_2SO_4 + 1% Thiourea and (b) 1% H_2SO_4 + 1% Thiourea + 10 mg L^{-1} of Cl^- for the direct determination experiments; 0.50 to 5.00 μg L^{-1} in (c) 1% H_2SO_4 and (d) 1% H_2SO_4 + 10 mg L^{-1} of Cl^- for the preconcentration experiments. The sample volume of the preconcentration and direct measurement experiments were 10.00 mL and 0.50 mL, respectively. The preconcentration experiments were carried out at optimum sample loading flow rate. The direct measurement experiments were begun from step (g) in Table 3.3, the eluent was replaced with standard mercury (II) solution and the preconcentration column was also replaced with blank column with no adsorbent.

3.3.8.5 Effect of interfering ions

Au (II), Ag (II) and Pb (II) ions were individually mixed with the mercury (II) ions in solution in order to observe the effect of the coexisting ions on percentage of Hg recovery. The effect of interfering ions was investigated by adding four concentration levels of these ions (10, 25, 50 and 100 μg L^{-1}) in solution containing 1.00 μg L^{-1} or 4.00 μg L^{-1} of mercury (II) ions.

3.3.8.6 Method validation

The method validation was performed by using standard mercury (II) ions at two concentration levels (1.00 μg L^{-1} and 4.00 μg L^{-1}). The analysis was repeated 10 times for each concentration level under the optimized condition. The calibration curve was obtained by analyzing 0, 0.50, 1.00, 2.00, 3.00, 4.00 and 5.00 μg L^{-1} standard mercury (II) ions solutions. Then the sample solution was determined. The accuracy and the precision were presented as percentage of recovery and the percentage of relative standard deviation, respectively. The limit of detection was calculated from the standard deviation of 10 measurements of reagent blank. The robustness of method was examined by repeating these experiments 5 times within 10 days.

3.3.8.7 Real sample analysis

The proposed method was applied to the determination of mercury (II) ions in real water samples: (i) tap water, (ii) natural water and (iii) sea water. All samples were collected with glass bottle then instantly preserved with sulfuric acid (pH < 2). All samples were filtered through a nylon 0.45 μm membrane before use and the samples were analyzed within 7 days after collection.

The accuracy of the proposed method was evaluated by adding 0.10 or 0.40 μg of mercury (II) ions into 100.00 mL of sample solution.

3.3.9 Preconcentration and quantification of mercury (II) ions by SG-PT-GF system

3.3.9.1 Effect of argon flushing flow rate (Argon #2, Scheme 3.7)

The argon flushing flow rate was set at 25, 30, 40 and 50 mL min^{-1}. The triplicated experiments were conducted by the procedures described in Table 3.4. The solution containing 0.50 μg L^{-1} mercury (II) ions was selected as the sample for all experiments and the background corrected peak height was considered.

3.3.9.2 Peak shape signal comparison of SG-PT and SG-PT-GF method

The SG-PT and SG-PT-GF experiments were setup to determine the standard mercury (II) solutions at the same concentration levels (1.00, 3.00 and 5.00 μg L^{-1}). The both methods were operated under their optimum conditions to observe the peaks shape signals. The improvement in analytical sensitivity was considered by the peak shape.

3.3.9.3 Method validation

The system validation was performed by using standard mercury (II) ions at two concentration levels (0.20 μg L^{-1} and 4.00 μg L^{-1}). The analysis was repeated 10 times for each concentration level under the optimized condition. The calibration curve was obtained by analyzing 0, 0.15, 0.50, 1.00, 2.00, 3.00, 4.00 and 5.00 μg L^{-1} mercury (II) ions solutions. Then the sample solution was determined. The accuracy and the precision were presented as percentage of recovery and the percentage of relative standard deviation, respectively. The limit of detection was calculated from the standard deviation of 10 measurements of reagent blank. The robustness of method was examined by repeating these experiments 5 times within 14 days.

3.3.9.4 Analysis of certified reference material

The accuracy of the proposed method was evaluated by determination of mercury (II) ions contained in certified reference materials (HG95-3, HG95-10, National Water Research Institute, Canada) compared to the certified values. The experiment was performed in triplicate.

Part II Preconcentration and determination of atmospheric mercury

3.4 Preconcentration and determination of atmospheric mercury

3.4.1 Fabrication of the DBD mercury detector

Two PTFE spacers (75 mm × 10 mm × 1 mm) were used as gaskets between two standard microscope glass slides (75 mm × 25 mm × 1 mm) to form a 5-mm wide 1-mm deep flow-through channel across the entire length of the slides where the DBD plasma was generated. While the assembly was clamped together, silicone adhesive was applied on all sides except the channel openings. One strip each of aluminum foil (50 mm × 10 mm) was affixed on the exterior of each glass slide with black electrical tape and a flat-headed bolt was attached at the gas entrance end of each Al-foil for facile electrical connection by two small pieces of Neodymium magnets (P/N B222, http://www.kjmegnetics.com). The spacing of the slides was close enough that the oppositely polarized magnet faces hold each other in place. The foils ended 10 mm from the exit of the DBD channel. Disc-shaped end caps/holders were machined from Glass-filled poly(tetrafluoroethylelene) (G-PTFE) for holding the microscope slide discharge assembly. The exit end cap was provided with a threaded axial aperture where a 10 mm diameter fused silica window (P/N NT45-308, http://www.edmundoptics.com) was placed. Experience showed that at high concentrations, mercury may adsorb on this window and this lowers the 254 nm light transmission efficiency dramatically. Therefore, for high concentration experiments, a flat ring-shaped heater (Polyimide Thermofoil®, P/N HK5186R25.0L12B, http://www.minco.com, 12.7 mm o.d., 2.4 mm i.d., 0.3 mm thickness) was placed atop the silica window. The heater was powered at 5 V that was sufficient to maintain the window at 150 °C. The window was held in place by the adhesive-backed heater. The fiber-optic (P600-025-SR, www.oceanoptics.com, 25 cm long, 600 μm core, SMA 905 terminated, numerical aperture 0.22, acceptance angle 25.4° in air), was put in a custom-machined insert. It held the assembly in place and allowed the detector to view the discharge. The exit end cap further contained a 1/4-28 threaded aperture on the circumference for gas exit. The entrance end cap contained a single 1/4-28 threaded aperture for gas entrance. The discharge voltage was provided by a 100× step-up neon sign transformer (P/N 12030P, http://www.franceformer.com) and

changed by adjusting the input voltage by a variable voltage transformer (P/N 3PN1010, http://www.stacoenergy.com).

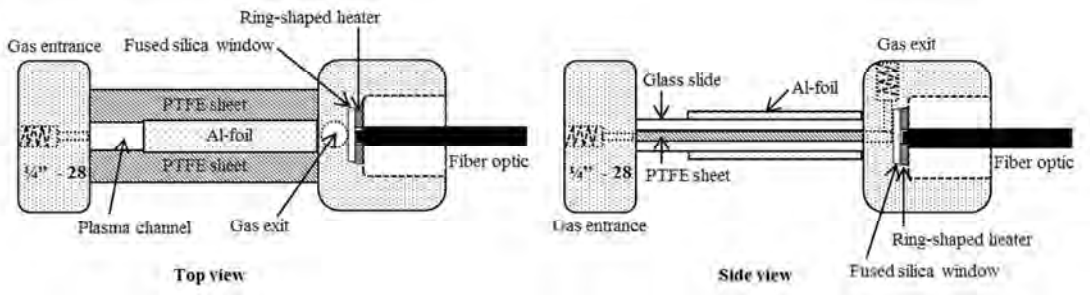

Scheme 3.8 The fabrication of DBD mercury detector.

3.4.2 Mercury calibration source

Elemental mercury was generated from gravimetrically calibrated permeation tubes [56] made in-house from low density polyethylene tubes (80 ± 5 mm × 2.08 mm o.d., 0.51 mm wall thickness). Four separate tubes thus made had average outputs of 12.5 ± 0.9 ng Hg^0 min^{-1} at 70 ± 0.2 °C; the tube used for most experiments had an output of 11.9 ± 0.7 ng min^{-1} over the time it was used. Dilution air was generated by mass flow controllers (Tylan General, Tylan) that were software-controlled by a A/D-D/A card (P/N USB-6009, 14-bit A/D, 12-bit D/A, http://www.ni.com). All mass flow controllers were calibrated by a NIST traceable primary flow calibrator (Gilibrator, http://www.sensidyne.com).

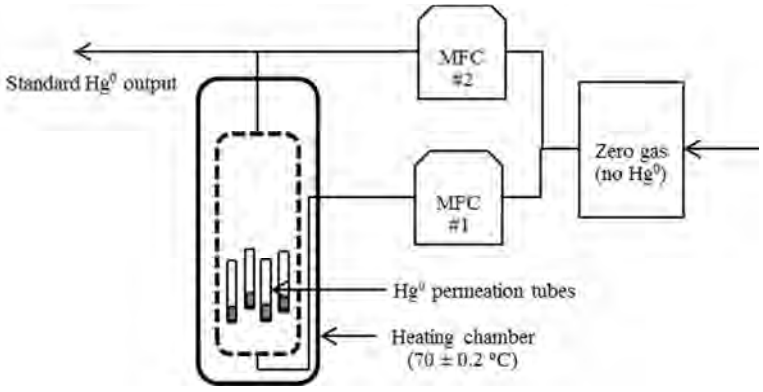

Scheme 3.9 The standard mercury source. (MFC = mass flow controller)

3.4.3 The mercury preconcentrator

Two gold-plated filaments (see Topic 3.3.7.2) were inserted, oppositely oriented, into two end caps machined from G-PTFE with a 40 mm glass tube (10 mm i.d., 12 mm o.d.) providing the flow enclosure. Each end cap was provided with 1/4-28 threaded apertures for gas in/out connections through the preconcentration cell; one end cap has two such apertures (vide infra) and the other just one. The lamp base was sealed in place by hot-melt adhesive and the glass tube was sealed into the G-PTFE holders with PTFE tape. For desorption, 9 V was applied to the filaments in parallel for 15 s via a relay (P/N JW2SN, http://www.digikey.com) actuated through one of the digital outputs.

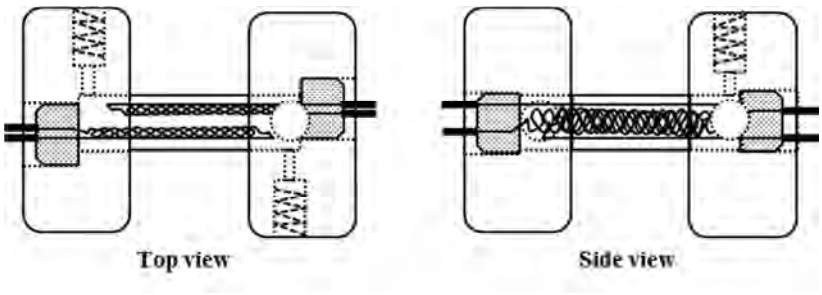

Scheme 3.10 The mercury preconcentrator**.**

3.4.4 General experimental setup

The instrument was setup as shown in scheme 3.11. Three of 3-ways fluorocarbon solenoid valves (SV#1 – SV#3, P/N 648K031, http://www.nresearch.com) configured as indicated. An operation cycle alternates between two modes, the sampling mode and the measurement mode. For the energy efficient operation, the solenoid valves (SV#1 – SV#3) configuration could be changed. The valve-port identities were therefore changed depending on whether the sampling period (t_s) was longer than the measurement period (t_m). The configuration shown in Scheme 3.10 is for $t_s > t_m$. During t_s the valves are not energized; the air sample or standard calibration sample enters through SV#2 which connected with preconcentration chamber, and flows through the preconcentor, through SV#1, through a short cartridge (0.375” o.d., 0.31” i.d., 6 cm long) filled with pelletized

iodized charcoal (P/N 05123, Fluka) to trap any residual mercury (needed only when high calibration concentrations are sampled) and then through the sampling mass flow controller (MFC #1, P/N FC280, Tylan) with the aspiration provided by an air suction pump (AP, P/N DOA-P120-FB, http://www.gastmfg.com). A small flow of argon, ~15 standard cubic centimeters per minute (sccm), is meanwhile maintained by a restrictor from a pressure regulated argon cylinder source through SV#3 into the DBD cell. During the measurement stage, the solenoid valves are energized simultaneously through a MOSFET switch controlled by one of the digital outputs from the multi-function universal serial bus data acquisition (USB-DAQ, P/N USB-1208FS, http://www.mccdaq.com). The sample was gone directly into the iodized charcoal column to maintain constant flow conditions on the standard mercury source, but for the real air sampling situation, the air suction pump was shut off via a relay. An argon flushing flow rate was controlled by MFC #2 (P/N UNIT UFC-1000, 1 SLM, http://www.siemens.com). Argon passed through SV #1, through the preconcentration chamber and through the port connected to SV #3 into the DBD cell and out. After air was completely removed from the preconcentration chamber, the gold-plated filaments were heated to release mercury. The desorbed mercury flowed into the DBD cell and the resulting emission was detected. In the ambient air sampling, a 47 mm PTFE particulate filter (0.5 μm pore size) was used in the sample inlet to remove particulate matter. The sequence of events is shown in table 3.5.

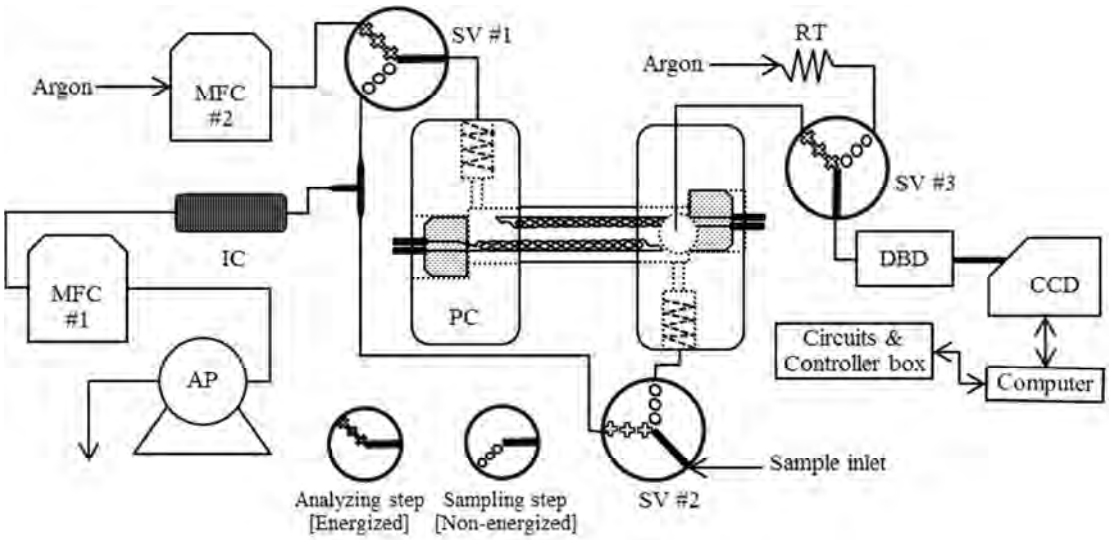

Scheme 3.11 System schematic**.** (AP = air pump, MFC = mass flow controller, IC = iodized charcoal column, SV #1 – SV #3 = solenoid valves (driven together), PC = preconcentration chamber, RT = restriction tube, DBD = dielectric barrier discharge cell, CCD = charge coupled device array spectrometer (other detectors were also used as indicated in text)

Table 3.5 Timing and sequence of the system operation[a]

Step No.	Unit operation	Duration	SV (#1-3)	Air pump	DBD power	DBD Aux flow*	Filaments power	Data acq.
1	Sample loading	Variable, 30 s – 60 min	OFF	ON	OFF	OFF	OFF	OFF
2	Flushing step (argon purge of preconcentrator)	2 min	ON	OFF	OFF	OFF	OFF	OFF
3	Start DBD plasma	2 min	ON	OFF	ON	OFF	OFF	OFF
4	Filaments heating	15 s	ON	OFF	ON	OFF	ON	ON
5	Data acquisition[b]	25 s	ON	OFF	ON	OFF	OFF	ON
6	Cooling step[c]	3 min	ON	OFF	OFF	OFF	OFF	OFF

[a] This sequence assumes a long sampling time – for this purpose DBD plasma power is turned off. *Auxiliary Ar flow is not used. Plasma power is turned on 1 min after flushing starts. For short sampling duration, auxiliary Ar flow remains and plasma power remains on at all times.

[b] Data acquisition starts simultaneously with filament power application.

[c] Cooling time may be longer than 3 min. if ambient temperature is high.

3.4.5 Effect of the plasma potential and plasma gas flow rate

The plasma potential and plasma gas flow rate were studied in the range of 0 to 8.0 kV and 88 sccm to 439 sccm, respectively. In order to evaluate the DBD detection performance, the instrument was setup as scheme 3.12. The constant concentration of Hg^0 (94 ng L^{-1}) was produced by the standard source at the flow rate of 597 sccm, two of 3-ways solenoid valves were used to switch between pure argon and standard Hg^0 to flow through the DBD cell. The MFC#4 and air suction pump were used to control the flow stream through DBD cell. The emission spectrum of standard Hg^0 and pure argon plasma were recorded by CCD spectrometer (P/N QE65000, Ocean Optics, http://www.oceanoptics.com). The signal to noise (S/N) ratio of individually conditions were calculated from the obtained data points at 253.7 nm (60 seconds continuous sampling, 10 Hz). The responses of the detector at various concentration of mercury and plasma flow rate were also investigated.

The concentration of standard Hg^0 was varied by the flow ratio of MFC#1 (fixed at 50 sccm) and MFC#2 (variable flow rate).

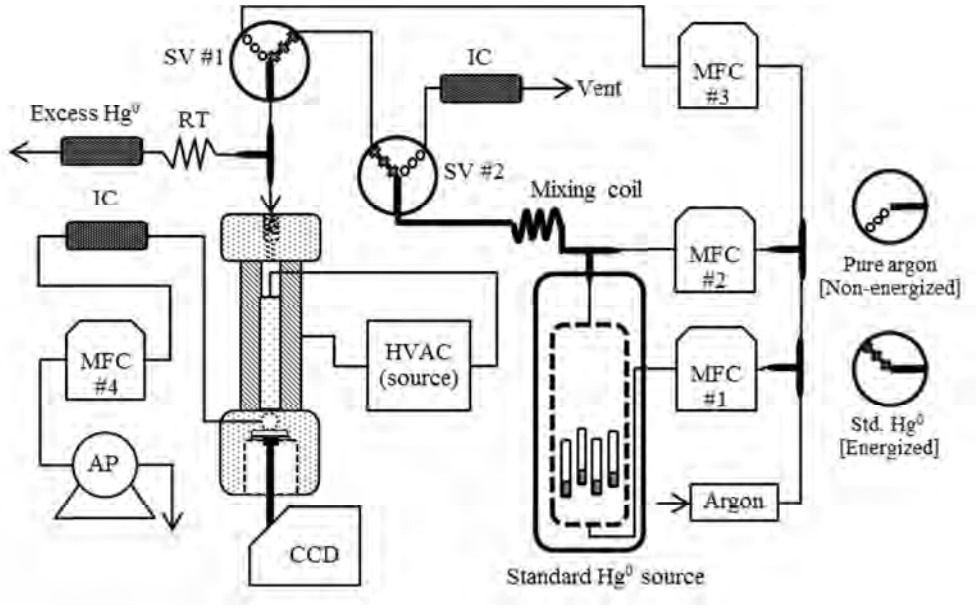

Scheme 3.12 System schematic in studying of the detection part**.** (AP = air pump, MFC = mass flow controller, IC = iodized charcoal column, SV#1 and SV#2 = solenoid valves (driven together), HVAC = high voltage alternative current, RT = restriction tube, CCD = charge coupled device array spectrometer.

3.4.6 Sensitivity comparison of different detectors

The several types of detectors were tested to compare their performance for the proposed. Three CCD-array detectors (P/N USB2000 and QE65000, http://www.oceanoptics.com and P/N C9404CA, http://www.hamamatsu.com) were equipped with their own monochromators and connected via optical fibers. Other detectors used were a head-on phototube (P/N R6800U-01) and photomultiplier tubes (P/N R7400U-09, H5784-06) all from http://www.hamamatsu.com; these were used with a modified end cap that allowed the placement of a narrow bandpass (half bandwidth 12 nm) high transmittance (> 65%) interference filter centered at 254 nm (P/N Hg01-254-25, MaxLamp^{TM}, http://www.semrock.com) ahead of the head-on

phototube and photomultiplier tubes. The arrangement is shown in scheme 3.13. The experiments were performed at the optimum conditions.

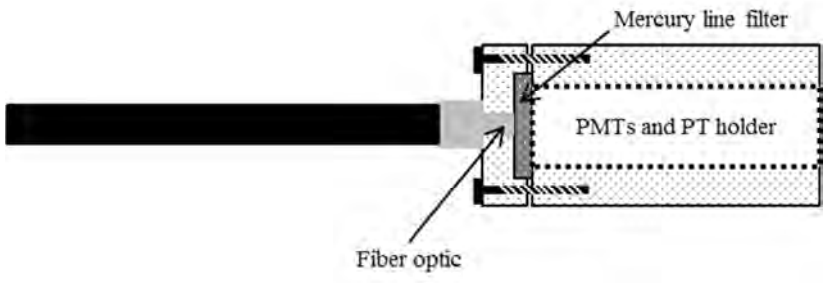

Scheme 3.13 The arrangement for phototube (PT) and photomultiplier tubes (PMTs) detection.

3.4.7 Effect of argon flushing flow rate during desorption step

The effect of argon flushing flow rate was investigated in the flow rate ranged of 90 to 440 sccm. The argon flushing flow rate was controlled by MFC#2 (scheme 3.11). The experiments were conducted by the following condition; standard Hg^0 concentration of 0.73 ng L^{-1}, sampling rate of 4.0 standard liters per minute (SLM) and sampling time of 60 seconds. The emission signals were recorded by the QE65000 CCD spectrometer.

3.4.8 Effect of sampling rate during preconcentration

The influence of the sampling flow rate on the sensitivity was studied in the ranged of 0.88 to 6.14 SLM. The sampling flow rate was controlled by MFC #1 (scheme 3.12). The experiments were conducted by the following condition; standard Hg^0 concentration of 0.64 ng L^{-1} and the sampling time of 30 seconds. The emission signals were recorded by the QE65000 CCD spectrometer.

3.4.9 Repeatability and limit of detection

The system was continuously operated over 7 days period to investigate the repeatability and stability of the system. A total of 19 calibrations were repeated with the following condition; standard Hg^0 calibration concentration of 0 to 6.6 ng L^{-1},

sampling flow rate of 0.88 SLM and sampling time of 120 seconds. The emission signals were recorded by the C9404CA CCD spectrometer.

3.4.10 Field application

The instrument was used to monitor the concentration of the gas phase mercury in the fluorescence lamp recycling plant (Environmental Light Recyclers Inc. Fort Worth, TX, USA). In consultation with plant personnel, the instrument was deployed in the plant over a 24 hours period. The experiments were conducted by the following condition; sampling flow rate of 2.64 SLM and sampling time of 30 seconds. The emission signals were recorded by the C9404CA CCD spectrometer.

CHAPTER IV

RESULTS AND DISCUSSIONS

This chapter is divided into two parts; part I: preconcentration and determination of mercury (II) in natural water samples and part II: preconcentration and determination of atmospheric mercury.

Part I Preconcentration and determination of mercury (II) in natural water samples

4.1 Synthesis and characterization of chemically modified MCM-41 and silica gel

4.1.1 Synthesis and characterization of chelating ligand

2-(3-(2-aminoethylthio)propylthio)ethanamine was synthesized through the reaction between Cystamine hydrochloride and 1,3-dibromopropane. The proton of thiol group was deprotonated by basic solvent. The terminal carbons were attached by sulfide groups to form the product, releasing the bromine gas. The synthesis is illustrated in scheme 4.1.

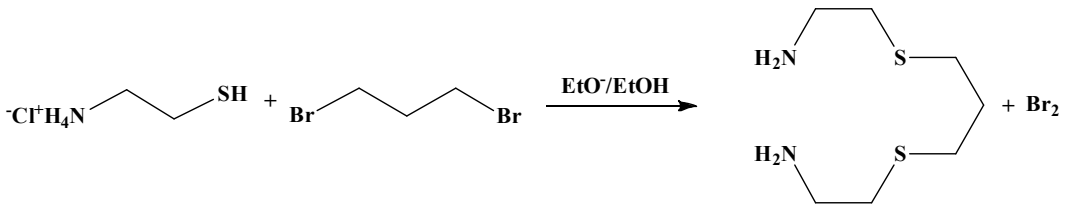

Scheme 4.1 Synthesis of 2-(3-(2-aminoethylthio)propylthio)ethanamine.

The pure product was confirmed by ^{1}H-NMR and ^{13}C-NMR spectrometer. The ^{1}H-NMR spectrum showed the signals of $-CH_2$ at 1.7 ppm (q, 2H), $S-CH_2$ and $S-CH_2-N$ at 2.5 ppm (t, 8H) and $N-CH_2$ at 2.8 ppm (t, 4H). The ^{13}C-NMR spectrum showed the signals of $-CH_2$ at 29.5 ppm, $S-CH_2$ at 30.4 ppm, $S-CH_2-N$ at 36.2 ppm and $N-CH_2$ at 41.2 ppm. The results indicate that the ligand was successfully synthesized.

4.1.2 Synthesis and characterization of modified MCM-41 and silica gel

The MCM-41 and silica gel were chemically modified with 2-(3-(2-amino ethylthio)propylthio)ethanamine following the scheme 4.2 below.

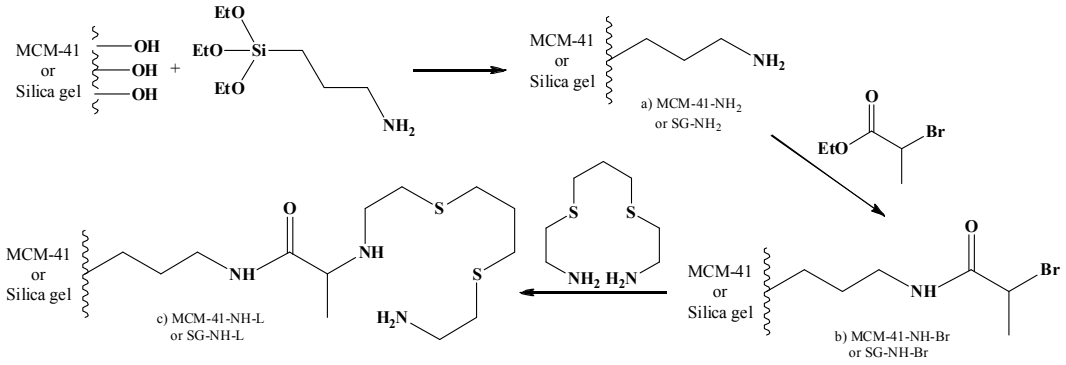

Scheme 4.2 Preparation of modified silica gel and modified MCM-41.

In this work, 2-(3-(2-aminoethylthio)propylthio)ethanamine was chemically modified on the silica gel and MCM-41 surface using 3-aminopropyltrietoxy silane and ethyl-2-bromopropionate as linker. Because the ligand contains sulfur and nitrogen donor atoms, mercury-ligand complex could be obtained. The characterization was performed to confirm that the desired product was successfully synthesized. The chemically modified silica gel and MCM-41 were characterized by XRD, TGA, surface analyzer and solid state ^{13}C-NMR before the sorption study. The results are shown in the following topics.

4.1.2.1 X-ray diffraction spectroscopy

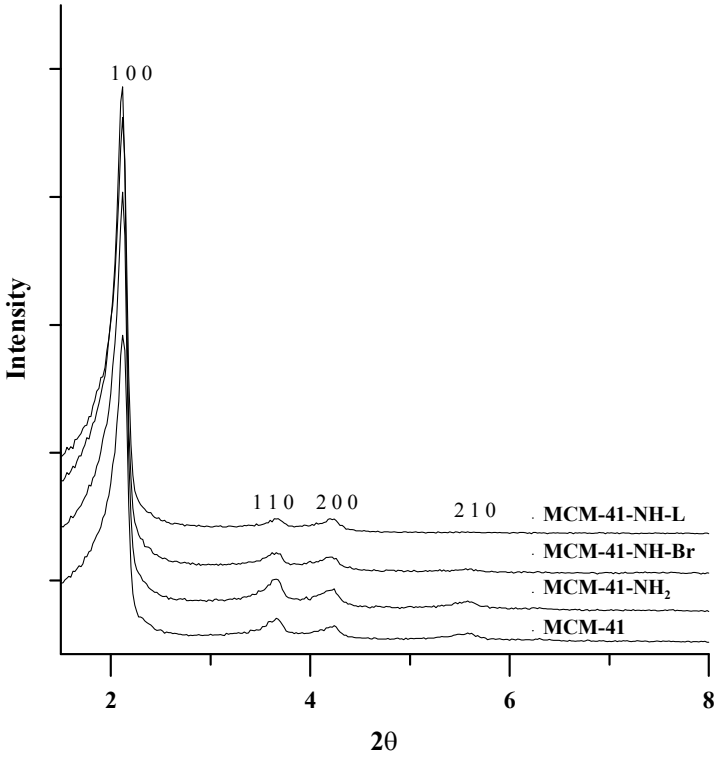

Figure 4.1 XRD pattern of MCM-41, MCM-41-NH_2, MCM-41-NH-Br and MCM-41-NH-L.

The XRD results present a well-resolved pattern at low 2Θ with a very sharp (1 0 0) diffraction peak at 2.12° and three additional higher order peaks (1 1 0, 2 0 0, 2 1 0) with lower intensities at 3.66°, 4.24° and 5.58°, respectively which are characteristic peaks of MCM-41 [52]. The *d*-spacing values for these XRD peaks were 41.65, 24.12, 20.83 and 15.82 Å, respectively. A major change in XRD pattern and *d*-spacing values was not observed after modification. The result indicates that the modification method did not lead to a structural change.

4.1.2.2 Thermogravimetric analysis

Thermogravimetric analysis of silica gel, MCM-41, modified silica gel and modified MCM-41 was performed. The results are shown in Fig 4.2. The TGA and differential TGA (DTGA) profiles indicate a difference in chemical composition of the adsorbents obtained from each step of the modification.

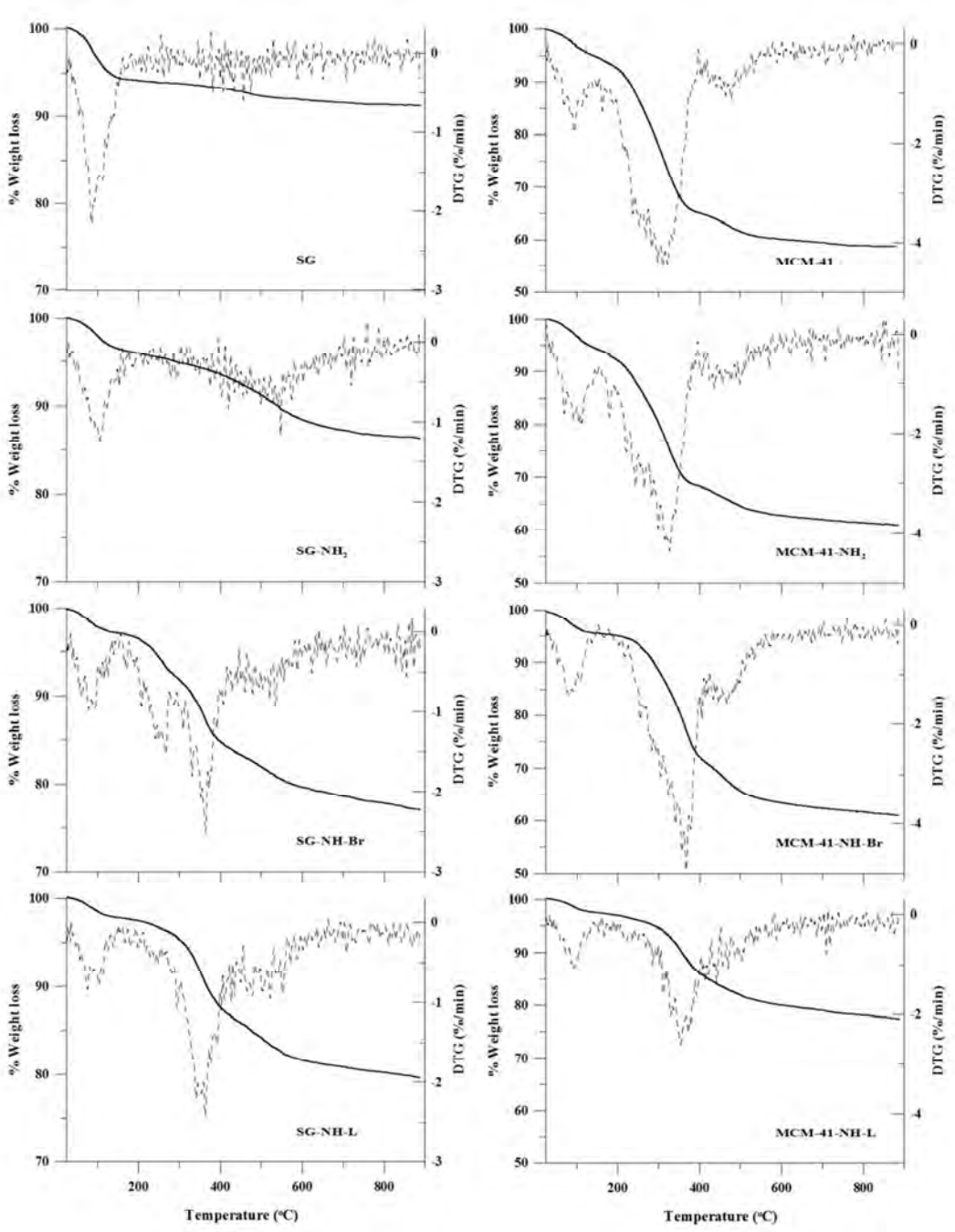

Figure 4.2 TGA and DTAG curves of SG, SG-NH_2, SG-NH-Br, SG-NH-L, MCM-41, MCM-41-NH_2, MCM-41-NH-Br and MCM-41-L.

The loss of moisture was found for both silica gel and MCM-41 at 60 – 150 ^{o}C. In the case of modified silica gels (SG-NH_2, SG-NH-Br and SG-NH-L), the profiles show a weight loss at 350 – 400 ^{o}C which could be attributed to the loss

of aminopropyl groups from the silica gel surface. The profiles of SG-NH-Br and SG-NH-L show a difference in weight loss at 150 – 300 ^{o}C indicating a difference in composition of these adsorbents. The loss of water from the silica surface appeared at 400-850 ^{o}C [57]. Unfortunately, the TGA and DTGA profiles of unmodified and modified MCM-41 were not different. The large weight loss was observed at 200 – 400 ^{o}C in the thermogram of MCM-41 which was believed to be a remaining surfactant in MCM-41 pores. Therefore, the losses of other organic molecules at the same temperature range in further steps were not clearly observed. Then the other techniques are required to confirm the modification of ligand onto the MCM-41 surface. The total organics loading on the surface of silica gel was calculated by equation (4-1) using the difference of weight loss data of silica gel and modified silica gel [58, 59]. The ligand loading on silica gel surface was found to be 0.36 mmol g^{-1} silica gel. On the other hand, the ligand loading on modified MCM-41 surface could not be obtained due to the presence of remaining surfactants on both modified and unmodified MCM-41.

$$Loading\ capacity\ \left(\frac{mmol\ ligand}{gram\ adsorbent}\right) = \frac{Difference\ weight\ loss\ (g)}{M.W.\ of\ organic\ compound \times Adsorbent\ (g)} \quad (4\text{-}1)$$

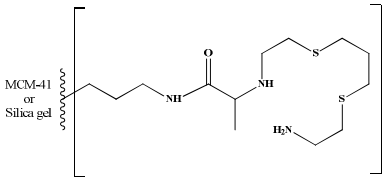

M.W. of organic compound = 307.52 g mol^{-1}

4.1.2.3 Surface area analysis

The surface area, pore volume and average pore size of the modified and unmodified adsorbents were determined and compared. The difference in physical surface properties of modified and unmodified adsorbents was clearly observed as shown in Table 4.1 and Fig 4.3. The modification leads to a reduction in surface area and pore volume. This is probably due to the occupation of the modified molecule on the surface and inside the pores of adsorbents.

Table 4.1 Physical parameters of the adsorbents obtained from by nitrogen adsorption-desorption isotherms

Sample	BET surface area (m^2 g^{-1})	Total pore volume (cm^3 g^{-1})	Average pore diameter (Å)	Pore size range (Å)
SG	515.67	0.69	53.54	20-100
SG-NH-L	201.93	0.30	59.05	20-100
MCM-41	852.60	0.75	35.31	20-40
MCM-41-NH-L	670.15	0.49	29.33	20-35

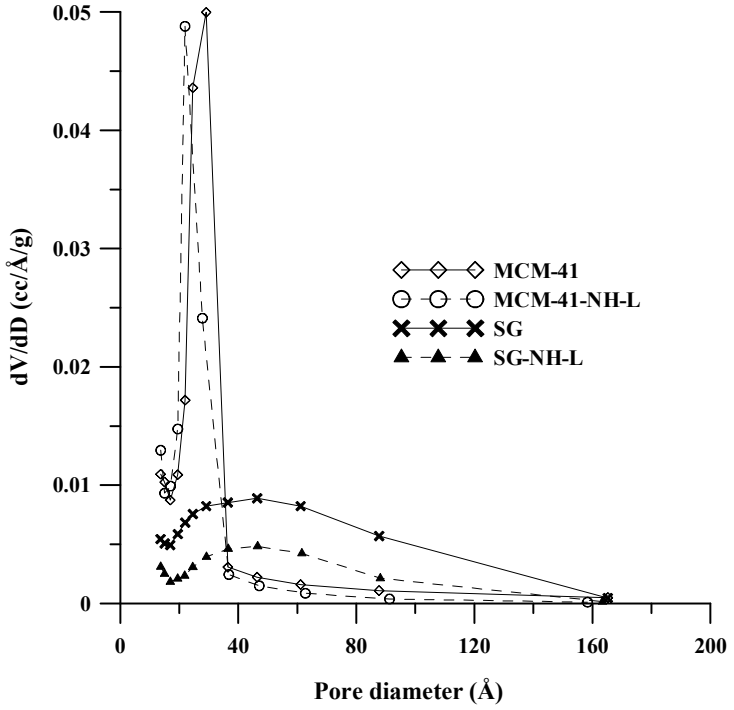

Figure 4.3 Pore size distribution of SG, SG-NH-L, MCM-41 and MCM-41-NH-L.

The results of pore size distribution indicate that the modification method had no effect on silica gel pore size range, while in the case of MCM-41, the reduction of pore size range was observed after modification. This is likely because amorphous silica gel has a wide range of pore sizes, therefore changes in pore size are difficult to observe. On the other hand, MCM-41 has a uniform and a narrow range of pore sizes. When this material is modified, the pore surface was coated with modified organic molecules and a significant change could be observed.

4.1.2.4 Solid state ^{13}C-NMR

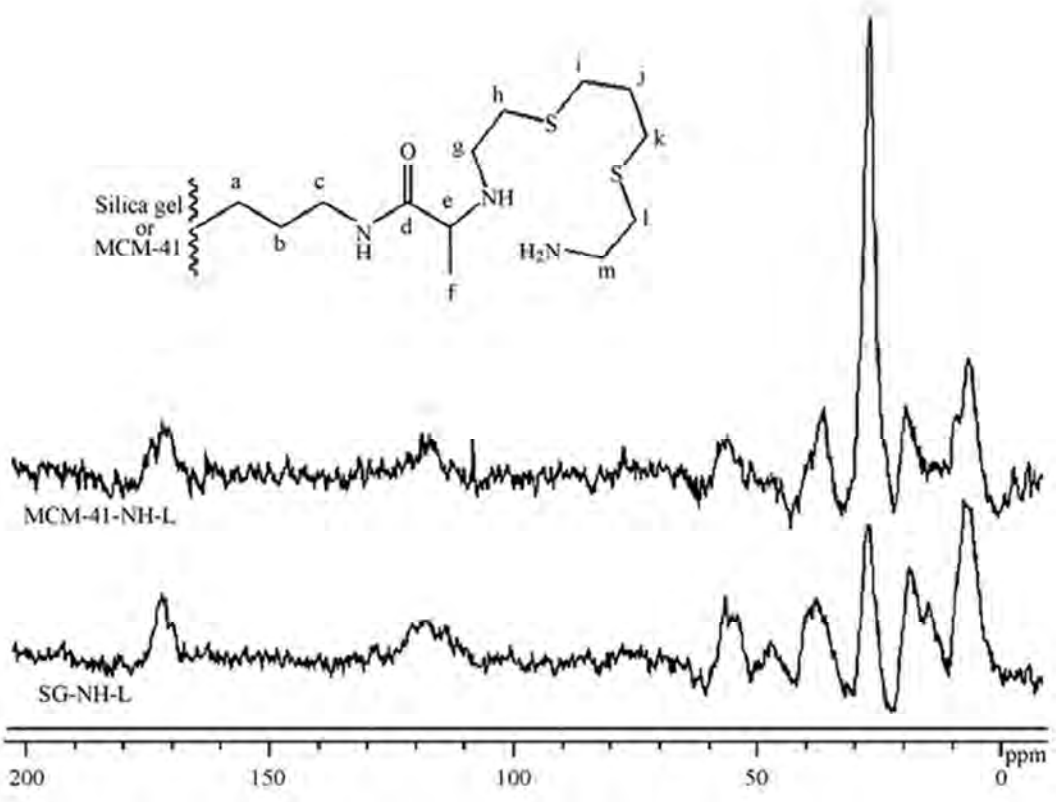

Figure 4.4 ^{13}C MAS NMR spectra of the SG-NH-L and MCM-41-NH-L [60].

The solid state ^{13}C-NMR spectra of SG-NH-L and MCM-41-NH-L are investigated. The methylene groups, labeled (a) and (b), gave signals at 7.3 and 19.1 ppm, respectively. The methylene groups (labeled (c), (g), (m)) and methyl group (labeled (f)) provided the signals at 38.2 ppm. The signals at 172.5 and 119.3 ppm were assigned to the carbonyl and methylene group, labeled (d) and (e), respectively. The six carbon atoms of ligand molecule (labeled (h) to (l)) provided the same signal at 27.5 ppm. The signals at 56.8 and 19.1 ppm belong to the methylene and the terminal methyl group of the remaining ethoxy groups on the silicon of the silylating agent (i.e. tetraethoxysilane), respectively [61]. These results confirm the successful modification of silica gel and MCM-41 with desired molecule. The unmodified silica gel spectra indicate no carbonaceous compound on it. On the

other hand, the signals of the residual surfactant template were observed in the spectrum of unmodified MCM-41 (21.1, 24.6, 28.3, 30.4, 5.17 and 64.9 ppm). Nevertheless, the spectrum of MCM-41-NH-L didn't show these signals except the peak at 27.5 ppm, revealing that some of the template was washed out during modification processes.

4.2 Adsorption study with batch method

4.2.1 Effect of pH of mercuric solutions

The solution pH is one of the major factors that influence the adsorption of metal ions. The protonation on the ligand binding sites may occur in acid solution, and moreover the metal-hydroxide complex or metal precipitation is present in basic solution.

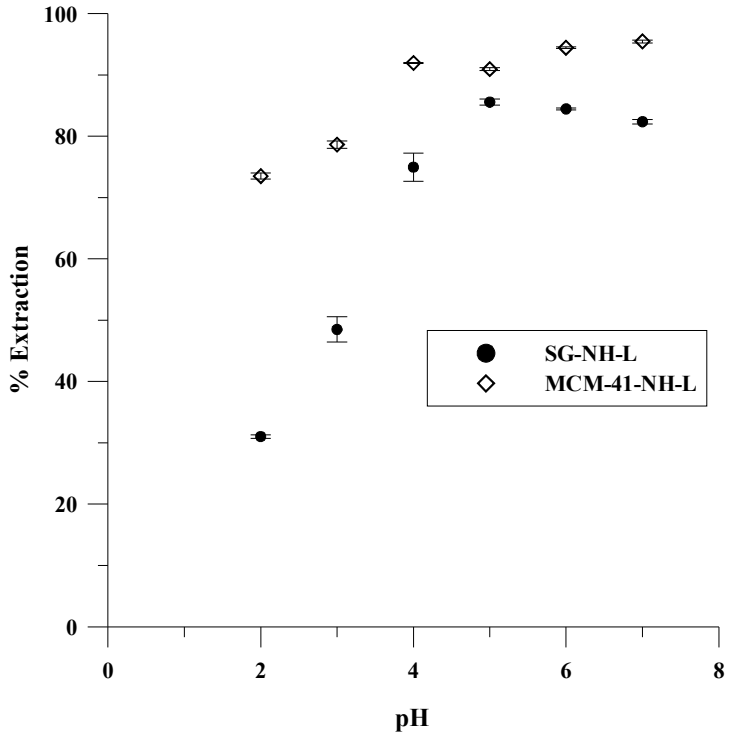

Figure 4.5 Effect of pH on the adsorption of mercury (II) ions by SG-NH-L and MCM-41-NH-L.

In this study, the effect of pH on mercury ion extraction by SG-NH-L and MCM-41-NH-L was investigated. The solution pHs were varied from 2 – 7 to avoid the breaking of Si-O-Si bond on adsorbent surface by hydroxide ion attack. The results of extraction of mercury (II) ions as a function of initial pH are shown in Figure 4.5. It was found that the pH of the solution at equilibrium increased to 7.1 – 7.3 when the initial pH was 4 and higher. The increase of the solution pH after extraction could be explained by the basic properties of ligand and silica surface, which may undergo the hydrolysis in aqueous solution. The results show that the adsorption behavior of adsorbents for mercury (II) ions was strongly affected by the change in pH and similar behavior was observed for SG-NH-L and MCM-41-NH-L. Low extraction efficiencies were observed at low pH values (pH 2 – 3), while the efficiency increased by increasing the pH of the solutions. The optimal pH for mercury (II) ion adsorption ranged from 4 to 7. In this study, the effect of pH on extraction efficiency seems to be related to the protonation of the ligand and the speciation of mercury (II) ions in solution. Theoretically, different species of mercury (II) ions are present in solution depending on the solution pH. At pH values lower than four, the major species of mercury (II) ions are Hg^{2+} cations, while $Hg(OH)_2$ species dominate at pH values higher than four. Moreover, at pH values lower than four, protonation of the amine group on the ligand is expected. The binding ability of the protonated ligand with Hg^{2+} cations is believed to be lower than that of the non-protonated molecule with $Hg(OH)_2$ at pH values higher than four. Thus, a low extraction efficiency of mercury (II) ions by the adsorbents was observed at pH 2 and 3.

Moreover, a higher degree of decrease in adsorption efficiency was observed when used the SG-NH-L, compared to MCM-41-L. Similar results were also observed by Walcarius and Delacote when they used mesoporous amorphous and ordered silica functionalized with thiol groups [38]. Regarding the structure of the adsorbent, when the ligands on mesoporous ordered silica were protonated, these positive charge bearing ligands may act as an electrostatic repulsion barrier to the entering proton [62]. This effect would be less pronounced in amorphous silica

because the positive charge is randomly distributed resulting in less electrostatic repulsion. It was found by Walcarius et al. that total protonation could be achieved with amorphous silica modified with aminopropyl, while lower degrees of protonation were observed with MCM-41 bearing the same functional group [62, 63]. In our study, it is possible that SG-NH-L could be protonated to a higher extent in comparison to MCM-41-NH-L. As a result, the extraction efficiency of SG-NH-L decreased more remarkably than that of MCM-41-NH-L due to the decreased complexation ability of the protonated ligands toward mercury (II) ions as proposed earlier.

4.2.2 Effect of extraction time

The effect of extraction time on the extraction of mercury (II) ions was investigated (Figure 4.6). The rapid adsorption of mercury (II) ions onto SG-NH-L and MCM-41-NH-L were observed. The adsorption reached equilibrium after ca. 5 minutes. And the MCM-41-NH-L showed faster adsorption kinetics than SG-NH-L, it is because the MCM-41-NH-L has a larger surface area than SG-NH-L. Moreover the homogeneity of pore size distriubution of MCM-41-NH-L structure could lead to the faster adsorption kinetics compared to SG-NH-L structure that had various pore sizes. The extraction of 30 minutes was performed for further batch experiments to assure that the adsorption equilibrium was reached.

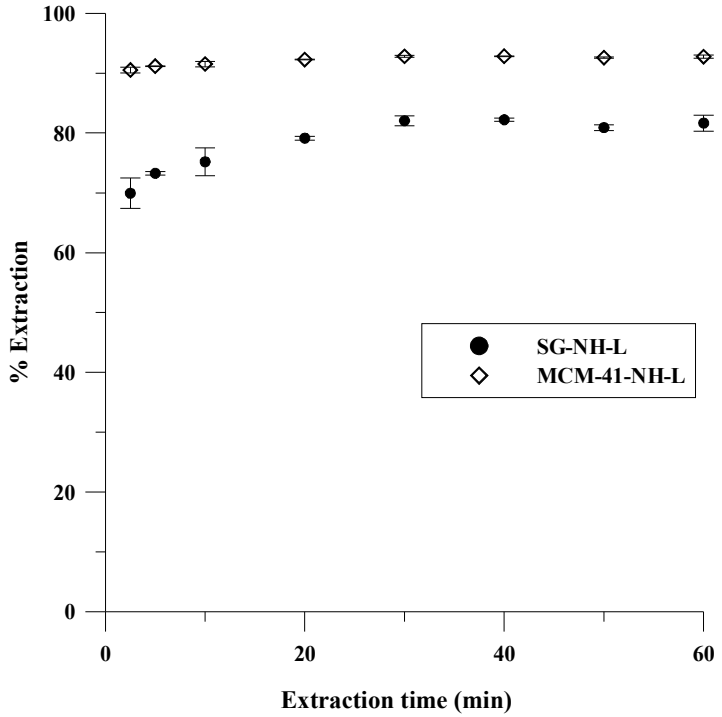

Figure 4.6 Effect of extraction time on the extraction of mercury (II) ions at pH 5 by SG-NH-L and MCM-41-NH-L.

4.2.3 Effect of ionic strength

In general, different ions would be present in water in different concentrations depending on the water source. The adsorption efficiency may be affected by a presence of ions at different concentrations. In this study, the effect of ionic strength on mercury (II) ion adsorption was investigated using $NaNO_3$ (Figure 4.7).

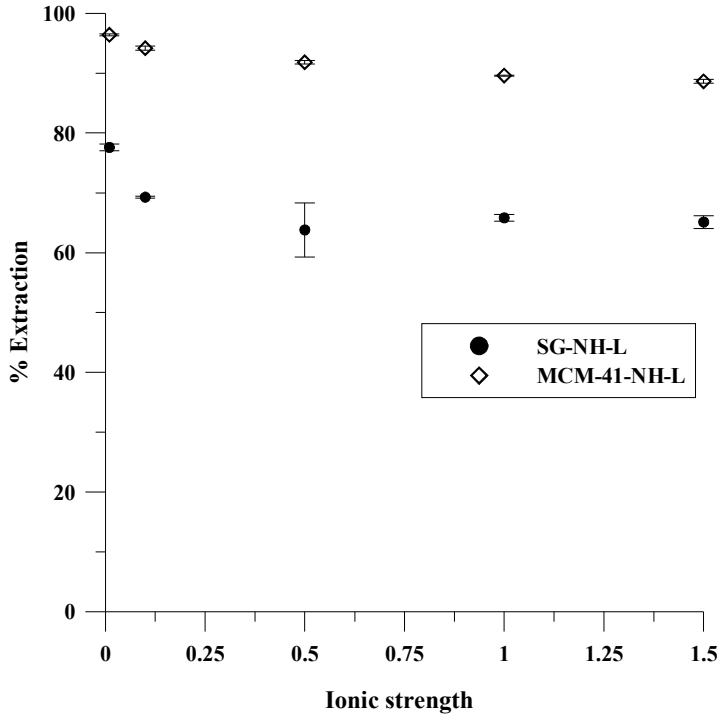

Figure 4.7 Effect of ionic strength on the extraction of mercury (II) ions at pH 5 by SG-NH-L and MCM-41-NH-L.

The slight decrease in extraction efficiency was observed in the both cases (SG-NH-L and MCM-41-NH-L) by increasing the ionic strength from 0.01 to 0.10 at pH 5. The ionic strength seems to have no significant effect on the extraction efficiency at ionic strength higher than 0.5 (using the two-tailed paired t-test at the 95% confidence level). The results indicate the adsorption of mercury (II) ions on the adsorbents occurred via specific complex formation with the modified ligand rather than by ion exchange mechanisms.

4.2.4 Effect of coexisting ions

The presence of coexist ions may influence the adsorption of mercury (II) ions due to: (i) the competition for the adsorption sites between mercury (II) ions and other ions, (ii) the complex formation of mercury (II) ions with certain anions, and (iii) the formation of mercury insoluble compounds (i.e. precipitation). In order to evaluate the

selectivity of adsorbents towards mercury (II) ions, the extraction of mercury (II) ions was carried out in the presence of several cations, anions and heavy metal ions.

4.2.4.1 Cations

The nitrate salts of Na^+, K^+, Mg^{2+} and Ca^{2+} were selected in this experiment in order to investigate the effect of coexisting cations on mercury (II) ions extraction efficiency by both adsorbents. These coexisting cations were studied at two levels of concentration (0.1 and 1.0 M) and the results are shown in Table 4.2.

Table 4.2 Effect of coexisting cations on the extraction of mercury (II) ions by SG-NH-L and MCM-41-NH-L

Salts	**Concentration (M)**	**% Extraction[a]**	
		SG-NH-L	**MCM-41-NH-L**
$NaNO_3$	0.1	81.69 ± 0.40	92.13 ± 0.16
	1.0	75.00 ± 0.83	88.96 ± 0.12
KNO_3	0.1	78.15 ± 0.99	91.87 ± 0.24
	1.0	75.00 ± 0.69	88.58 ± 0.17
$Mg(NO_3)_2$	0.1	77.30 ± 0.77	89.27 ± 0.24
	1.0	74.99 ± 0.63	85.42 ± 0.62
$Ca(NO_3)_2$	0.1	76.29 ± 0.96	88.23 ± 0.30
	1.0	72.63 ± 0.13	86.30 ± 0.14

[a] Mean ± S.D. (n=3)

No significant effect of these cations on extraction of mercury (II) ions onto both modified amorphous silica gel and MCM-41 are observed. This observation indicates that the modified adsorbents are more selective towards mercury (II) ions

over alkaline and alkaline earth metals due to the hard/soft acid/base principle [64]. Considering that the common adsorption mechanism for alkaline and alkaline earth metal ions on the adsorbents may be an ion-exchange, the results show that these co-existing ions did not affect the extraction of mercury (II) by the adsorbents. Therefore the extraction of mercury (II) ions via the complex formation with the ligand on the adsorbents is confirmed.

4.2.4.2 Anions

The effect of anions (NO_3^-, SO_4^{2-} and Cl^-) on mercury (II) ion extraction was studied. The extraction of mercury (II) ions in the presence of these anions was performed and the results are listed in Table 4.3. The mercury (II)-anions complex formation could be occurred in the solution and the formation constants are shown in Table 4.4.

Table 4.3 Effect of coexisting anions on the extraction of mercury (II) ions by SG-NH-L and MCM-41-NH-L

Salts	**Concentration (M)**	**% Extraction[a]**	
		SG-NH-L	**MCM-41-NH-L**
$NaNO_3$	0.1	73.83 ± 1.25	94.03 ± 0.66
	1.0	69.99 ± 0.15	88.88 ± 0.77
Na_2SO_4	0.1	70.45 ± 0.27	90.04 ± 0.97
	1.0	68.76 ± 0.25	89.55 ± 0.40
NaCl	0.1	87.83 ± 1.01	61.45 ± 1.81
	1.0	65.52 ± 1.81	39.22 ± 0.64

[a] Mean ± S.D. (n=3)

The presence of both NO_3^- and SO_4^{2-} in mercury (II) solution did not affect the extraction efficiency significantly. On the other hand, the significant effect on the extraction efficiency was observed when Cl^- was ions present in the solution. Moreover, the Cl^- ion effect seems to be dependent on Cl^- ion concentration and the adsorbents type. A hypothesis to explain these results are proposed by considering of the formation constants. It is possible that the ligand can reduce mercury (II) to mercury (I) ions which would precipitate with Cl^- as Hg_2Cl_2 (K_{sp} = 1.3 x 10^{-18}, [65]). Both mercury-ligand complexation and mercury chloride precipitation are proposed for the extraction of mercury ions in the presence of Cl^- ions. This would result in the high extraction efficiency of SG-NH-L observed in the presence of 0.1 M Cl^-. On the other hand, no precipitation occurred in both cases of other anions, the extraction of mercury was only the result of complexation of mercury species with the ligand on the adsorbent. In order to test this hypothesis, the free ligand solution (in MeOH) was added in the individual solutions containing (i) $HgCl_2$, (ii) Hg^{2+} ions and NaCl and (iii) Hg^{2+} ions and $NaNO_3$ with concentration similar to those used in the extraction experiments. After adding the ligand solution into solution (i) and (ii) which contained Cl^-, a white precipitate was immediately obtained, while no precipitation was observed in the solution (iii) with no Cl^- contained. These results showed that mercury (II) ions can be reduced by the ligand and form the white precipitate as Hg_2Cl_2. Nevertheless, when increased the concentration of Cl^- ions (0.1 to 1.0 M) in solution, decreasing in extraction efficiency was found. It is probably because the different concentration of Cl^- provides a different dominant mercury species in solution. In calculation by using the formation constants (Table 4.4), in 0.1 M NaCl, the dominant species are $HgCl_2$ (41%), $HgCl_3^-$ (29%) and $HgCl_4^{2-}$ (29%) while $HgCl_2$ (1%), $HgCl_3^-$ (9%) and $HgCl_4^{2-}$ (90%) species were found in the 1.0 M NaCl solution. Moreover the standard reduction potential of these mercury species are 0.91, 0.63 and 0.54 V for Hg^{2+}, $HgCl_2$ and $HgCl_4^{2-}$, respectively [66]. Thus, $HgCl_2$ could be reduced more easily than $HgCl_4^{2-}$. Therefore, in solution containing 0.1 M NaCl, it would contain different mercury species that could be reduced by the ligand more easily and then adsorbed on the adsorbent in higher amount, compared to the solution with 1.0 M NaCl which contained mainly $HgCl_4^{2-}$.

The effect of Cl^- on Hg(II) ions extraction was more pronounced in the case of MCM-41-NH-L than in the case of SG-NH-L. It is possible that the restricted access of different species of Hg-Cl complexes through the small and uniform pore size of the MCM-41-NH-L occurred, therefore, the extraction efficiency of mercury (II) ions in the presence of Cl^- was found to be less than those of the other anions.

Table 4.4 Aqueous speciation reactions and equilibrium constants of mercury (II) ions [65, 67]

Reaction	**log *K***
$Hg^{2+} + H_2O \leftrightarrow HgOH^+ + H^+$	-2.70
$Hg^{2+} + 2H_2O \leftrightarrow Hg(OH)_2 + 2H^+$	-6.19
$Hg^{2+} + NO_3^- \leftrightarrow HgNO_3^+$	0.45
$Hg^{2+} + Cl^- \leftrightarrow HgCl^+$	6.74
$Hg^{2+} + 2Cl^- \leftrightarrow HgCl_2$	13.22
$Hg^{2+} + 3Cl^- \leftrightarrow HgCl_3^-$	14.07
$Hg^{2+} + 4Cl^- \leftrightarrow HgCl_4^{2-}$	15.07
$Hg^{2+} + Cl^- + H_2O \leftrightarrow HgClOH + H^+$	3.23
$Hg^{2+} + SO_4^{2-} \leftrightarrow HgSO_4$	1.39
$Hg^{2+} + SO_4^{2-} + 2H_2O \leftrightarrow Hg(OH)_2SO_4^{2-} + 2H^+$	-4.83[a]

[a] Conditional equilibrium constant (log *K*, ionic strength = 0.1) optimized using the Hg(II)-SO_4-quartz and Hg(II)-PO_4-quartz system data.

4.2.4.3 Heavy metal ions

Table 4.5 Effect of coexisting heavy metal ions on the extraction of mercury (II) ions by SG-NH-L and MCM-41-NH-L

Metals	Concentration (mM)	% Extraction[a]	
		SG-NH-L	MCM-41-NH-L
$NaNO_3$ (blank)	0.1 x 10^3	79.20 ± 0.04	87.38 ± 0.10
Ni (II)	0.01	81.39 ± 0.43	-
	0.10	81.46 ± 0.51	-
	0.05	-	87.05 ± 0.51
	0.50	-	86.63 ± 0.26
Cd (II)	0.01	80.01 ± 0.39	-
	0.10	82.01 ± 1.36	-
	0.05	-	85.87 ± 0.31
	0.50[b]	-	-
Co (II)	0.01	79.44 ± 1.26	-
	0.10	79.59 ± 1.15	-
	0.05	-	87.14 ± 0.29
	0.50	-	85.08 ± 0.10

Initial concentration of mercury (II) ions was 0.01 mM for SG-NH-L and 0.05 mM for MCM-41-NH-L.

[a] Mean ± S.D. (n=3)

[b] Cadmium precipitated as cadmium hydroxide.

The effect of heavy metal ions toward the extraction efficiency of mercury (II) ions was studied. The mercury (II) solutions were prepared in two different concentrations. Ni (II), Cd (II) and Co (II) was individually added into those solutions at concentration equal to or 10 times higher than that of mercury (II) ion. All results

are summarized in Table 4.5. It was found that the extraction of mercury (II) ions by the adsorbents was not affected by the presence of these foreign ions. This result shows a high mercury (II) selective property of the both SG-NH-L and MCM-41-NH-L.

4.2.5 Adsorption isotherms

The adsorption behavior of the metal ions on adsorbents surface at equilibrium was usually explained by the adsorption model. Freundlich isotherm and Langmuir isotherm have been widely used to predict adsorption behavior and adsorption capabilities of metals on the solid sorbent.

The Langmuir relation assumes monolayer sorption onto the homogeneous surface with specific number of equivalent sites. The Langmiur equation [30] and the linearized expression are presented in equation 4.2 and 4.3, respectively,

$$N_f = \frac{bN_f^S C}{1+bC} \tag{4.2}$$

$$\frac{C}{N_f} = \frac{C}{N_f^S} + \frac{1}{bN_f^S} \tag{4.3}$$

where N_f is the amount of metal ion adsorbed per gram of adsorbent (mg g^{-1}), C is the equilibrium concentration of the metal ion (mg L^{-1}), $b = K_{eq}/a$ (where a represents the activity of the solute in solution, K_{eq} is the equilibrium constant) and N_f^S is the maximum sorption capacity of the sorbent (mg g^{-1}). The Langmuir constant (b) is related to the bonding energy between the metal ion and the adsorbent.

The Freundlich relation [31] describes multilayer sorption and the adsorption on heterogeneous surface. The relationship can be expressed as:

$$N_f = K_f C^{\frac{1}{n}} \tag{4.4}$$

where N_f is the amount of metal ion added per gram of sorbent (mg g^{-1}), C is the equilibrium concentration of the metal ion (mg L^{-1}), K_f is Freundlich constants and

n is the numerical value of Freundlich constant. The information can be obtained by fitting experimental data to the following linear equation.

$$\log N_f = \log K_f + \frac{1}{n}\log C \tag{4.5}$$

The values of $1/n$ and K_f can be obtained from the slope and the intercept, respectively.

The experiments were carried out at 298 K using a batch method with the studied solutions containing initial concentration of mercury (II) ions ranged from 0.5 to 4.0 mM at pH 3. The results are shown in Fig 4.8 and the Langmuir plots are presented in Fig 4.9.

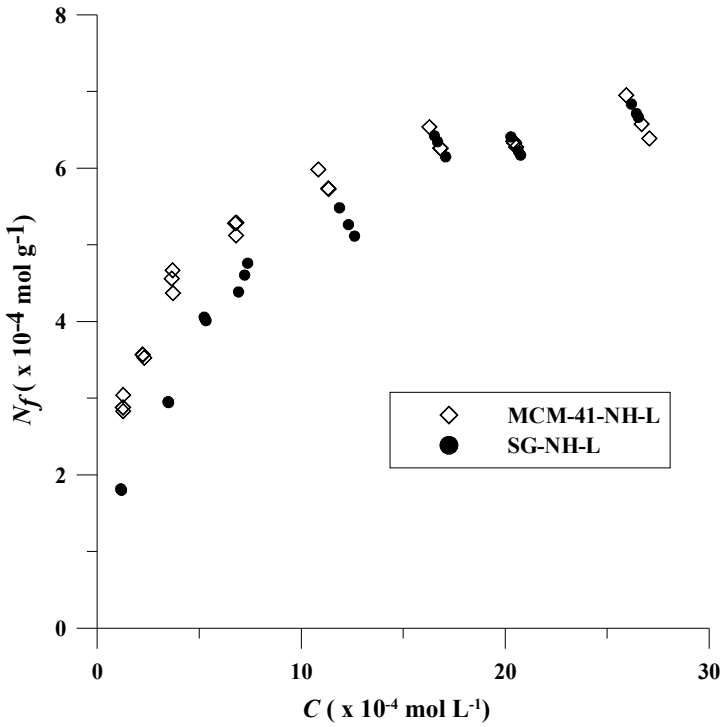

Figure 4.8 Adsorption isotherms of mercury (II) ions onto SG-NH-L and MCM-41-NH-L at 298 ± 0.5 K.

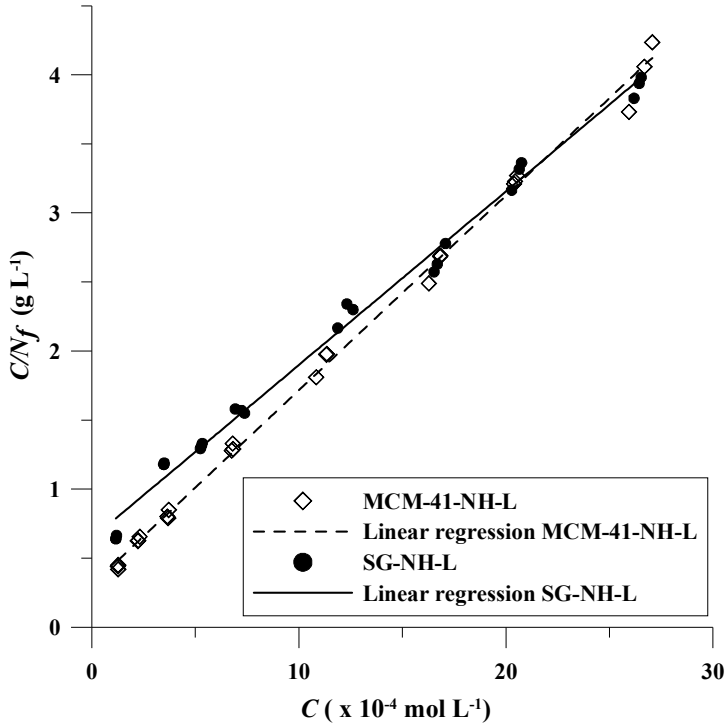

Figure 4.9 Langmuir adsorption model plot of the mercury (II) ions adsorption onto SG-NH-L and MCM-41-NH-L at 298 ± 0.5 K.

The results were well fit to the Langmuir model and provide important thermodynamic adsorption parameters. The slope of the linear model represents a maximum sorption capacity ($N_s^f = \frac{1}{slope}$) and the intercept indicates the equilibrium constant ($K_{eq} = \frac{a}{intercept\ x\ N_f^s}$), high K_{eq} value indicates chemically coordination between metal ion and ligand site on adsorbents surface. Moreover, K_{eq} does not depend on kinetic of metal ion adsorption [68]. The results from SG-NH-L adsorbent seem to be fit with the Freundlich model also. All Langmuir and Freudlich parameters are summarized in Table 4.6.

Table 4.6 Thermodynamic parameters of Langmuir adsorption isotherm at 298 ± 0.5 K

Phases	**Langmuir constants**			**Freundlich constants**		
	N_f^s **(mmol g^{-1})**	***b*** **(L mol^{-1})**	R^2	K_f	N	R^2
SG-NH-L	0.79	1955.7	0.993	9150	4.66	0.986
MCM-41-NH-L	0.70	5263.5	0.998	35843	2.24	0.839

The monolayer coverage of the metal ions on the MCM-41-NH-L occurred with a maximum adsorption capacity of 0.70 mmol g^{-1}. On the other hand, in the case of SG-NH-L, it seems that the concentration of mercury (II) ions used in this study was not sufficient to reach the saturation level of the binding sites on the adsorbent and the concentration is still in the monolayer regime. Therefore, metal adsorption can be described by both isotherm models. However, higher concentration of mercury (II) ions could not be employed in the experiments because of the precipitation of hydroxide species ($Hg(OH)_2$). The maximum adsorption capacity was 0.79 mmol g^{-1} for SG-NH-L. Regarding the maximum adsorption capacity results, the SG-NH-L seems to have more active sites for mercury (II) than MCM-41-NH-L, while MCM-41-NH-L has higher surface area. The lower adsorption capacity of MCM-41 was probably due to the fact that the MCM-41 had some residual surfactant left in the pore from the preparation step as presented in the ^{13}C NMR spectra of unmodified MCM-41. Therefore, the amount of 3-aminopropyltriethoxysilane grafted onto the surface was limited by the number of remaining active sites, resulting in lower ligand loading on the adsorbents. In order to increase the adsorption capacity of modified MCM-41, the removal of residual surfactant was attempted by calcination at 500 ^oC for 3 hours. The calcined MCM-41 (cal-MCM-41) was modified following the method for MCM-41-NH-L and SG-NH-L. Unfortunately, the adsorption capacity of the cal-MCM-41-NH-L (21 mg g^{-1}) was about 2 times lower than adsorption capacity of MCM-41-NH-L (44 mg g^{-1}) under the same experimental condition. It was found that the XRD patterns of cal-MCM-41-NH-L showed less intense characteristic peaks, indicating a change in its original structure after modification. This observation may

explain the lower adsorption capacity. Moreover, the cal-MCM-41 probably lost a silanol group on surface by calcination [69], resulting in a decrease in available site for modification. Thus, another method for removing the surfactant i.e. solvent extraction is suggested.

Furthermore, the adsorption behavior of these adsorbents, which are different in structure, could be differentiated by the *b* values (equation 4.2) observed. MCM-41-NH-L, which has ordered porous structure showed a much larger *b* value than SG-NH-L, which has amorphous structure. This result indicates that MCM-41-NH-L has the ability to adsorb mercury (II) ions from solution better than SG-NH-L. This observation may be explained that the access of mercury (II) ions through uniform mesopore channels of MCM-41 is more favorable than the non-uniform pore channels of the amorphous silica gel. The adsorbents were compared with the other literatures as shown in Table 4.7.

Table 4.7 The maximum adsorption capacity for Hg(II) ions of modified adsorbents from the literature.

Material	**Ligand (method of modification)**	**[a]N_f (mmol g^{-1})**	**Reference**
Hexagonal mesoporous silica	2-Mercaptothiazoline (co-condensation method)	2.34	[58]
Silica gel	2-Mercaptobenzimidazole (Heterogeneous method) (Homogeneous method)	 1.35 1.43	[70]
Sol-gel silica	1,5-Diphenylcarbazide (doping method)	0.029	[71]
Silica gel	Dithizone (grafting method)	0.32	[72]
MCM-41	2-Mercaptopyridine (Heterogeneous method) (Homogeneous method)	 0.09 0.12	[10]
MCM-41	2-Mercaptothiazoline (Heterogeneous method) (Homogeneous method)	 0.25 0.70	[11]
MCM-41 Silica gel	2-(3-(2-Aminoethylthio)propylthio) ethanamine (heterogeneous method)	[b]0.70 [b]0.79	This work

[a]Results from adsorption isotherms at pH 6.

[b]Results from adsorption isotherms at pH 3.

The results from the adsorption study show that both modified MCM-41 and modified silica gel have a good potential in mercury (II) ions extraction. Therefore, the materials were further employed in the preconcentration of mercury (II) ions prior to the determination by cold vapor atomic absorption spectrometer. The automated system for on-line preconcentration was built in the lab.

4.3 Development of an automated system for online preconcentration

In the determination of mercury (II) in water sample by the developed systems, the modified silica gel was used as the solid phase adsorbent in the preconcentration column. The modified MCM-41 was not suitable for the systems because the modified MCM-41 with smaller particle size produced high pressure in the systems.

The automated online preconcentration and cold vapor introduction system for mercury determination was setup in two different systems. The simple system SG-PT (Scheme 4.3), the mercury (II) in water sample was preconcentrated and then converted into cold vapor (Hg^0) before introducing to AAS. The 1% Thiourea in 1% H_2SO_4 was used as the eluent which completely eluted quantitatively the collected mercury (II) from the preconcentration column. A gold surface trapping was added to SG-PT to improve the sensitivity of the system (Scheme 4.4, SG-PT-GF). The cold vapor (Hg^0) was trapped on the gold surface and then released in short period.

4.3.1 Preconcentration and quantification of mercury (II) ions in sample by SG-PT system

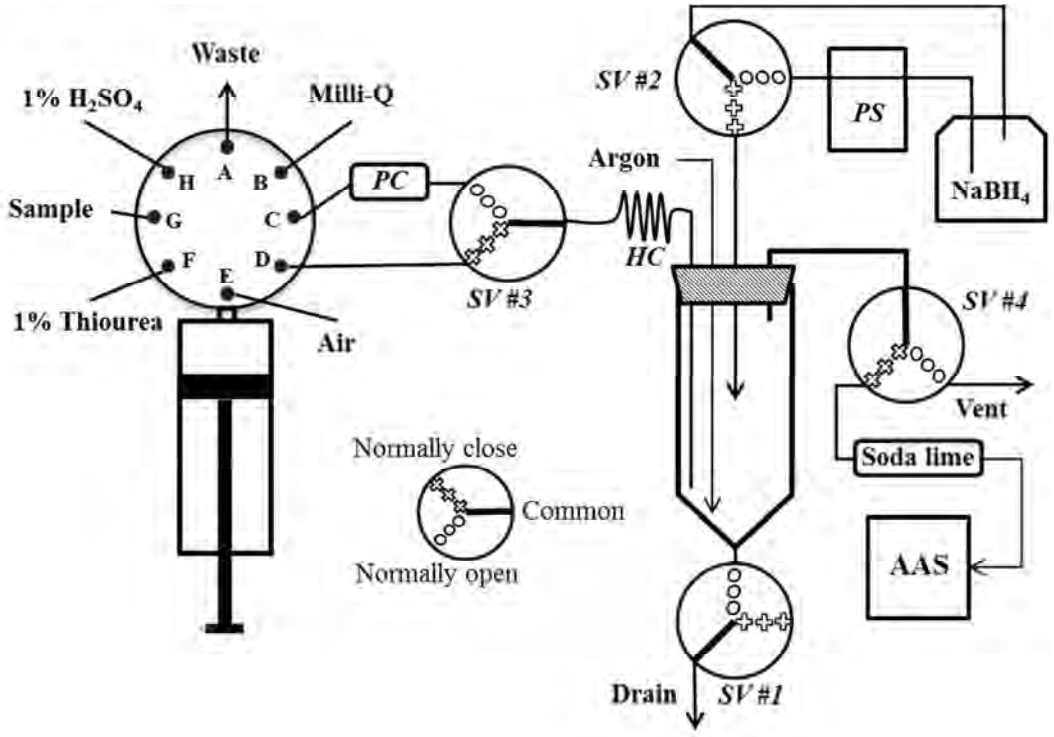

Scheme 4.3 The automated sample preconcentration and cold vapor introduction to atomic absorption spectrometer. (PC = preconcentration column, HC = holding coil, PS = peristaltic pump, SV = solenoid valve)

4.3.1.1 Effect of argon flushing flow rate

The argon flushing flow rate is an important parameter for the cold vapor introduction. The peak shape of signal depends on the flow rate of argon carrier. In order to find the optimized flow rate, the background corrected peak height of the signal after preconcentration of mercury (II) ions in solution (0.5 and 5.0 μg L^{-1}) was considered. Non-significant change in background corrected peaks height was observed with argon flushing flow rate of 50, 100 and 150 mL min^{-1}. Moreover the similar peaks shape was observed at the flow rates of used. Therefore, the 50 mL min^{-1} of argon carrier was selected as the argon flushing flow rate for the further experiments.

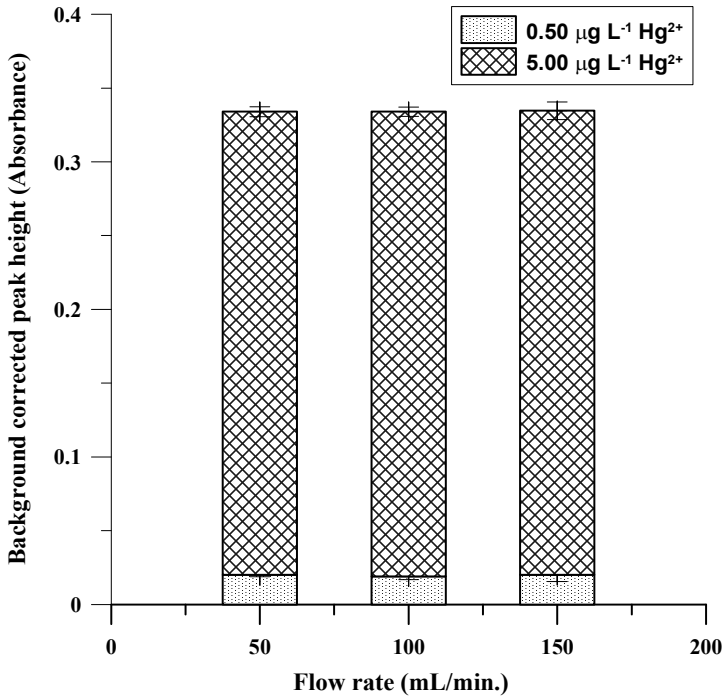

Figure 4.10 Effect of argon flow rate on the signal of mercury (II) after preconcentration. (Condition: SG-NH-L 30 mg, Hg (II) 0.50 and 5.00 μg L^{-1})

4.3.1.2 Effect of sample loading flow rate

The sample loading flow rate can affect the extraction efficiency of preconcentration column and also the analysis time. At high sample loading flow rate, the mercury (II) ions in the sample solution is passed through the column quickly and the contact time between adsorbent and the mercury (II) ions in the solution may not sufficient for the complete mercury (II) retention. The contact time increases when the low sample loading flow rate is used, resulting in high extraction efficiency. In order to maintain the high extraction efficiency and shorten the analysis time, the sample loading flow rate was optimized.

The effect of sample loading flow rate on the preconcentration and quantification was studied at the flow rate of 3.0, 5.0 and 7.0 mL min^{-1}. The results are shown in Figure 4.11. The 3.0 and 5.0 mL min^{-1} sample loading flow rate show non-different in signal and provide higher extraction efficiency than 7.0 mL min^{-1}. Moreover, a large back pressure was generated at 7.0 mL min^{-1} and caused the high deviation of signal. The optimized sample loading flow rate was 5.0 mL min^{-1} and it was used for the further experiments.

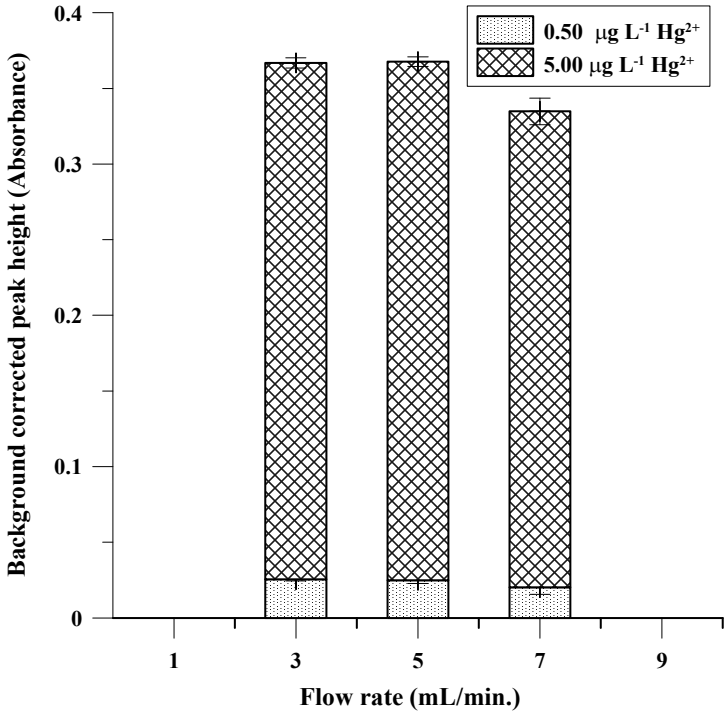

Figure 4.11 Effect of sample loading flow rate on signal of mercury (II) after preconcentration. (Condition: SG-NH-L 30 mg, Hg (II) 0.50 and 5.00 μg L^{-1})

4.3.1.3 Effect of chloride ions on the extraction efficiency

Regarding the strong effect of co-existing chloride ions in mercury (II) ions solution observed in batch experiment, the effect of the presence of chloride ions was also studied in this preconcentration system (Fig 4.12). The results show that, the signal after preconcentration of 1.00 and 4.00 μg L^{-1} mercury (II) ions solution increased by adding the chloride ions in the solutions. Moreover, no-significant difference in the extraction efficiency was observed when increased Cl^- concentration from 10 to 1000 mg L^{-1}. Therefore, the appropriate amount of Cl^- ions would be added into mercury (II) ion standard or sample to maintain 10 mg L^{-1} of Cl^- in solution for further experiments.

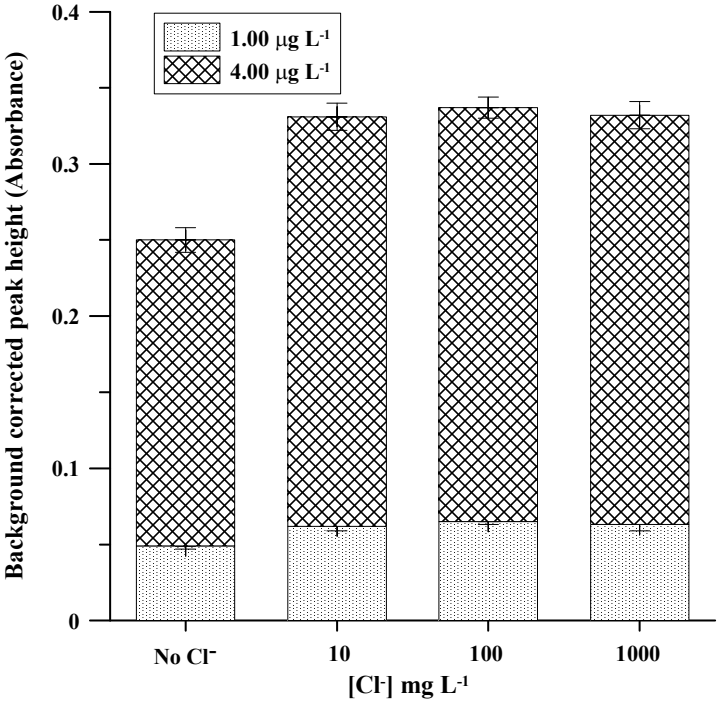

Figure 4.12 Effect of chloride ions on signal of mercury (II) ion after preconcentration. (Condition: SG-NH-L 30 mg, Hg (II) 1.00 and 4.00 μg L^{-1})

4.3.1.4 Comparison of the calibration curve obtained from direct determination and preconcentration procedure

In order to investigate the mercury (II) extraction efficiency and effect of chloride ion in the extraction and analyzing step, four sets of calibration experiment were setup. The standard solutions containing 0.50 to 5.00 μg L^{-1} of mercury (II) ions were prepared in (i) 1 % H_2SO_4 or (ii) 1 % H_2SO_4 and 10 mg L^{-1} of Cl^- ions for the preconcentration experiments. These calibration plots are shown in Figure 4.13. The results show that, the presence of chloride ions improved the sensitivity of the preconcentration method. It is probably because the SG-NH-L adsorbent has higher extraction efficiency for mercury(II)-chloro complex than the other mercury (II) species in acid solution.

It is also possible that the presence of chloride ions has the effect in the analyzing step. In order to confirm that the presence of chloride had no effect on the determination of mercury but the extraction, the direct determination of mercury ions in standard solutions containing chloride ions was performed without preconcentration step and compared to the standard mercury solutions. In this experiment, the standard calibration solutions containing 10 to 100 mg L^{-1} of mercury (II) ions were prepared in the eluent matrix i.e. (iii) 1 % H_2SO_4 / 1 % Thiourea or (iv) 1 % H_2SO_4 / 1 % Thiourea / 10 mg L^{-1} of Cl^- ions. The calibration plot of the direct determination is shown in Figure 4.14. The results show that the presence of 10 mg L^{-1} Cl^- ions in the standard solutions has no effect in the analyzing step. This observation confirms that the presence of chloride ions was actually improving the extraction efficiency of mercury (II) ion by SG-NH-L in the preconcentration step. Moreover, the signals obtained from preconcentration method were not different significantly from those obtained by the direct determination method (Figure 4.15), indicating that the exhaustive extraction was achieved in the preconcentration step over the entire concentration range.

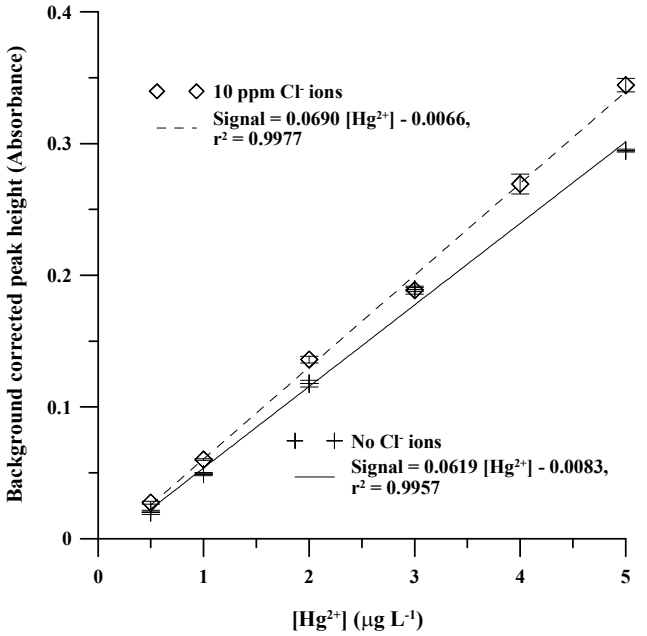

Figure 4.13 The calibration plots of preconcentration and determination of mercury in the presence and absence of chloride ions in standard solutions. (Condition: SG-NH-L 30 mg, Hg (II) 0.50 to 5.00 μg L^{-1})

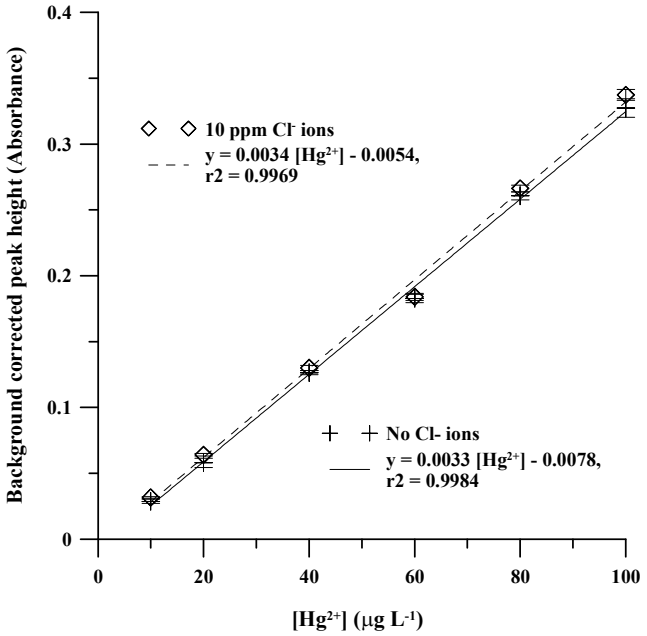

Figure 4.14 The calibration plots of direct determination of mercury in the presence and absence of chloride ions in standard solutions. (Condition: Hg (II) 10 to 100 μg L^{-1})

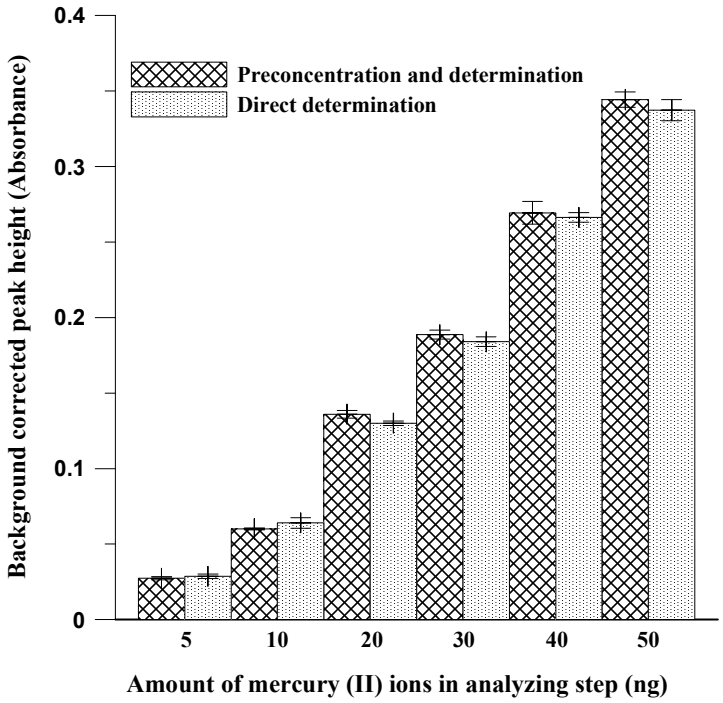

Figure 4.15 Background corrected signal of mercury from direct determination and from preconcentration method. (Condition: Amount of Hg (II) 5 to 50 ng)

4.3.1.5 Effect of interfering ions

Because the extraction of mercury (II) ions by SG-NH-L occurred via metal-ligand complex formation process following the hard/soft acid/base theory, the soft acid metals ion (Au (III), Ag (I) and Pb (II)) were selected as the potential interfering ions. Those metals ions were individually added into mercury (II) ion solutions (1.00 and 4.00 μg L^{-1}) at concentration of 10, 25, 50 and 100 μg L^{-1}. All solutions were analyzed by the proposed method and the results are shown in Table 4.8. The results show that Ag(I) ion has the greatest effect on the recovery of mercury, compared to Au(III) and Pb(II). In the 4.00 μg L^{-1} of mercury (II) solutions, the presence of Au(III) and Pb(II) at all concentrations (up to 100 μg L^{-1}) did not interfere the determination of mercury by proposed method, regarding the % recovery found. On the other hand, in 1.00 μg L^{-1} mercury (II) solutions, the Au(III) and Pb(II) had interfering effect at the concentration higher than 25 and 50 μg L^{-1}, respectively. This is because the competitive adsorption between Au(III) or Pb(II) and Hg(II) ions on the solid phase,

resulting in the mercury (II) extraction efficiency decreased. In case of Ag(I) ion, the interfering behavior was observed at all concentrations. In order to find out how Ag(I) ion interfere the determination of mercury by the proposed method, a quick experiment was setup by direct determination of mercury (II) solutions contain Ag(I) ions at several concentrations. It was found that the absorption signal of elemental mercury decreased by increasing the concentration of Ag(I) ions. This is probably due to the formation of mercury-silver amalgam, resulting in lower amount of elemental mercury that flow through the absorption cell. Moreover, when the mixture was mixed with the reducing agent, the reduced mixture turned to dark solution in the presence of Ag(0). The same change was observed in both preconcentration and direct determination methods.

Table 4.8 Effect of interfering ions on the recovery of mercury

Metals ion	**Concentration ($\mu g\ L^{-1}$)**	**Metals : Hg^{2+} (equi-valent)**	**1.00 $\mu g\ L^{-1}$ of Hg (II)**		**Metals : Hg^{2+} (equi-valent)**	**4.00 $\mu g\ L^{-1}$ of Hg (II)**	
			% recovery	**% RSD**		**% recovery**	**% RSD**
Ag(I)	10	19	87	12	5	80	3.3
	25	46	54	20	12	58	4.5
	50	93	50	21	23	39	6.8
	100	186	40	27	46	37	7.2
Au(III)	10	10	99	11	3	101	2.7
($AuCl_4^-$)	25	25	99	11	6	100	2.5
	50	51	86	12	12	100	2.5
	100	102	59	22	25	99	2.6
Pb(II)	10	10	99	13	2	102	2.8
	25	24	103	10	6	100	2.5
	50	48	94	10	12	100	2.5
	100	97	66	16	24	99	2.6

4.3.1.6 Method validation

After the optimum condition for the proposed method was obtained, the method was validated by establishing the performance characteristics related to the accuracy and precision of the method, reported in the term of the percentage of recovery and percentage of relative standard deviation, respectively. The limit of detection was also determined. The robustness of the method was examined and reported in term of standard deviation of the calibrations slope. All the results are summarized in Table 4.9. The results show that the accuracy and precision of this method in mercury (II) determination are acceptable, according to the widely used criteria of analyte recovery and precision at different concentrations (Table 4.10). The reusable of preconcentration column was found to be over 100 times of used. The relative standard deviation of the calibration slope was less than 4 % (n = 5) over 10 days, indicating the robustness of the method.

Table 4.9 Accuracy, precision and limit of detection of the proposed method for mercury (II) determination

Hg [II] concentration ($\mu g\ L^{-1}$)	**Recovery (%)**		**RSD (%)**		**LOD ($\mu g\ L^{-1}$)**	
	[a]Intra-day	**[b]Inter-day**	**[a]Intra-day**	**[b]Inter-day**	**[a]Intra-day**	**[b]Inter-day**
1.00	95 - 102	95 - 106	3.7	3.7 - 14	0.24	0.24 - 0.33
4.00	98 - 103	96 - 105	2.6	2.6 - 5.2		

[a] n = 10

[b] Results from 5 experiments over 10 days

Table 4.10 Acceptable values of analyte recovery and relative standard deviation of the determination of analyte at different concentrations [73]

Analyte, %	Analyte ratio	Unit	Mean recovery, %	RSD, %
100	1	100 %	98 – 102	1.3
10	10^{-1}	10 %	98 – 102	2.8
1	10^{-2}	1 %	97 – 103	2.7
0.1	10^{-3}	0.1 %	95 – 105	3.7
0.01	10^{-4}	100 ppm	90 – 107	5.3
0.001	10^{-5}	10 ppm	80 – 110	7.3
0.0001	10^{-6}	1 ppm	80 – 110	11
0.00001	10^{-7}	100 ppb	80 – 110	15
0.000001	10^{-8}	10 ppb	60 – 115	21
0.0000001	10^{-9}	1 ppb	40 – 120	30

4.3.1.7 Real sample analysis

The proposed method was applied to determine mercury (II) ions in real samples using spiked method. The results are shown in Table 4.11. The recoveries of mercury (II) ions from spiked samples at both concentration levels are acceptable. Therefore, the proposed method can be used to determine the mercury (II) ions contained in water samples.

Table 4.11 Determination of mercury (II) ions in real samples

Sample	Added ($\mu g\ L^{-1}$)	Found ($\mu g\ L^{-1}$) (n = 3)	Recovery (%)
Tap water	-	n.d.	-
	1.00	0.97 (± 0.13)	97.0
	4.00	3.91 (± 0.21)	97.8
Natural water	-	n.d.	-
	1.00	1.01 (± 0.16)	97.2
	4.00	4.03 (± 0.19)	99.9
Sea water	-	n.d.	-
	1.00	1.07 (± 0.22)	104.3
	4.00	4.18 (± 0.16)	103.7

4.3.2 Preconcentration and quantification of mercury (II) ions in sample by SG-PT-GF system

The SG-PT-GF system was developed to improve the sensitivity of the SG-PT system. The first stage elemental mercury that was formed in the reducing chamber was trapped again on the gold-plated filament which placed in the GT (Scheme 4.4). The GT chamber has much lower internal volume than the reducing chamber, this design will reduce the dispersion of the elemental mercury vapor. Moreover the trapped elemental mercury would be released at almost the same time, this also again reduces the dispersion of the elemental mercury vapor before detection. All of these steps were called re-focusing.

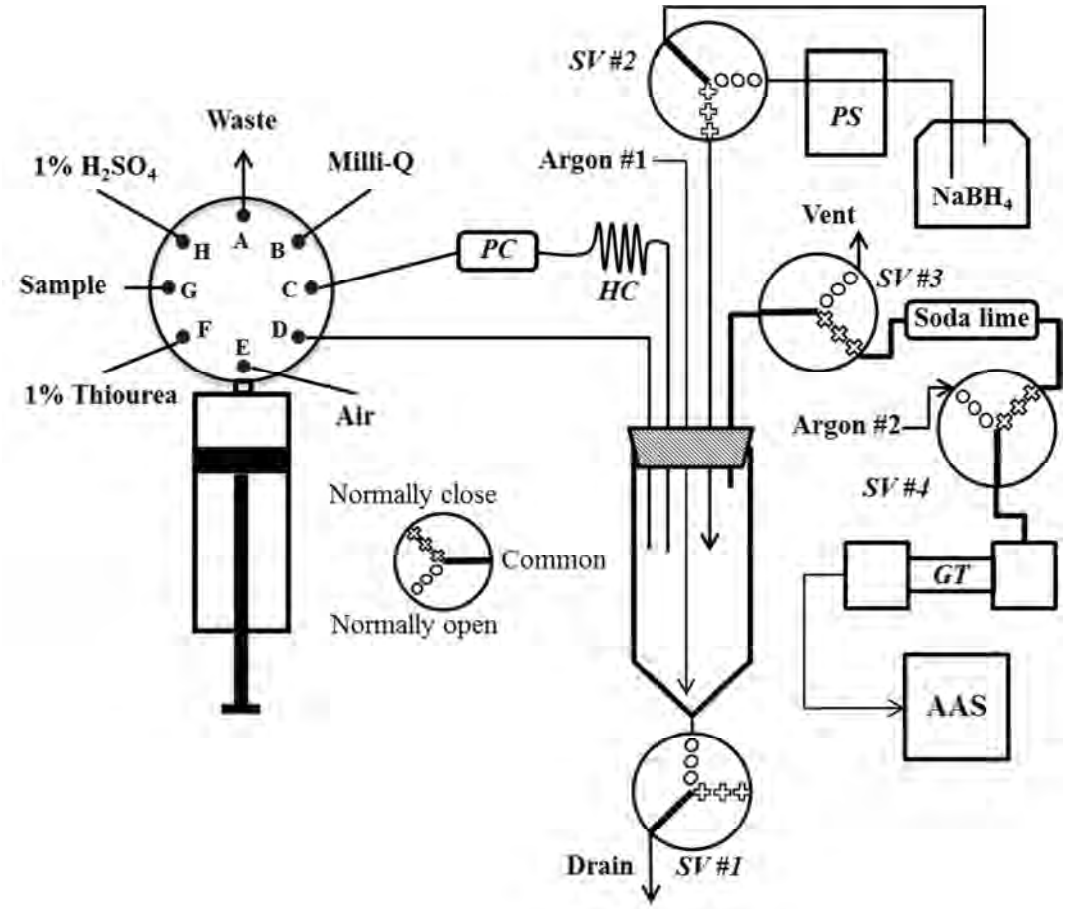

Scheme 4.4 The automated sample preconcentration and cold vapor with gold trap introduction to atomic absorption spectrometer (PC = preconcentration column, HC = holding coil, PS = peristaltic pump, SV = solenoid valve, GT = gold trap).

4.3.2.1 Effect of argon flushing flow rate

The effect of argon flushing flow rate (Argon #2, Scheme 4.4) was studied. The flow rate had to be sufficient to sweep off the moisture in a reasonable period of time but not too high to dilute the released elemental mercury. The peak shape of signal also depended on the flow rate of argon #2. The results are shown in Figure 4.16. The results show that the signal decreased by increasing the flow rate of argon, because the residence time of released elemental mercury in the absorption cell was shortened at a high flow rate. However, the low argon flow rate will result in the broad peak signal and this was observed at the flow rate lower than 25 mL min^{-1}.

Therefore, the argon flow rate of 30 mL min^{-1} was selected for flushing in the further experiments to ensure the moisture was removed before heating the filament resulting in long lifetime for gold-plated filament and the quantitative amount of mercury was flushed to the absorption cell.

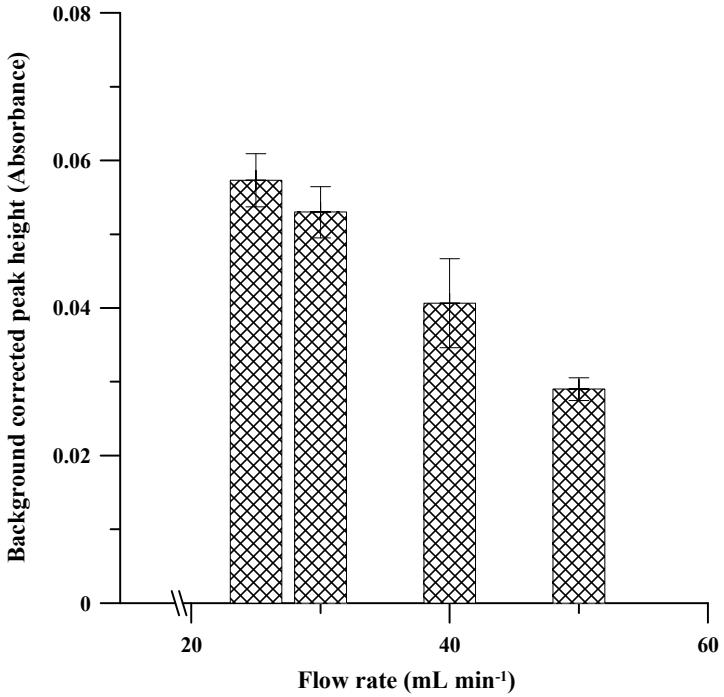

Figure 4.16 Effect of argon flushing flow rate. (Argon #2, Scheme 4.4) (Condition: SG-NH-L 30 mg, Hg (II) 0.50 μg L^{-1})

4.3.2.2 Comparison of signal peak shape obtained from SG-PT and SG-PT-GF method

The determination of mercury was performed by SG-PT and SG-PT-GF, operated at their optimum conditions. The background corrected signals were shown in Figure 4.17. The reduction in peak broadening and the increase in peak height were observed when SG-PT-GF was used, compared to SG-PT. The Full-Width Half-Maximum (FWHM) of the peaks from SG-PT method was about 3.7 times reduced

when using the SG-PT-GF method, indicating that the sensitivity was improved by SG-PT-GF method.

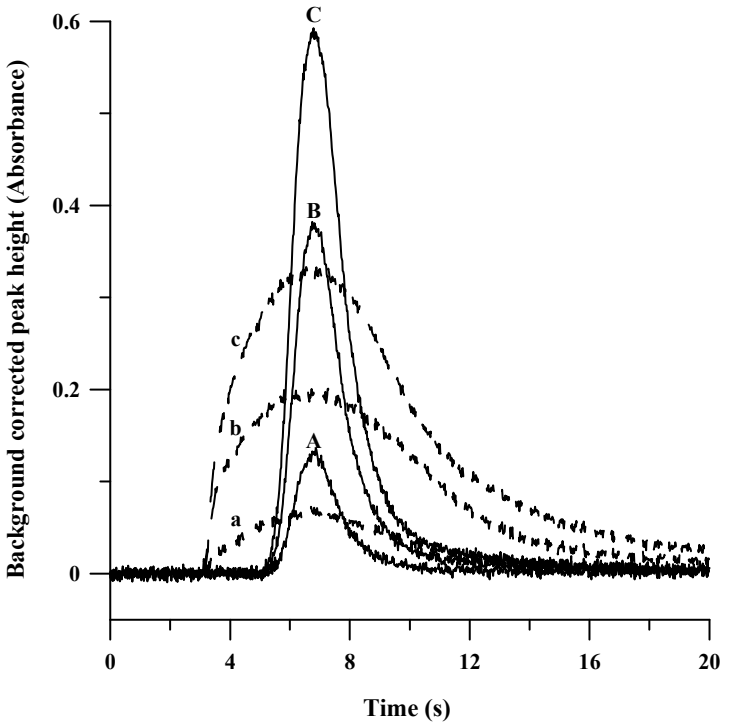

Figure 4.17 Peak shape signal of mercury solutions obtained by SG-PT and SG-PT-GF method. (SG-PT: a = 1.00 μg L^{-1}, b = 3.00 μg L^{-1}, c = 5.00 μg L^{-1}; SG-PT-GF: A = 1.00 μg L^{-1}, B = 3.00 μg L^{-1}, C = 5.00 μg L^{-1})

4.3.2.3 Method validation

After the optimum condition for the proposed method was achieved, the method was validated. All the experiments are performed as same as the validation of SG-PT method except the concentrations range of standard solutions. The calibration is plotted in Figure 4.18. All the results are summarized in Table 4.12. The results show that the accuracy and precision of this method in mercury (II) determination are acceptable, according to the widely used criteria of analyte recovery and precision at

different concentrations [73]. The relative standard deviation of the calibration slope was less than 4 % (n = 5) over 14 days, indicating the robustness of the method.

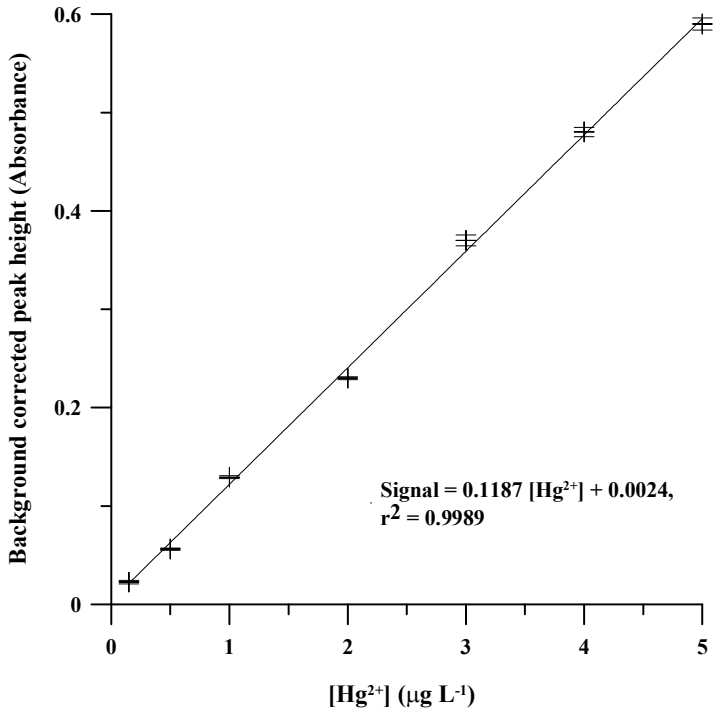

Figure 4.18 The calibration plot of SG-PT-GF system.

Table 4.12 Accuracy, precision and limit of detection of the SG-PT-GF method for mercury (II) determination

Hg [II] concentration ($\mu g\ L^{-1}$)	Recovery (%)		RSD (%)		LOD ($\mu g\ L^{-1}$)	
	[a]Intra-day	[b]Inter-day	[a]Intra-day	[b]Inter-day	[a]Intra-day	[b]Inter-day
0.20	85 - 110	80 - 115	12	12 - 21	0.035	0.035 - 0.066
4.00	95 - 106	93 - 108	5.5	5.5 - 7.3		

[a] n = 10

[b] Results from 5 experiments over 14 days

4.3.2.4 Analysis of certified reference material

The accuracy of the SG-PT-GF method was examined by determining the mercury (II) content in certified reference material (HG95-3, HG95-10) compared to the certified values. The results are shown in Table 4.13. Regarding the certified value and acceptable limit mentioned in the CRMs, the acceptable results were obtained by using the SG-PT-GF method. Therefore, the proposed method can be applied to analysis of water samples with acceptable accuracy. Noted that the efficiency of preconcentration column was reduced after 3 times of use when analyzing the CRMs, this is probably because of potassium dichromate (0.05%) used as the preservative for CRMs.

Table 4.13 Analytical results of mercury (II) determination in certified reference materials by SG-PT-GF method.

CRM	**Assigned value ($\mu g\ L^{-1}$)**	**Acceptable limit ($\pm\mu g\ L^{-1}$)**	**Found ($\mu g\ L^{-1}$) (n = 3)**	**% Recovery**
HG95-3	0.157	0.0484	0.138 (± 0.028)	87.9
HG95-10	0.240	0.0718	0.203 (± 0.024)	84.5

Part II Preconcentration and determination of atmospheric mercury

4.4 Optimization of mercury detection by DBD

To optimize the parameters affecting the detection of mercury by DBD, the experiments were performed using the setup shown in scheme 4.5. The effect of plasma potential and plasma gas flow rate, response behavior of the detector and sensitivity comparison of the radiation detectors were investigated.

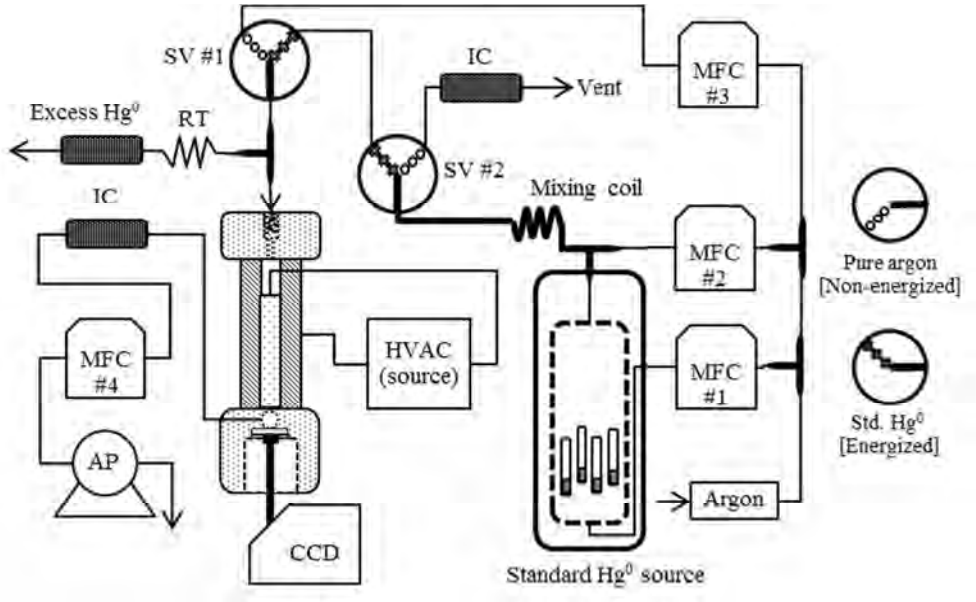

Scheme 4.5 System schematic in studying of the detection part**.** (AP = air pump, MFC = mass flow controller, IC = iodized charcoal column, SV#1 and SV#2 = solenoid valves (driven together), HVAC = high voltage alternative current, RT = restriction tube, CCD = charge coupled device array spectrometer.

4.4.1 Emission spectra of the system

The emission spectral of pure argon plasma (blank) and 82.7 ng L^{-1} of Hg^0 were shown in Figure 4.19. The emission of mercury in the plasma was observed at 253.7 nm which is a characteristic wavelength of mercury.

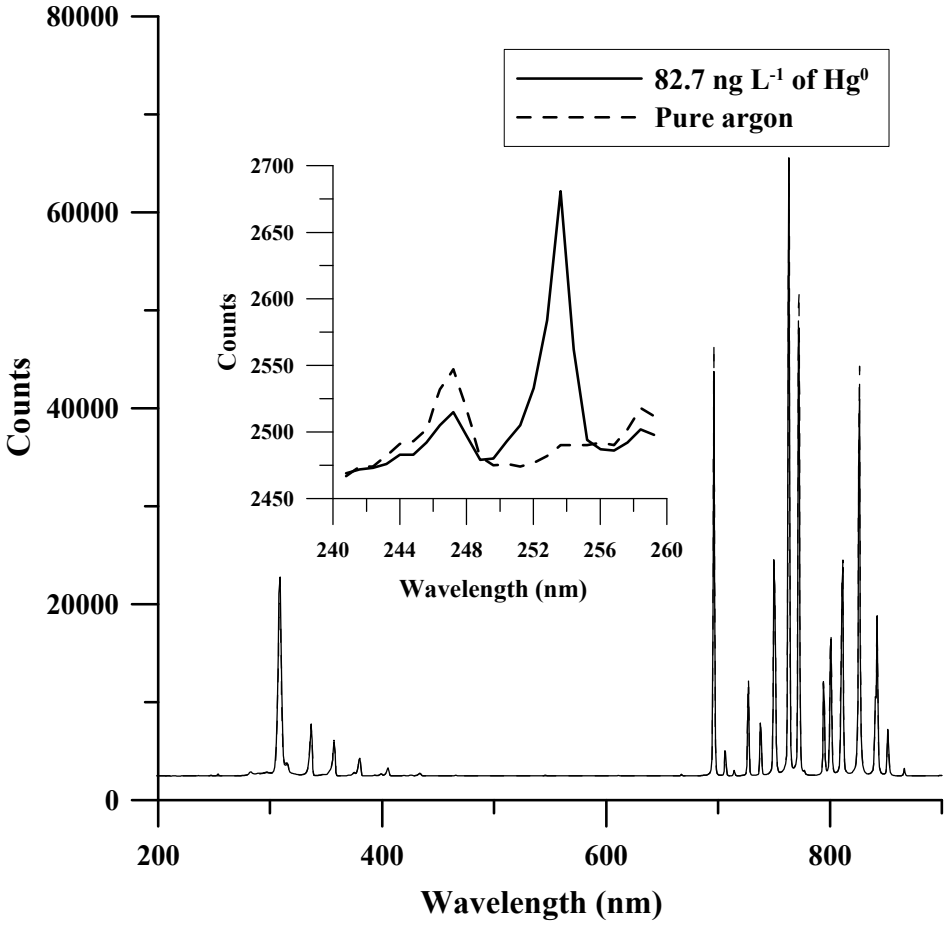

Figure 4.19 The spectra of pure argon plasma and 82.7 ng L^{-1} of mercury in argon plasma. The spectra were collected at 200 millisecond of the integration time; Ocean Optics QE65000. (Inserted figure is a close up plots around the emission line)

4.4.2 Effect of the plasma potential and plasma gas flow rate

The initial ignition potential for argon plasma was 1.5 kV and the maximum voltage that could be safely applied before sparking occurred was 8.0 kV. The heat

generated by the plasma was minimal under the operated conditions (plasma potential < 8.0 kV, plasma gas flow rate range of 88 – 439 sccm). The change in S/N of 94 ng L^{-1} Hg^0 as a function of applied voltage is shown in Figure 4.20. In the whole plasma gas flow rate (88 – 439 sccm) ranged, the S/N increased by increasing the applied voltage, and the maximum S/N was observed at the maximum applied voltage that the plasma could be operated in. It is because more excitation energy transferred to the mercury when applied higher potential, compared to the lower applied potential.

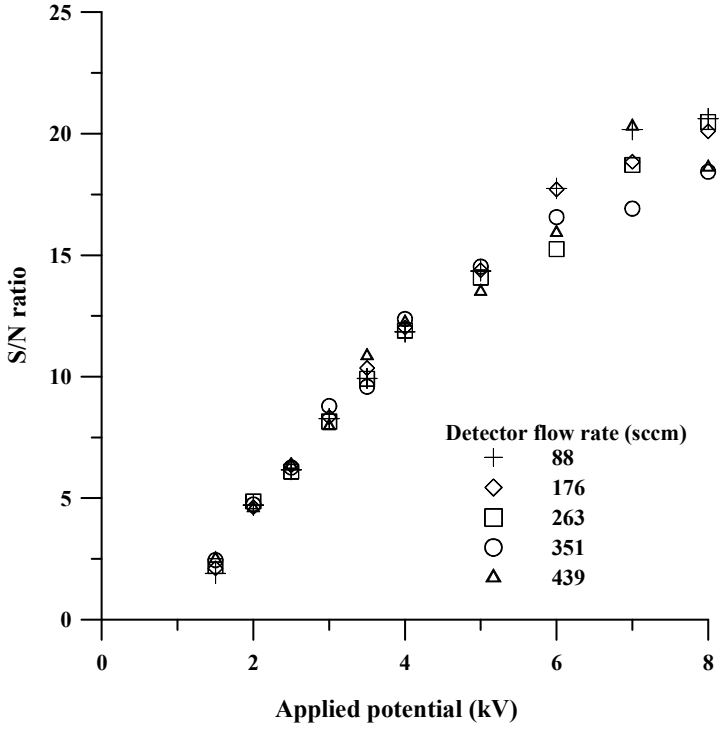

Figure 4.20 Signal to noise ratio as a function of plasma gas flow rate and applied voltage for argon plasma gas, 94 ng L^{-1} Hg in DBD cell. Ocean Optics QE65000 detector. Spectra were acquired with 100 ms integration times. All spectra acquired over 60 s were averaged.

4.4.3 Response behavior

The response of the system to varying mercury concentrations in argon plasmas (operated at 8.0 kV) is shown in Figure 4.21. The system showed linear response up to high Hg concentrations at all gas flow rates. Therefore, the argon plasma operated at 8.0 kV was used for further work and the system could be operated in wide range of plasma gas flow rate (88-439 sccm).

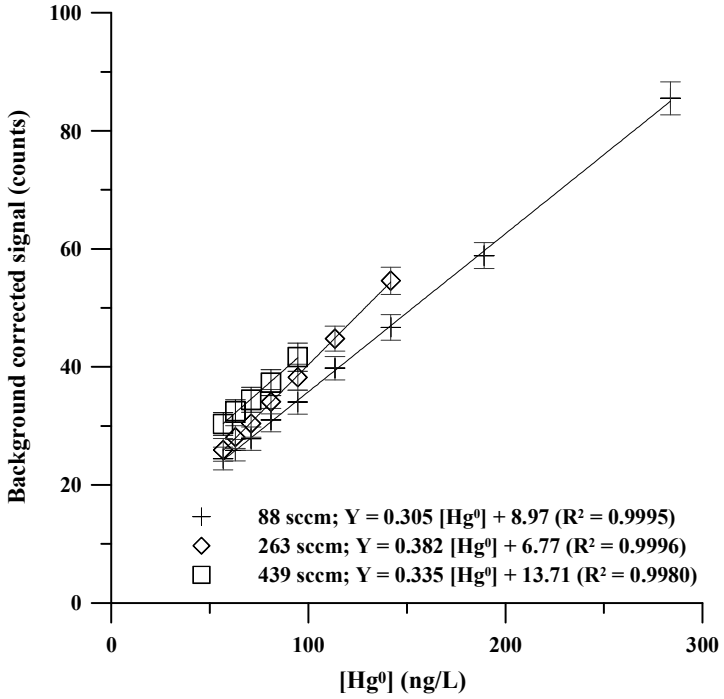

Figure 4.21 Response behavior of the detection system. The data were obtained by the Hamamatsu C9404CA CCD spectrometer, 100 ms integration time. All spectra acquired over 60 s were averaged.

4.4.4 Sensitivity comparison of different detectors

Several types of detectors were tested to check their performance in the detection of mercury emission in DBD cell. The results are shown in Table 4.14. Note that the integration times for the CCDs were 100 ms as opposed to 1 s for the photo(multiplier)tubes. The unamplified phototube could not sense any light either for

the background plasma or in the presence of mercury. The solar blind (P/N R6800U-01) photomultiplier tube which has a response range of 160 – 320 nm, provided twice better S/N than the H5784 PMT sensor module. Because the H5784 responds to visible light as well (185 – 650 nm) and the interference filter could not completely remove the whole visible wavelength (> 580 nm can pass through the filter).

For the CCD spectrometers detection, the low-cost USB-2000 spectrometer did not really provide enough sensitivity to perform trace analysis. While the QE65000 showed good sensitivity and ability to detect the mercury emission. The Hamamatsu CCD spectrometer showed the best performance with the highest S/N ratio (approximately 60 times better than the USB-2000) and was used for further work.

Table 4.14 Relative performance of different detection systems[a]

Detector CCD spectrometer	**Operating range (nm)**	**Slits / resolution**	**Operating conditions**	**Sample**	**Counts / 100 ms (sd)**	**S/N**
Hamamatsu C9404CA	200 – 400	140 μm / 3 nm	100 ms integration	Blank 82.7 ng L^{-1} Hg^0	1164 (19) 2860 (55)	31
Ocean Optics QE65000	200 – 1100	25 μm / 2.6 nm	100 ms integration	Blank 82.7 ng L^{-1} Hg^0	2460 (1.5) 2494 (2.0)	17
Ocean Optics USB2000	200 – 1100	25 μm / 1.5 nm	100 ms integration	Blank 82.7 ng L^{-1} Hg^0	113.5 (2.3) 134.9 (2.5)	0.6
Detector Photo(multiplier) tube	**Response range (nm)**	**Interference filter**	**Gain / Power**	**Sample**	**mV (sd)**	**S/N**
Hamamatsu PMT R7400U-09	160 – 320	12 nm halfwidth	- 850 V applied	Blank 82.7 ng L^{-1} Hg^0	89.6 (6) 96.5 (4)	
Hamamatsu PMT module H5784-06	185 – 650	12 nm halfwidth	Gain control 0.85 V	Blank 82.7 ng L^{-1} Hg^0	403 (5) 398 (9)	
Hamamatsu PT R6800U-01	185 – 320	12 nm halfwidth	- 15 V applied	Blank 82.7 ng L^{-1} Hg^0	No light detected	N/A

[a]Argon flow rate 88 sccm, 8.0 kV plasma potential.

sd = standard deviation of the signal (counts)

4.5 Preconcentration and determination of atmospheric mercury

In the analysis of trace amount of atmospheric mercury, gold plated filaments made in-house were included in the system to preconcentrate mercury prior to the determination by DBD. The setup is shown in scheme 4.6. The sample or the standard mercury was introduced to the system via SV#2.

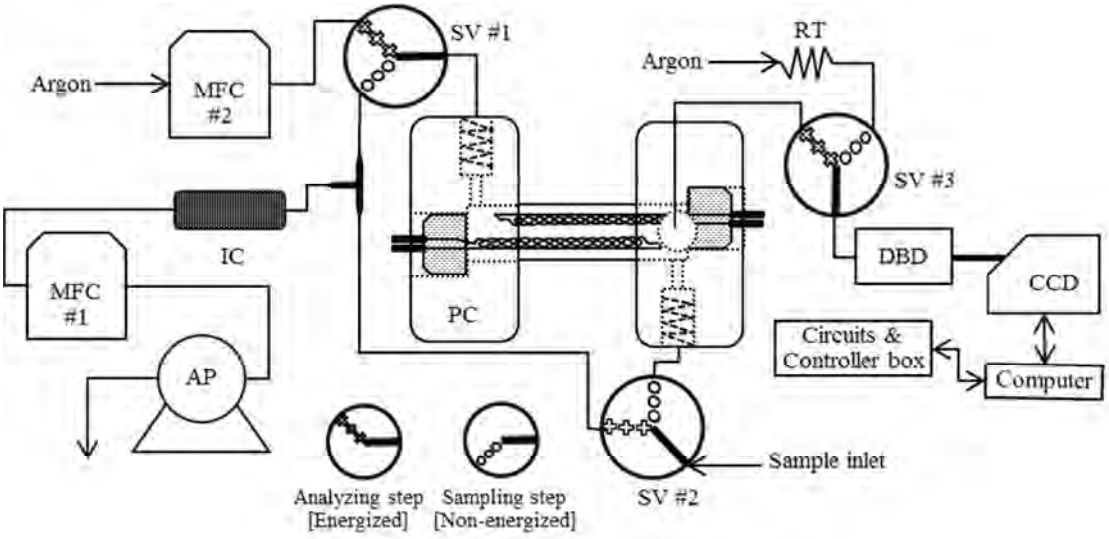

Scheme 4.6 System schematic**.** (AP = air pump, MFC = mass flow controller, IC = iodized charcoal column, SV#1 – SV#3 = solenoid valves (driven together), PC = preconcentration chamber, RT = restriction tube, DBD = dielectric barrier discharge cell, CCD = charge coupled device array spectrometer (other detectors were also used as indicated in text)

4.5.1 Argon flushing flow rate during desorption step

The effect of argon flushing flow rate during desorption step was studied by the system presented in Scheme 4.6. The flushing flow rate had to be sufficient to sweep off the air in a reasonable period, when switched the mode of operation from sampling mode to analyzing mode, but not too high to dilute the desorbed Hg^0. However, too low flow rate would not only broaden out the signal, it would also

increase the analytical cycle time. The effect of argon flushing flow rate varied between 90 to 440 sccm on the signal is shown in Figure 4.22. The signal increasing was observed when the flow rate increased from 90 to 180 sccm, while no significant change in signal was observed for the range of 180 to 440 sccm. Therefore a flushing flow rate of 180 sccm was used for further work.

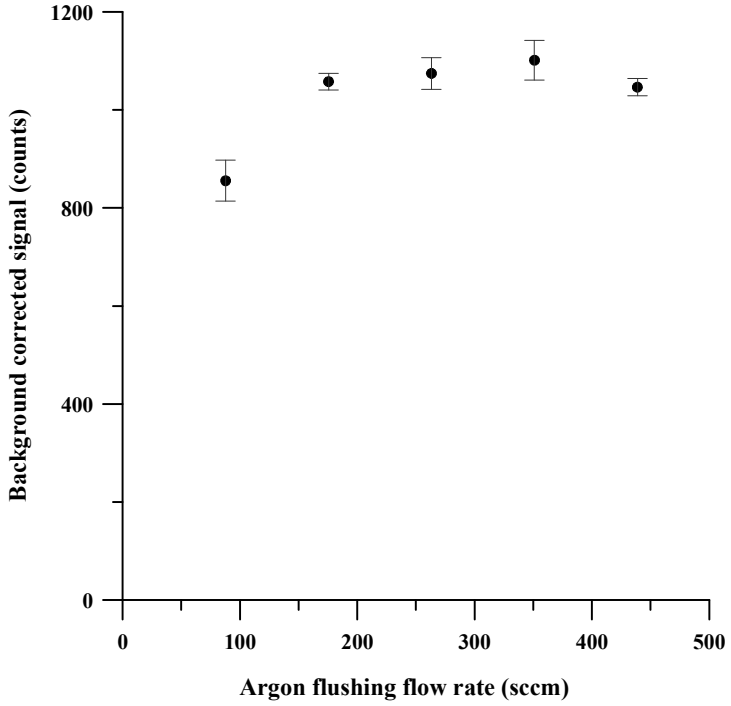

Figure 4.22 Signal of 0.73 ng L^{-1} mercury (preconcentrated for 60 s at 4.0 SLM) at different argon flushing flow rate.

4.5.2 Sampling rate during preconcentration

The sampling rate during preconcentration step was investigated by a test with mercury concentration of 0.64 ng L^{-1} and the sampling rate of 0.88 to 6.14 SLM. The dependence of the response per unit amount of mercury sampled on the sampling flow rate is presented in Figure 4.23. In a simple tubular system, the collection efficiency decreases with flow rate [74]. The reproducible collection is an important concern for the determination of mercury in the air, and the reproducible collection

was observed in the range of operation. Therefore, the whole range of sampling rate could be used. In this study, the sampling rate of 0.88 SLM was chosen to obtain a high analytical sensitivity in mercury determination.

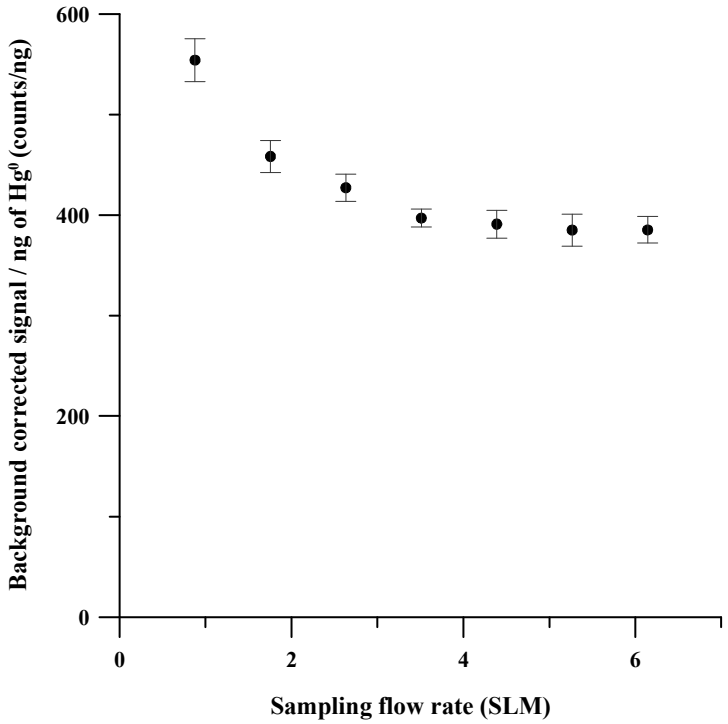

Figure 4.23 The mercury signal response per unit amount of mercury as a function of sampling flow rate.

4.5.3 Repeatability and limit of detection

A total of 19 such calibrations were repeated in an automated fashion over a 7-consecutive-day period. The calibrations plot and the signals are presented in Figure 4.24. The calibration equation for the combined data was:

$$\text{Signal counts} = 557(\pm 4.8)\,[Hg^0] + 56.8(\pm 18.2)$$

The relative standard error of the calibration slope was less than 1%, indicating the robustness of the technique. The standard deviation of the responses at individual concentration points varied from 2.8 to 4.9%. Given the signal magnitude of the

lowest concentration for this flow rate and this sampling period and the uncertainty of the blank measured under these same conditions, the calculated limit of detection of 0.12 ng L^{-1} was observed based on the three standard deviations over blank criterion.

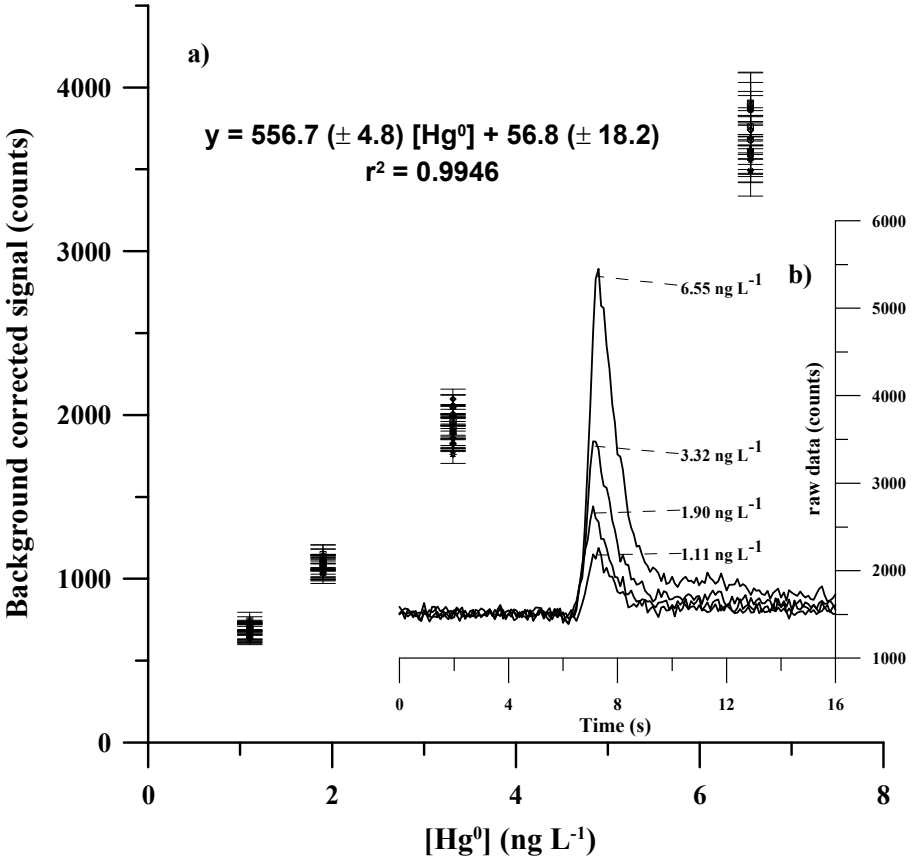

Figure 4.24 a) Calibrations data plot of 19 automated four-concentration calibration plots executed over 1 week, b) signal profiles for 1.1 – 6.6 ng L^{-1} Hg^0 preconcentrated at 0.88 SLM for 120 s, 180 sccm flushing flow rate.

4.4.8 Field application

The experiment was conducted at a lamp recycling plant. The instrument was deployed in the plant over a 24 h period. The air handling system was shut down after work hours; Figure 4.25 shows that the mercury concentration rises remarkably in the enclosed area and then the mercury concentration drops again after the work hour begins.

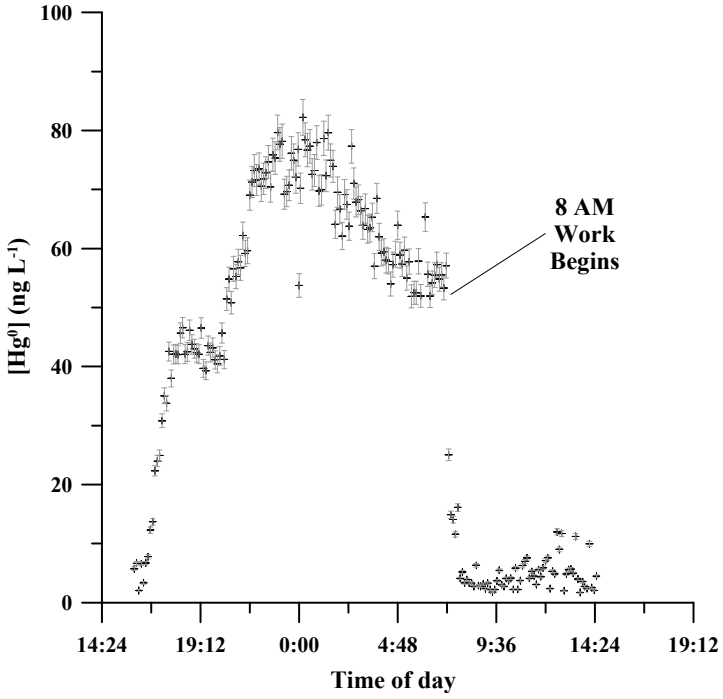

Figure 4.25 Gaseous mercury concentrations in the air at a fluorescent lamp recycling plant. The air sample was collected at 2.64 SLM for 30 s. Note that mercury concentration drops abruptly as work begins and air handlers are started.

CHAPTER V

CONCLUSIONS

Part I Preconcentration and determination of mercury (II) in natural water samples

MCM-41 and silica gel functionalized with The 2-(3-(2-aminoethylthio) propylthio)ethanamine were prepared as the adsorbents for mercury (II) ions (MCM-41-NH-L and SG-NH-L). The successful modification was confirmed by the X-ray diffractometer, thermo gravimetric analyzer, surface area analyzer and solid state ^{13}C-NMR spectrometer. The mercury (II) extraction properties were examined by batch method. The adsorbents showed a high selectivity toward mercury (II) ions over other metal ions. The SG-NH-L and MCM-41-NH-L showed similar adsorption capacity at pH 3, while the MCM-41-NH-L showed faster adsorption kinetics over the SG-NH-L due to its uniform structure. All the results show that the modified MCM-41 and silica gel have a good potential to be used as selective adsorbents for mercury (II) ions and the modified silica gel was also applied to preconcentrate and determine the mercury (II) ions in natural water samples.

The automated sample preconcentration and cold vapor introduction system were developed and coupled to AAS. The SG-NH-L was applied to the system as a solid phase extraction for mercury (II) ions. The parameters affecting the determination of mercury (II) ions by the proposed method were optimized. The characteristics and performance of the proposed method are shown in Table 5.1.

Table 5.1 The analytical performance of mercury (II) analysis

Features	**System**	
	SG-PT	**SG-PT-GF**
Detection limit (3 SD) (μg L^{-1})	0.24	0.035
Precision (RSD, n = 10) (%)	3.7[b], 2.6[c]	12[a], 5.5[c]
Accuracy (Recovery, n = 10) (%)	95 - 102[a], 98 - 103[b]	85 - 110[a], 95 - 106[c]
Linear range (μg L^{-1})	0.50 - 5.00	0.15 - 5.00
Sample volume (mL)	10.00	10.00
Eluent volume (mL)	0.50	0.50
Sample flow rate (mL min^{-1})	5.0	5.0
Eluent flow rate (mL min^{-1})	1.0	1.0
Preconcentration factor	20	20
Analysis time (minutes : seconds)	12 : 22	14 : 20

[a]$[Hg^{2+}]$ = 0.2 μg L^{-1}, [b]$[Hg^{2+}]$ = 1.00 μg L^{-1}, [c]$[Hg^{2+}]$ = 4.00 μg L^{-1}

The accuracy of the proposed method was investigated by determination of mercury (II) ions contained in certified reference materials. The SG-PT-GF method which is capable to determine the mercury (II) ions at low concentration range provided the accurate results for CRMs. Finally, the methods were successfully applied for the determination of mercury (II) in water samples.

Part II Preconcentration and determination of atmospheric mercury

The gold-on-tungsten filament preconcentrator coupled with a DBD emission detector was built as an automated atmospheric mercury detector. The major parameters which affected the sensitivity and reproducibility of the system were optimized. The system provides an excellent performance to measure atmospheric mercury and the 0.12 ng L^{-1} of detection limit was obtained. The system was successfully applied for field application.

Suggestions for future work

Part I Preconcentration and determination of mercury (II) in natural water samples

According to the analysis time of sequential injection analysis method is longer than flow injection analysis method due to the filling and cleaning step, the analysis time could be reduced by combine the FIA and SIA together for the systems for example, using the FIA in the sample loading step. Moreover the configuration of syringe pump used in this method has more risk in syringe contamination, because the syringe has to directly connect to the common port of selection valve. Some of cleaning step could be avoided when using the other configuration of syringe pump which has a holding coil between the syringe and selection valve, resulting in shorter analysis time.

Part II Preconcentration and determination of atmospheric mercury

In the emission light detection with photomultiplier tubes, the replacement of the interference filter by a high resolution wavelength selector, should provide higher sensitivity of the system. Moreover the total cost could be reduced by using the photomultiplier tubes instead of the expensive CCD spectrometer.

REFERENCES

[1] Namasivayam, C. and Kadirvelu, K. Uptake of mercury (II) from wastewater by activated carbon from an unwanted agricultural solid by-product: coirpith. Carbon 37 (1999) 79-84.

[2] Ranganathan, K. Adsorption of Hg(II) ions from aqueous chloride solutions using powdered activated carbons. Carbon 41 (2003) 1087-1092.

[3] Yavuz, E., Senkal, B.F. and Bicak, N. Poly(acrylamide) grafts on spherical polyvinyl pyridine resin for removal of mercury from aqueous solutions. React. Funct. Polym. 65 (2005) 121-125.

[4] Sun, C. and others. A chelating resin containing S, N and O atoms: Synthesis and adsorption properties for Hg(II). Eur. Polym. J. 42 (2006) 188-194.

[5] Tonle, I. K., Ngameni, E., Njopwouo, D., Carteret, C. and Walcarius, A. Functionalization of natural smectite-type clays by grafting with organosilanes: physico-chemical characterization and application to mercury(ii) uptake. Phys. Chem. Chem. Phys. 5 (2003) 4951-4961.

[6] Mahmoud, M. E. and Gohar, G. A. Silica gel-immobilized-dithioacetal derivatives as potential solid phase extractors for mercury(II). Talanta 51 (2000) 77-87.

[7] Soliman, E. M., Saleh, M. B. and Ahmed, S. A. New solid phase extractors for selective separation and preconcentration of mercury (II) based on silica gel immobilized aliphatic amines 2-thiophenecarboxaldehyde Schiff's bases. Anal. Chim. Acta 523 (2004) 133-140.

[8] Antochshuk, V., Olkhovyk, O., Jaroniec, M., Park, I.-S. and Ryoo, R. Benzoylthiourea modified mesoporous silica for mercury(II) removal. Langmuir 19 (2003) 3031-3034.

[9] Bibby, A. and Mercier, L. Mercury(II) Ion Adsorption Behavior in Thiol-Functionalized Mesoporous Silica Microspheres. Chem. Mater. 14 (2002) 1591-1597.

[10] Pérez-Quintanilla, D., del Hierro, I., Fajardo, M. and Sierra, I. Mesoporous silica functionalized with 2-mercaptopyridine: Synthesis, characterization and employment for Hg(II) adsorption. Micropor. Mesopor. Mat. 89 (2006) 58-68.

[11] Pérez-Quintanilla, D., del Hierro, I. d., Fajardo, M. and Sierra, I. 2-Mercapto thiazoline modified mesoporous silica for mercury removal from aqueous media. J. Hazard. Mater. 134 (2006) 245-256.

[12] Pérez-Quintanilla, D., del Hierro, I. d., Fajardo, M. and Sierra, I. Preparation of 2-mercaptobenzothiazole-derivatized mesoporous silica and removal of Hg(ii) from aqueous solution. J. Environ. Monitor. 8 (2006) 214-222.

[13] Bravo-Sánchez, L. R., de la Riva, B. S. V., Costa-Fernández, J. M., Pereiro, R. and Sanz-Medel, A. Determination of lead and mercury in sea water by preconcentration in a flow injection system followed by atomic absorption spectrometry detection. Talanta 55 (2001) 1071-1078.

[14] Duan, T., Song, X., Xu, J., Guo, P., Chen, H. and Li, H. Determination of Hg(II) in waters by on-line preconcentration using Cyanex 923 as a sorbent – Cold vapor atomic absorption spectrometry. Spectrochim. Acta B 61 (2006) 1069-1073.

[15] Martinis, E. M., BertÓn, P., Olsina, R. A., Altamirano, J. C. and Wuilloud, R. G. Trace mercury determination in drinking and natural water samples by room temperature ionic liquid based preconcentration and flow injection cold vapor atomic absorption spectrometry. J. Hazard. Mater. 167 (2009) 475-481.

[16] Sequential Injection Analysis SciTopics. Online available from: http://www.scitopics.com/Sequential_Injection_Analysis.html [2011, February 10].

[17] Lin, C.J. and Pehkonen, S.O. The chemistry of atmospheric mercury: a review. Atmos. Environ. 33 (1999) 2067-2079.

[18] Renner, R. Rethinking atmospheric mercury. Environ. Sci. Technol. 38 (2004) 448A-449A.

[19] Telliard, W. A. U.S. Environmental Protection Agency Method 245.7 (2005).

[20] de Wuilloud, J. C. A., Wuilloud, R. G., Silva, M. F., Olsina, R. A. and Martinez, L. D.,. Sensitive determination of mercury in tap water by cloud point extraction pre-concentration and flow injection-cold vapor-inductively coupled plasma optical emission spectrometry. Spectrochim. Acta B. 57 (2002) 365-374.

[21] Engel, U., Bilgi, A. M., Haase, O., Voges and Broekaert E. A Microwave-induced plasma based on microstrip technology and its use for the atomic emission spectrometric determination of mercury with the aid of the cold-vapor technique. Anal. Chem. 72 (1999) 193-197.

[22] Martínez, R., Pereiro, R., Sanz-Medel, A. and Bordel, Mercury speciation by HPLC-cold-vapour radiofrequency glow-discharge optical-emission spectrometry with on-line microwave oxidation.N. Fresen. J. Anal. Chem. 371 (2001) 746-752.

[23] Yu, Y., Du, Z., Chen, M. and Wang, J. Atmospheric-pressure dielectric-barrier discharge as a radiation source for optical emission spectrometry. Angew. Chem. Int. Edit. 47 (2008) 7909-7912.

[24] Zhu, Z., Chan, G. C. Y., Ray, S. J., Zhang, X. and Hieftje, G. M. Microplasma source based on a dielectric barrier discharge for the determination of mercury by atomic emission spectrometry. Anal. Chem. 80 (2008) 8622-8627.

[25] Eliasson, B., Egli, W. and Kogelschatz, U. Modelling of dielectric barrier discharge chemistry. Pure Appl. Chem. 66 (1994) 1275-1286.

[26] Rose, M., Knaggs, M., Owen, L. and Baxter, M. A review of analytical methods for lead, cadmium, mercury, arsenic and tin determination used in proficiency testing. J. Anal. Atom. Spectrom. 16 (2001) 1101-1106.

[27] Li, X. and Wang, Z. Determination of mercury by intermittent flow electrochemical cold vapor generation coupled to atomic fluorescence spectrometry. Anal. Chim. Acta 588 (2007) 179-183.

[28] Jiang, X., Gan, W., Wan, L., Zhang, H. and He, Y. Determination of mercury by electrochemical cold vapor generation atomic fluorescence spectrometry using polyaniline modified graphite electrode as cathode. Spectrochim. Acta B. 65 (2010) 171-175.

[29] Leopold, K., Foulkes, M. and Worsfold, P.J. Preconcentration techniques for the determination of mercury species in natural waters. Trac-Trend. Anal. Chem. 28 (2009) 426-435.

[30] Langmuir, I., The adsorption of gases on plane surfaces of glass, mica and platinum. J. Am. Chem. Soc. 40 (1918) 1361-1403.

[31] Freundlich, H.M.F. Over the adsorption in solution. Z. Phys. Chem. 57A (1906) 385-470.

[32] Ruzicka, J. and Hansen, E.H. Flow injection analyses: Part I. A new concept of fast continuous flow analysis. Anal. Chim. Acta 78 (1975) 145-157.

[33] Burguera, J.L. and Burguera, M. Pretreatment of oily samples for analysis by flow injection-spectrometric methods. Talanta 83 (2011) 691-699.

[34] Chiarle, S., Ratto, M. and Rovatti, M. Mercury removal from water by ion exchange resins adsorption. Water Res. 34 (2000) 2971-2978.

[35] Dujardin, M.C., Cazé, C. and Vroman, I. Ion-exchange resins bearing thiol groups to remove mercury.: Part 1: synthesis and use of polymers prepared from thioester supported resin. React. Funct. Polym. 43 (2000) 123-132.

[36] Starvin, A.M. and Rao, T.P. Removal and recovery of mercury(II) from hazardous wastes using 1-(2-thiazolylazo)-2-naphthol functionalized activated carbon as solid phase extractant. J. Hazard. Mater. 113 (2004) 75-79.

[37.] Olkhovyk, O., Antochshuk, V. and Jaroniec, M. Benzoylthiourea-modified MCM-48 mesoporous silica for mercury(II) adsorption from aqueous solutions. Colloid. Surface. A. 236 (2004) 69-72.

[38.] Walcarius, A. and Delaĉte, C. Mercury(II) binding to thiol-functionalized mesoporous silicas: critical effect of pH and sorbent properties on capacity and selectivity. Anal. Chim. Acta 547 (2005) 3-13.

[39.] Aguado, J., Arsuaga, J.M. and Arencibia, A. Adsorption of aqueous mercury(II) on propylthiol-functionalized mesoporous silica obtained by cocondensation. Ind. Eng. Chemres. 44 (2005) 3665-3671.

[40] Krata, A., Pyrzyńska, K. and Bulska, E. Use of solid-phase extraction to eliminate interferences in the determination of mercury by flow-injection CVAAS. Anal. Bioanal. Chem. 377 (2003) 735-739.

[41] Pourreza, N. and K. Ghanemi, Determination of mercury in water and fish samples by cold vapor atomic absorption spectrometry after solid phase extraction on agar modified with 2-mercaptobenzimidazole. J. Hazard. Mater. 161 (2009) 982-987.

[42] Soliman, E.M., Saleh, M.B. and Ahmed, S.A. Alumina modified by dimethyl sulfoxide as a new selective solid phase extractor for separation and preconcentration of inorganic mercury(II). Talanta 69 (2006) 55-60.

[43] Ahmed, S.A. Alumina physically loaded by thiosemicarbazide for selective preconcentration of mercury(II) ion from natural water samples. J. Hazard. Mater. 156 (2008) 521-529.

[44] Mahmoud, M.E., Osman, M.M. and Amer, M.E. Selective pre-concentration and solid phase extraction of mercury(II) from natural water by silica gel loaded dithizone phases. Anal. Chim. Acta 415 (2000) 33-40.

[45] Moghimi, A. Selective Pre-concentration and Solid Phase Extraction of Mercury(II) from Natural Water by Silica Gel-loaded (E)-N-(1-Thien-2′-ylethylidene)-1,2-phenylenediamine Phase. Chinese J. Chem. 25 (2007) 1536-1541.

[46] Seibert, E. L., Dressler, V. L., Pozebon, D. and Curtius, A. J. Determination of Hg in seawater by inductively coupled plasma mass spectrometry after on-line pre-concentration. Spectrochim. Acta B. 56 (2001) 1963-1971.

[47] Fitzgerald, W.F. and Gill, G.A. Subnanogram determination of mercury by two-stage gold amalgamation and gas phase detection applied to atmospheric analysis. Anal. Chem. 51 (1979) 1714-1720.

[48] Yoshida, Z. and Motojima, K. Rapid determination of mercury in air with gold-coated quartz [silica] wool as collector. Anal. Chim. Acta 106 (1979) 405-410.

[49] Sallsten, G. and Nolkrantz, K. Determination of trace amounts of mercury vapour in humid air: performance of gold traps in an atomic fluorescence system. Analyst 123 (1998) 665-668.

[50] McNerney, J.J., Buseck, P.R. and Hanson, R.C. Mercury detection by means of thin gold films. Science 178 (1972) 611-612.

[51] McNerney, J. J. Thin gold films based mercury sensor. Sensors 3 (1986) 39-41.

[52] Chen, H. and Wang, Y. Preparation of MCM-41 with high thermal stability and complementary textural porosity. Ceram. Int. 28 (2002) 541-547.

[53] Choudhury, S. B., Ray, D. and Chakravorty, A. Sulfur-ligated nickel oxidation states. Chemistry of a family of NizS2N4 (z = +2, +3, +4) complexes incorporating hexadentate thioether-imine-oxime binding. Inorg. Chem. 30 (1991) 4354-4360.

[54] Puanngam, M., Ohira, S. I., Unob, F., Wang, J. H. and Dasgupta, P. K. A cold plasma dielectric barrier discharge atomic emission detector for atmospheric mercury. Talanta 81 (2010) 1109-1115.

[55] Saouter, E. and Blattmann, B. Analyses of Organic and Inorganic mercury by atomic fluorescence spectrometry using a semiautomatic analytical system. Anal. Chem. 66 (1994) 2031-2037.

[56] Larsson, T., Frech, W., Bjorn, E. and Dybdahl, B. Studies of transport and collection characteristics of gaseous mercury in natural gases using amalgamation and isotope dilution analysis. Analyst 132 (2007) 579-586.

[57] Lee, B., Kim, Y., Lee, H. and Yi, J. Synthesis of functionalized porous silicas via templating method as heavy metal ion adsorbents: the introduction of surface hydrophilicity onto the surface of adsorbents. Micropor. Mesopor. Mat. 50 (2001) 77-90.

[58] Evangelista, S. M., DeOliveira, E., Castro, G. R., Zara, L. F. and Prado, A. G. S. Hexagonal mesoporous silica modified with 2-mercaptothiazoline for removing mercury from water solution. Surf. Sci. 601 (2007) 2194-2202.

[59] Alekseev, S. A., Zaitsev, V. N. and Fraissard, J. Organosilicas with Covalently Bonded Groups under Thermochemical Treatment. Chem. Mater. 18 (2006) 1981-1987.

[60] Puanngam, M. and Unob, F. Preparation and use of chemically modified MCM-41 and silica gel as selective adsorbents for Hg(II) ions. J. Hazard. Mater. 154 (2008) 578-587.

[61] Arakaki, L. N. H. and others. Thioglycolic acid grafted onto silica gel and its properties in relation to extracting cations from ethanolic solution determined by calorimetric technique. J. Colloid Interf. Sci. 273 (2004) 211-217.

[62] Walcarius, A., Etienne, M. and Lebeau, B. Rate of Access to the Binding Sites in Organically Modified Silicates. 2. Ordered Mesoporous Silicas Grafted with Amine or Thiol Groups. Chem. Mater. 15 (2003) 2161-2173.

[63] Walcarius, A. and Delacôte, C. Rate of Access to the Binding Sites in Organically Modified Silicates. 3. Effect of Structure and Density of Functional Groups in Mesoporous Solids Obtained by the Co-Condensation Route. Chem. Mater. 15 (2003) 4181-4192.

[64] Beerbower, A. and B. Jensen, W. The HSAB principle and extended solubility theory. Inorg. Chim. Acta 75 (1983) 193-197.

[65] Dean, J. A. Lange's Handbook of Chemistry. 13th ed. Singapore: McGraw-Hill, 1987.

[66] Patnaik, P. Dean's Analytical Chemistry Handbook. 2nd ed. Singapore: McGraw-Hill, 1995.

[67] Sarkar, D., Essington, M. E. and Misra, K. C. Adsorption of Mercury(II) by Kaolinite. Soil Sci. Soc. Am. J. 64 (2000) 1968-1975.

[68] Filho, N. L. D., Gushikem, Y., Polito, W. L., Moreira, J. and Ehirim, E. O. Sorption and preconcentration of metal ions in ethanol solution with a silica gel surface chemically modified with benzimidazole. Talanta 42 (1995) 1625-1630.

[69] Zhang, C., Zhou, W. and Liu, S. Synthesis and Characterization of Organofunctionalized MCM-41 by the Original Stepped Templated Sol Gel Technology. J. Phys. Chem. B 109 (2005) 24319-24325.

[70] Alcântara, E. F. C. and others. Modification of silica gel by attachment of 2-mercaptobenzimidazole for use in removing Hg(II) from aqueous media: A thermodynamic approach. J. Colloid Interf. Sci. 311 (2007) 1-7.

[71] Khan, A., Mahmood, F., Khokhar, M. Y. and Ahmed, S. Functionalized sol-gel material for extraction of mercury (II). React. Funct. Polym. 66 (2006) 1014-1020.

[72] Cestari, A. R., Vieira, E. F. S., Lopes, E. C. N. and da Silva, R. G. Kinetics and equilibrium parameters of Hg(II) adsorption on silica-dithizone. J. Colloid Interf. Sci. 272 (2004) 271-276.

[73] Mark, R. L. Validation and Qualification in Analytical Laboratories. Illinois: Interpharm Press, 1999.

[74] Toda, K. and Dasgupta, P. K. Chapter 22 Environmental Applications: Atmospheric Trace Gas Analyses. Compr. Anal. Chem. 54 (2008) 639-683.

VITA

Mr. Mahitti Puanngam was born on July 8th, 1981 in Bangkok, Thailand. After completing his secondary school from Benchamaratrangsarit school, he entered the Faculty of Science, Burapha University in 2000. Then he received his Bachelor of Science (Chemistry) in March 2003. He then entered the Department of Chemistry, Faculty of Science, Chulalongkorn University (2004) and become a member of Environental Analysis Research Unit under the supervision of Assistant Professor Dr. Fuangfa Unob. In 18-20 October 2007, he attended the 33rd Congress of Science and Technology of Thailand in the title of "Chemically Modified MCM-41 and Silica Gel as Adsorbents for Hg(II) Ions" with a poster presentation. And the following year, in January 30th – 1st February 2008, he attended the Pure and Applied Chemistry International Conference 2008 in the title of "Chemically Modification of MCM-41 and Silica Gel for the Use as Selective Adsorbents for Hg(II) Ions" in an oral presentation. He received the scholarship from Thailand Research Fund through Royal Golden Jubilee Ph.D. Program in 2008. He went to do his research at University of Texas at Arlington under the supervision of Professor Purnendu K. Dasgupta, from August 2009 to February 2010. Then he has finished his Doctoral degree of Science in 2011. His present address is 98/149 Pracharadbumpen Road, Huaykwang, Bangkok, 10310 Thailand. Contact number is 086-779-1958.